Coupling of spatial and GTPase cycle of Rheb enables growth factor signaling to mTORC1

Inaugural-Dissertation

zur

Erlangung des Doktorgrades

Dr. rer. nat.

der Fakultät für

Biologie

an der

Universität Duisburg-Essen

vorgelegt von

Marija Kovacevic

geboren in Teslic

Februar 2017

Die der vorliegenden Arbeit zugrunde liegenden Experimente wurden in der Abteilung von Prof. Dr. Philippe Bastiaens am Max Planck Institut für Molekulare Physiologie in Dortmund durchgeführt.

1. Gutachter: Prof. Dr. Martin Schuler
2. Gutachter: Prof. Dr. Michael Ehrmann
3. Gutachter: Prof. Dr. Philippe Bastiaens

Vorsitzender des Prüfungsausschusses: Prof. Dr. Perihan Nalbant

Tag der mündlichen Prüfung: 29 Mai 2017

“My dear, here we must run as fast as we can, just to stay in place.
And if you wish to go anywhere you must run twice as fast as that.”

-Lewis Carroll, Alice in Wonderland

For my family.
Thank you for teaching me how to run.

Table of Contents

LIST OF FIGURES

LIST OF TABLES

ABBREVIATIONS

4EBP1	eukaryotic translation initiation factor 4E-binding protein 1
α	fraction of interacting proteins
Akt	protein kinase B
AMPK	AMP-activated protein kinase
APD	avalanche photo diode
APT	acyl protein thioesterase
Arf	ADP ribosylation factor
Arl	ADP ribosylation factor like GTPase
ATG13	autophagy related protein 13
ATP	adenosine triphosphate
BAX	Bcl-2 associated X protein
BSA	bovine serum albumin
Cas9	CRISPR-associated 9 endonuclease
CIP	calf intestinal phosphatase
CRISPR	clustered regularly interspaced short palindromic repeats
crRNA	Crispr RNA
Deptor	DEP domain-containing mTOR interacting protein
DMEM	Dulbecco´s Modified Eagle´s Medium
dNTP	deoxynucleoside triphosphates
DSB	double stranded DNA break
ER	endoplasmatic reticulum
Erk	extracellular signal-regulated kinase
FCS	fetal calf serum
FCS	fluorescence correlation spectroscopy
FLIM	flurescence lifetime imaging microscopy
FOXO	forkhead box protein O
FPR1	yeast ortholog of FKBP12
FRAP	FKBP12–rapamycin-associated protein
FRAP	fluorescence recovery after photobleaching
FRET	Förster resonance energy transfer
G protein/domain	guanine nucleotide binding

GAP	GTPase activating protein
GATOR	GAP activity towards Rags
GDF	GDI-displacement factor
GDI	guanosine nucleotide dissociation inhibitors
GDP	guanosine diphosphate
GEF	guanine nucleotide exchange factor
GPCR	G-protein coupled receptors
GppNhp	5´-guanylyl imidodiphosphate
GTP	guanosine triphosphate
GTPase	enzyme that hydrolyses GTP
H-Ras	Harvey rat-sarcoma
HIF1α	hypoxia-inducible factor 1 α
HNH	homing endonuclease
HVR	hypervariable region
IGF-1	insulin-like growth factor 1
INDEL	insertion/deletion
INPP5E	inositol polyphosphate-5-phosphatase E
IRS-1	insulin receptor substrate 1
K-Ras	Kirsten rat-sarcoma
LAMP	lysosomal-associated membrane protein
LB	lysogeny broth
LPS	lipopolysaccharide
MAPKAP-K/p90^{rsk}	MAPK-activated protein kinase-1
MEF	mouse embryonic fibroblast
mLST8	mammalian lethal with SEC13 protein 8
mSin1	mammalian *s*tress-activated protein kinase [SAPK] interacting protein
mTOR	mechanistic target of rapamycin kinase
mTORC	mTOR complex
NEAA	non-essential amino acids
NHEJ	non-homologous end joining
NMR	nuclear magnetic resonance spectroscopy
N-Ras	neuroblastoma rat-sarcoma
PAM	protospacer adjacent motif

PAT	palmitoyltransferase
PCR	polymerase chain reaction
PDEδ	phosphodiesterase δ
PDK1	phosphoinositide-dependent kinase 1
PI3K	phosphatidylinositol 3- kinase-related kinase
PIP2	phosphatidylinositol (4,5)-bisphosphate
PIP3	phosphatidylinositol (3,4,5)-trisphosphate
PLA	proximity ligation assay
PMT	photo-multiplier tube
PPARγ	peroxisome proliferator-activated receptor γ
PRAS40	proline-rich Akt substrate of 40 kDa
Protor	protein observed with Rictor
PTEN	phosphatase and tensin homolog
Rab	Ras related in brain
Raf	rapidly accelerated fibroblastoma kinase
RAFT1	FKBP12 target 1
Rag	Ras related
Ran	Ras related nuclear protein
RAPT1	rapamycin target 1
Ras	rat sarcoma
RCE1	RAS converting enzyme 1
REDD1	regulated in development 1
RGK	Rem, Rad, Gem, Kir (Ras subfamily)
Rheb	Ras homologue enriched in brain
Rho	Ras homologue
Rictor	rapamycin insensitive companion of mTOR
RNAi	RNA interference
RSK	Erk activated ribosomal S6 kinase
RTCA	real-time cell analyzer
RTK	receptor tyrosine kinase
S2	Schneider 2
SEP	sirolimus effector protein
sgRNA	single guide RNA
SH2	Src homology 2

siRNA	silencing RNA
S6K-1	ribosomal protein S6 kinase beta-1
S6P	ribosomal S6 protein
τ	fluorescence lifetime
TBC1D7	Tre2-Bub2-Cdc16 1 domain family, member 7
TCSPC	time correlated single photon counting
TCTP	translationally controlled tumor protein
TFP	teal fluorescent protein
tracrRNA	trans-activating RNA
TSC	tuberous sclerosis complex
TSC1	tuberous sclerosis 1 (hamartin)
TSC2	tuberous sclerosis 2 (tuberin)

1. INTRODUCTION

1.1. How cells sense their environment?

Environment can be any biotic and abiotic surrounding of a living matter, which includes the factors that have an influence on its survival, development and evolution. For cells, the most important and challenging task is to couple the ever-changing environmental conditions with their own robust hereditary unit, gene. This gene-environment communication is manifested as an essential set of events necessary to maintain the cell as an entity, by promoting various biochemical processes and determining cellular physiology. In order to respond to the fluctuations in the environment, cells have created sophisticated communication channels, which receive, process, amplify and, in the end, respond to a variety of inputs by developing a regulatory mechanism responsible for changes in their physiology. These channels make a network of different proteins that respond to one input, providing specificity for each signal, but have intersection regions as well, enabling integration of diverse signals, resulting in various metabolic states of the cell.

The start of all signaling cascades begins at the plasma membrane, where diverse signaling molecules, which are too big or too charged to enter to the cell, bind to receptors, causing its conformational change. This triggers the production of secondary messengers, which activate downstream protein kinases that can phosphorylate and activate further proteins involved in the cascade. In each of these events, the signal is amplified, and at some parts of the cascades, there are checkpoints responsible to either propagate or stop the signal from inducing some biochemical reaction. The “checkpoint” role is mostly visible in a subset of guanine nucleotide binding (G) proteins that have a major role in propagating the signal through various points in the cytoplasm until it reaches nucleus. These proteins act as a “molecular switch”, cycling from inactive, guanosine diphosphate (GDP)-bound to active, guanosine triphosphate (GTP)-bound state, depending on the input strength and availability.

They regulate numerous processes, most of them promoting activation of genes involved in cell growth, differentiation and survival. Mutations in these genes lead to over activation even in the absence of growth factors, and this aberrant signaling is one of the main reasons behind various pathological processes in organisms.

The biggest group of small GTPases involved in signal transduction is Rat sarcoma (Ras) family. Apart from the regulation of guanine nucleotide binding, the function of these proteins is determined by their localization. The majority of them are associated with the lipid bilayers of plasma membrane or endomembranes due to their posttranslational modifications that additionally regulate protein-protein interactions and protect them from degradation **(Konstantinopoulos, Karamouzis, and Papavassiliou 2007)**.

The maintenance of this spatial segregation of small GTPases is necessary to keep the signaling cascade operative and responsive to inputs. All small GTPases have a tendency to localize to a certain locus in the cell, where they promote or stop the signal propagation, however, they undergo dynamic changes in their structure and localization in order to keep this steady state.

This spatial cycle, therefore, keeps the number of entities (small GTPases in this case) in a system (cell) constant over time, but with their constant flux from one distinct location in the system to another (**Vartak and Bastiaens 2010**). The spatial cycle of small GTPases in the cells is independent on their nucleotide bound state. However, due to its occurrence, the regulators of the activity state of the GTPase can act on it, thereby enabling biochemical processes to occur.

In this thesis, I describe the spatial cycle of the small GTPase Ras homologue enriched in brain (Rheb), which relies on the phosphodiesterase 6D (PDEδ)-mediated solubilization in the cytosol, and its subsequent release on the perinuclear membranes through ADP ribosylation factor like 2 (Arl2)-GTP activity. Here, the spatial cycle is coupled to the GTPase cycle of Rheb, as TSC2 GTPase activating protein (GAP) activity on membranes regulates the level of GTP-hydrolysis on Rheb, while (re) solubilization by PDEδ is necessary for the new GTP-loading of Rheb.

1.1.1. Small GTPases and their role in signaling

G-proteins are a protein class that transmits signal from various stimuli from cellular exterior to its interior by acting as a molecular switch. They can reversibly shift from 'on' to 'off' state, which is determined by their capacity to hydrolyze GTP to GDP **(Vetter and Wittinghofer 2001**) (**Figure 1**).

G-proteins are divided into two groups: heterotrimeric G-protein complexes and monomeric small GTPases. Heterotrimeric G-proteins consist of alpha (α) and tightly associated beta (β) and gamma (γ) subunits. When a ligand in a form of growth factor, sugar, lipid or another protein activates G-protein coupled receptors (GPCRs), it promotes a conformational change that allows the GPCR to act as a guanine nucleotide exchange factor (GEF) for $G_{\alpha,}$ which dissociates from $G_{\beta\gamma}$ and the GPCR. Both G_{α}-GTP and $G_{\beta\gamma}$ can now activate signaling cascades, while the GPCR can activate the next G-protein. Upon GTP-hydrolysis on G_{α}, the re-association with $G_{\beta\gamma}$ occurs and the new cycle of activation can begin. Hydrolysis is enhanced by activity of regulator of G-protein signaling proteins (RGSs), which act as GAPs for G_{α} subunits (**Oldham and Hamm 2008**).

Small GTPases are homologous to the G_{α} subunit of heterotrimeric G-proteins, but unlike G_{α}, which needs other two subunits in order to promote signaling events, they function independently as hydrolase enzymes (**Biou and Cherfils 2004**). In addition to GEFs and GAPs, the activity of small GTPases is regulated by guanosine nucleotide dissociation inhibitors (GDIs), which maintain small GTPases in inactive, GDP-bound state by stabilizing the inactive form and covering the lipid modification of the GTPase as a cytosolic complex (**Seabra and Wasmeier 2004**).

Superfamily of Ras GTPases is the best-known group of small GTPases. They consist of more than 150 members, 20-25 kDa in size, divided into six families: Ras, Rho, Rab, Ran, Arf and Rad/Rem/Gem/Kir (RGK) GTPases. Each subfamily shares a conserved N-terminal G-domain, with two flexible regions (Switch I and Switch II) providing the nucleotide exchange activity, while the C-terminal part possesses features important for their subcellular localization, commonly modified with lipid posttranslational modifications such as myristoylation, palmitoylation and prenylation. These modifications allow

interaction with the phospholipids, and are responsible for membrane localization and GDI binding (**Hancock et al. 1991; Hancock et al. 1989; Cox and Der 2002; Michaelson et al. 2005**).

Proteins from the Ras homologue (Rho) family are involved in a wide array of cellular processes, such as cytoskeletal reorganization, cell migration, transformation and metastasis. Ras-related nuclear protein (Ran) subfamily is necessary for nuclear transport of macromolecules and start of mitosis (**Etienne-Manneville and Hall 2002**). Ras-related in brain (Rab) proteins regulate the vesicular transport from various organelles as Golgi or ER to the plasma membrane, with each protein having an organelle-specific subcellular localization (**Pereira-Leal and Seabra 2001; Zerial and McBride 2001**). ADP ribozylation factor (Arf) subfamily consists of Arf and Arf-like proteins. They regulate vesicle trafficking and membrane fusion. This is the most diverse family of proteins in the entire group of small GTPases and in contrast to all the others, is not regulated by GDIs (**Pasqualato, Renault, and Cherfils 2002; Nie, Hirsch, and Randazzo 2003**). RGK subfamily has various physiological functions such as controlling cardiac hypertrophy, inhibiting insulin-stimulated glucose uptake in myocyte and adipocyte cell lines, as well as inhibiting voltage dependent calcium channels (**Correll et al. 2008**).

Members of Ras family of proteins have a prominent role in oncogenic transformation of the cells, with 15% of all human cancers having a point mutation in one of these proteins leading to their constitutive activation (**Repasky, Chenette, and Der 2004**). First characterized Ras proteins, Harvey and Kirsten rat-sarcoma (H- and K-Ras (alternatively spliced into two isoforms: K-Ras4A and K-Ras4B) were isolated from oncogenic viruses in rats: Harvey sarcoma and Kirsten sarcoma virus, and later found in human cells (**Chang et al. 1982**). Neuroblastioma rat-sarcoma (N-Ras) was identified in human neuroblastoma cells in 1980's (**Marshall, Hall, and Weiss 1982; Hall et al. 1983; Shimizu et al. 1983**). All of these proteins are similar in structure and function, which is positively regulating proliferative processes.

The process of guanine nucleotide exchange occurs on the N-terminal G domain, while the membrane localization is mediated by the C-terminal hypervariable region (HVR), which ends in common CAAX motif (C- cysteine, A-alyphatic amino acid, X-any amino acid)**(Willumsen et al. 1984; Vetter and**

Wittinghofer 2001). All three Ras proteins are enriched at the plasma membrane of the cell, through an active reaction-diffusion system **(Schmick et al. 2014**) that will be discussed in the following chapters. Presence of growth factors enhances Ras-mediated enrichment of its effector, rapidly accelerated fibroblastoma (Raf) kinase at the plasma membrane, which enables its phosphorylation and activation by several other protein kinases residing at the plasma membrane. This allows for further signal transduction to downstream effectors, such as extracellular signal-regulated kinase (Erk), resulting in cell proliferation (**Nan et al. 2013**). Rheb is another Ras-like protein, which shares significant homology with other members of the group, but differs in certain aspects as well. Opposite to Ras, Rheb is an endomembrane bound protein, residing mostly at the late endosomal/lysosomal structures (**Sancak et al. 2008)**. It is a direct activator of mechanistic target of rapamycin (mTOR) kinase, which integrates various environmental cues in order to promote anabolic and inhibit catabolic cellular processes (**Laplante and Sabatini 2012**). Numerous pathways and inputs involved in the building up/breaking down processes in the cell must be well coordinated and balanced. Various pathways are involved in maintenance of the metabolic state of the cell, with mTOR complex 1 (mTORC1) signaling having a significant role.

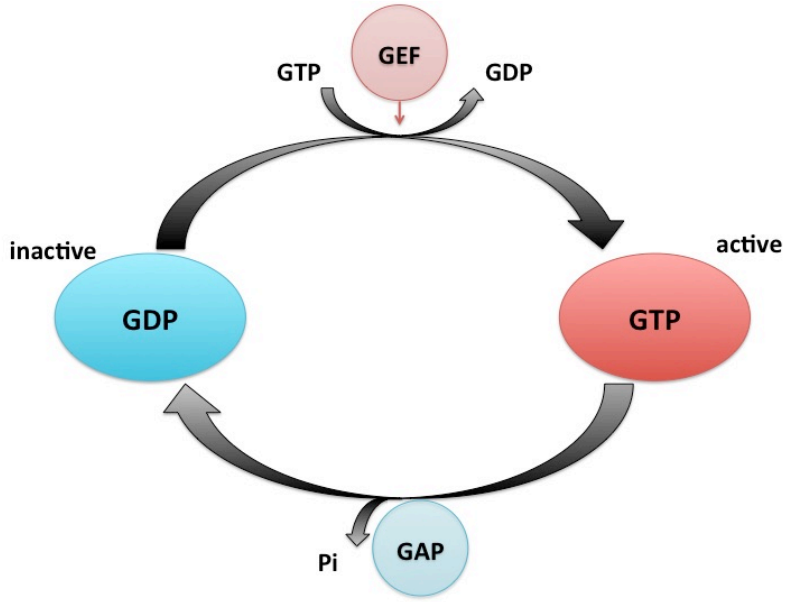

Figure 1. GTPase cycle of a G-protein

Guanylate binding proteins constantly cycle from guanosine triphosphate (GTP) bound, active, state in which they promote signal propagation to guanosine diphosphate (GDP), inactive state, where the signal propagation is halted. The cycling from GDP to GTP state is mediated by guanosine nucleotide exchange factors (GEFs), whilst GTPase activating proteins (GAPs) mediate GTP-hydrolysis, resulting in inactivation.

1.2. mTORC1 signaling

1.2.1. Mechanistic target of rapamycin (mTOR)

The serine/threonine kinase mTOR belongs to a family of phosphatidylinositol 3- kinase-related kinases (PI3Ks) and is found in two distinct multiprotein complexes in the cell. Both mTORC1 and 2 regulate cell growth, proliferation, protein and lipid biosynthesis, while actin cytoskeleton is regulated by mTORC2 specifically (**Wullschleger, Loewith, and Hall 2006; Guertin and Sabatini 2007; Laplante and Sabatini 2012**).

Yeast studies first identified FPR1 (yeast ortholog of FKBP12), TOR1 and TOR2 as the targets of rapamycin, and that mutation in each of their coding genes leads to rapamycin resistance (**Heitman, Movva, and Hall 1991**). Rapamycin is the antifungal substance isolated from the soil of Rapa Nui (Easter Island), coming from the bacterium *Streptomyces hygroscopicus* (**Vezina, Kudelski, and Sehgal 1975**). Originally, it was used as an immunosuppressant following organ transplantation, as it arrests T-

lymphocytes in mammals in G1 phase (**Abraham and Wiederrecht 1996**).

In 1994, mTOR was found to be an ortholog of the yeast TOR1/2 proteins. Several groups described mTOR independently by using names as FKBP12–rapamycin-associated protein (FRAP) (**Brown et al. 1994**), FKBP12 target 1 (RAFT1) (**Sabatini et al. 1994**), rapamycin target 1 (RAPT1) (**Chiu, Katz, and Berlin 1994**) and sirolimus effector protein (SEP) (**Chen et al. 1995**). Due to ubiquitous expression of mTOR in various eukaryotic organisms, it was decided that 'm' would stand for 'mechanistic', not 'mammalian'.

As mentioned, there are two mTOR complexes in the cell, of which mTORC1 is highly researched and well known. However, it is known that mTORC2 has a direct positive effect on protein kinase B (Akt) activation, by phosphorylating Akt at Ser 247; indicating its involvement in anabolism (**Betz and Hall 2013**). Additionally, it promotes cell motility and building of the actin cytoskeleton (**Zhou and Huang 2011**).

mTORC1 and 2 share some of the subunits within the complex besides mTOR kinase. Those are mammalian lethal with SEC13 protein 8 (mLST8) and DEP domain-containing mTOR interacting protein (Deptor). mLST8 interacts directly with mTOR and enhances its activity (**Kim et al. 2003**), while Deptor was found to have an inhibitory activity on mTOR within mTORC1.

Additional components within mTORC2 are rapamycin insensitive companion of mTOR (Rictor), mammalian *s*tress-activated protein kinase [SAPK]-interacting protein (mSin1) and protein observed with Rictor (Protor) (**Sarbassov et al. 2004; Frias et al. 2006**) (**Figure 2, right**), all necessary for efficient activation of Akt at Ser 473. This might facilitate the phosphorylation of Akt on Thr 308 by phosphoinositide-dependent kinase 1 (PDK1), which is a prerequisite for full activation (**Sarbassov et al. 2004; Sarbassov et al. 2005**).

mTORC1, besides mTOR, mLST8 and Deptor is composed of two other subunits: regulatory-associated protein of mTOR (Raptor) and proline-rich Akt substrate of 40 kDa (PRAS40) **(Kim et al. 2002; Sarbassov et al. 2005; Hay and Sonenberg 2004**) (**Figure 2, left**). mLST8 not only interacts directly with mTOR and enhances its activity (**Kim et al. 2003**), but as well favors Raptor-

mediated activation of the mTORC1 activity, by stabilizing mTOR-Raptor interaction (**Hara et al. 2002; Kim et al. 2002; Schalm et al. 2003**). These stimulative activities are balanced with negative regulators PRAS40 and Deptor. Activation of mTORC1, which occurs in response to nutrients and growth factors, results in phosphorylation of both PRAS40 and Deptor by mTORC1. This leads to dissociation of PRAS40 and Deptor from the complex and relieves the inhibitory constraint on its activity (**Vander Haar et al. 2007; Peterson et al. 2009**).

The activation of mTORC1 is a consequence of converged signals on Rheb, which in a GTP-bound state can bind and activate mTORC1. This complex functions as a nutrient/energy/redox sensor and it responds to growth factors, hormones, nutrient, energy, oxygen and amino acid availability by promoting cell growth, protein and lipid biosynthesis, as well as ribosomal biogenesis. Two main activatory paths are involved in activation of mTORC1, both mediated by different GTPases, and that is growth factor signaling, dependent on Rheb and amino acid sensing, dependent on Ras-related (Rag) GTPases.

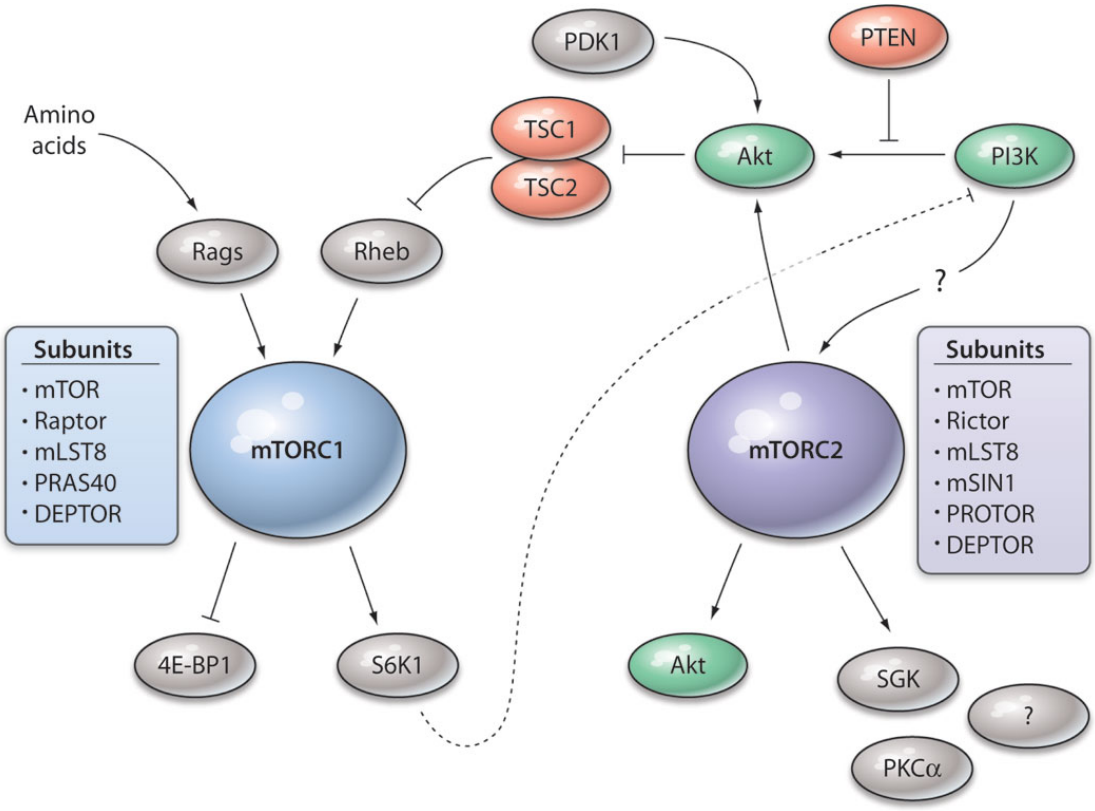

Figure 2. Structure of mTOR complexes

(adapted from: Guertin and Sabatini, 2009)

The mTOR protein kinase is the catalytic core of two multiprotein complexes, mTORC1 and mTORC2. mTORC1 (blue) additionally contains positive regulatory subunits called Raptor and mLST8 and two negative regulators, PRAS40 and Deptor. mTORC2 (purple) also contains mLST8 and the negative regulator Deptor as well as three positive regulatory subunits, Rictor, mSIN1 and Protor. Signaling events both upstream and downstream of mTORC1 are a result of growth factor signaling via PI3K/Akt/TSC axis. mTORC2 role in signaling is not well known, other than the fact that by phosphorylating Akt it wires into the mTORC1 signaling. Role specific to mTORC2 is involvement in cell motility and cytoskeleton organization by acting on protein kinase C α (PKCα). Negative regulators of mTORC activities represented in red, positive regulators represented in green.

1.2.2. mTORC1 regulation by growth factors

Growth factors are one of the most important regulators of the mTORC1 activity. Sensing of growth factor in the extracellular environment is crucial for keeping the cell growth, protein synthesis and other anabolic processes happening. The activation of mTORC1 via growth factors occurs through receptor tyrosine kinase/phosphoinositide 3-kinase/ protein kinase B (RTK/PI3K/Akt) signaling axis (**Manning and Cantley 2007**). Activation of PI3K can be accomplished through 3 different ways. One of them is by binding to activated Ras at the plasma membrane, which results in PI3K activation (**Ong et al. 2001**). Two other ways start with activation of receptors from a family of RTKs by an extracellular ligand. Two of the most prominent ligands activating mTORC1 are insulin and insulin-like growth factor 1 (IGF-1), which bind to their respective receptors, thereby activating them. This activation is manifested in dimerization of the monomers forming a receptor, and heterologous auto phosphorylation of the monomers. Tyrosine phosphorylation of insulin receptor substrate 1 (IRS-1) by insulin or IGF-1 receptor is necessary for binding and activation of PI3K, as it introduces binding sites for proteins bearing Src homologue 2 (SH2) homology domain (**Schlessinger 2002; Pawson 2002**). Additionally, PI3K can bind directly to a phosphorylated RTK (**Domchek et al. 1992**). The active PI3K can migrate to inner side of the plasma membrane and phosphorylate phosphatidylinositol (4,5)-bisphosphate (PIP2) to create phosphatidylinositol (3,4,5)-trisphosphate (PIP3). PIP3 can recruit Akt and the activation occurs by phosphorylation on Thr308 site by PDK-1. Akt is one of the most prominent proto-oncogenes with a lot of substrates. For example, it can bind to Bcl-2 associated X protein (BAX) and reduce its ability to form holes in mitochondrial membrane and

cause apoptosis (**Cantley 2002**). Additionally, active Akt causes ubiquitination of forkhead box protein O (FOXO) and its subsequent proteasomal degradation, thereby triggering cell proliferation (**Zhang et al. 2011**). But, one of the most important roles of Akt is inhibition of Rheb GAP, tuberous sclerosis complex (TSC), by phosphorylating subunit tuberin (TSC2) on Ser 939 and Thr 1462. This results in relocalization of TSC to cytoplasm and guanine nucleotide exchange on Rheb. This active, GTP-bound Rheb can bind to and activate mTOR. The activation of numerous downstream effectors, such as ribosomal protein S6 kinase beta-1 (S6K-1) and ribosomal S6 protein (S6P), finally leads to protein synthesis (**Ma and Blenis 2009**) (**Figure 3**).

As mentioned before, binding to the activated Ras GTPase can activate PI3K. Ras GTPase is activated by growth factors, cytokines, polypeptide hormones etc. and starts the signaling cascade that results in activation of Erk and promotes survival, cell proliferation and motility. The Ras-Erk and PI3K-mTOR signaling axis have some points of cross talk that end in either cross-activation or cross inhibition. One of the main lanes for cross-activation is phosphorylation of TSC2 by Erk and its substrate, MAPK-activated protein kinase-1 (MAPKAP-K or $p90^{rsk}$). The phosphorylation of TSC2 through Erk involves different sites compared to ones of Akt (discussed in detail in **1.3.2.**), but the function is the same- to inhibit its GAP activity towards Rheb.

The cross-inhibitory function involves strong IGF-1 stimulation where Akt phosphorylates inhibitory Raf sites in the N-terminus, thereby inhibiting Erk activation, but longterm, mTORC1 activation as well (**Mendoza, Er, and Blenis 2011**).

The degree of activation of each axis depends on the various factors, such as amount and species of the growth factor and the balance of cross-reactivity processes. The role of the small GTPases (Ras and Rheb) are of high importance in order to propagate the signal. Activation of Rheb is the most important step in the activation of the mTOR signaling axis in general, as various upstream stimuli are all integrated in the tightly controlled TSC-Rheb relationship.

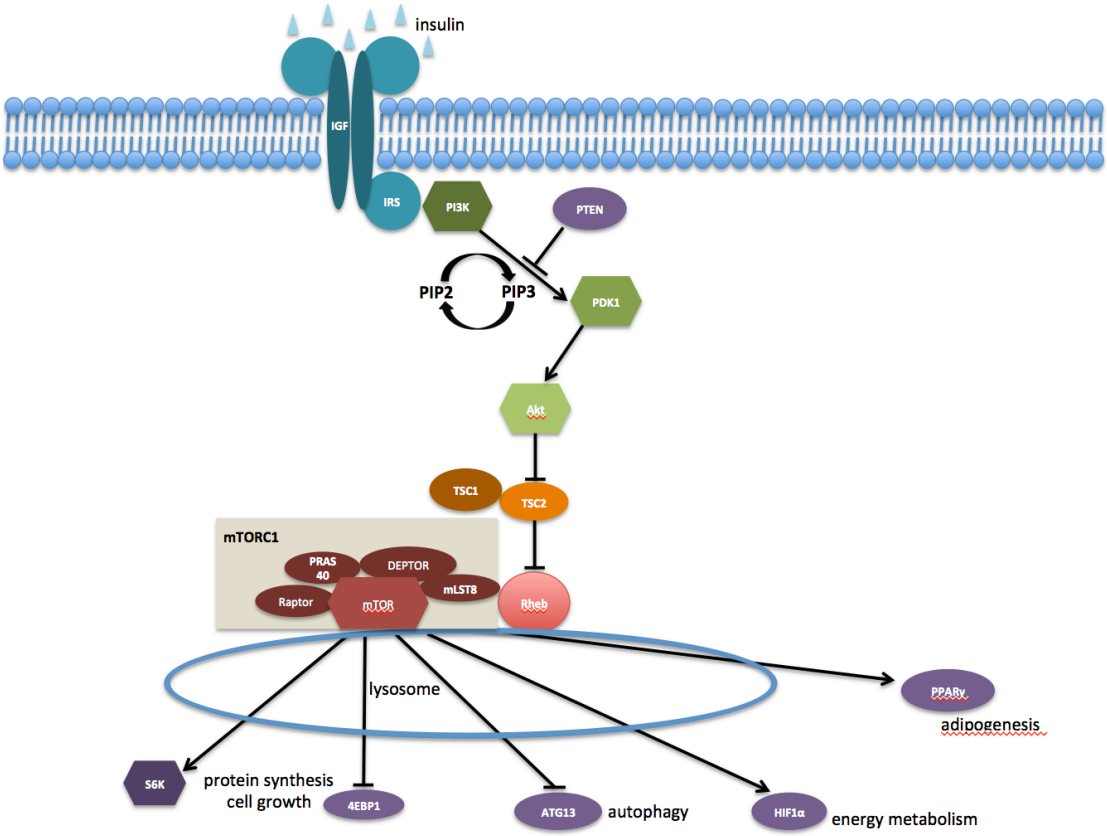

Figure 3. mTORC1 activation via growth factors

Insulin/growth factor stimulation activates PI3-kinase (PI3K). PI3K catalyzes the conversion of PIP2 to PIP3, resulting in recruitment of Akt. Inactivation of phosphatase and tensin homolog (PTEN) and phosphorylation via PDK1 activates Akt. Once Akt is activated, it directly phosphorylates TSC2 resulting in inactivation of TSC. Inactivation of the GAP TSC results in guanine nucleotide exchange on Rheb, which in GTP-bound state binds and activates mTORC1. mTORC1 further phosphorylates downstream effectors that promote protein synthesis and cell growth (ribosomal S6 kinase (S6K), eukaryotic translation initiation factor 4E-binding protein 1 (4EBP1)), energy metabolism (hypoxia-inducible factor 1 α (HIF1α)) and adipogenesis (peroxisome proliferator-activated receptor γ (PPARγ)) and inhibit autophagy (autophagy related protein 13 (ATG13)).

1.2.3. mTORC1 regulation by amino acids

Investigations in rat muscles revealed that amino acids are necessary building blocks for protein synthesis (**Preedy and Garlick 1986**). Later research done in 2D cell culture revealed that a mixture of amino acids positively regulates mTORC1 signaling, while a combination of amino acids and growth factors is needed for phosphorylation of all downstream effectors (**Hara et al. 1998; Wang et al. 1998**).

By regulating intracellular localization of mTORC1, amino acids regulate the signaling as well. When cells are deprived of amino acids, mTORC1 is located in the cytoplasm, whilst upon addition of amino acids it translocates to the

lysosomal surface, where it can be activated by Rheb (**Sancak et al. 2008; Sancak et al. 2010**) (**Figure 4**).

Cell-reconstitutive assays suggested that amino acid sensing comes from the lysosomal lumen, where they accumulate after their extracellular addition (**Zoncu et al. 2011**). This particular stimulus sensing differs from the other activating paths, as it involves Rag GTPases. They were discovered as binding partners of Raptor through immunoprecipitation-mass spectrometry analysis and the screening of small GTPases using RNA interference (RNAi) in *Drosophila melanogaster*. Rag GTPases are obligate heterodimers consisting of functionally redundant Rag A/B and Rag C/D, localized at the lysosomal surface, where they recruit mTORC1 in amino acid dependent manner (**Sancak et al. 2008**).

They do not rely on lipid modifications to tether them to membranes, but on a multiprotein complex Ragulator, which serves as a GEF for Rag A/B. Myristoylation and palmitoylation of Ragulator subunits tether Rag GTPases to the lysosome, and the Ragulator complex was reported to preferentially bind to nucleotide-free Rag A/B in vitro, which represents a classic GEF-GTPase reaction. The Ragulator activity is regulated through amino acid dependent conformational changes mediated by lysosomal v-ATPase (**Bar-Peled et al. 2012**).

GAP activity towards Rags 1 (GATOR 1) is a subunit of GATOR complex and a GAP for Rag A/B, acting as a tumor suppressor and regulating their activity. Besides GATOR1, GATOR complex consists of GATOR2. GATOR2 has an inhibitory role towards GATOR1, and it is known that its activity is regulated through sestrins. Sestrins interact with GATOR2 in amino acid-dependent manner and have an inhibitory role toward mTORC1 (**Chantranupong et al. 2014**). It was reported that they act as GDIs towards Rag A/B. Sestrin overexpression inhibits amino-acid-induced Rag guanine nucleotide exchange and mTORC1 translocation to the lysosome, while mutation of the conserved GDI motif creates a dominant-negative form of sestrin that renders mTORC1 activation insensitive to amino acid deprivation (**Peng, Yin, and Li 2014**).

While role of Rag A/B is well established, role of Rag C/D in the amino acid sensing is still relatively unknown. It is known, however, that in order to recruit mTORC1 from the cytoplasm to the lysosomes RagC/D, unlike Rag A/B,

needs to be GDP bound. This hydrolysis is regulated through folliculin, GAP for Rag C/D (**Tsun et al. 2013**).

The role of TSC2 is crucial in growth factor signaling and mTORC1 regulation as it acts as a GAP for Rheb. However, recently it has been shown that it has a role in the amino acid sensing as well. Upon amino acid removal, Rag GTPases recruit TSC2 to the lysosome, where it can act on Rheb. It is necessary that both Rheb and Rag GTPases are fully inactive to relocalize mTORC1 to the cytoplasm from the lysosome. TSC2-null cells do not release mTORC1 fully from the lysosome, which results in constant propagation of the signal (**Demetriades, Doumpas, and Teleman 2014**). This suggests that TSC2 is a central protein in sensing cellular environment, and regulating the proper cellular response.

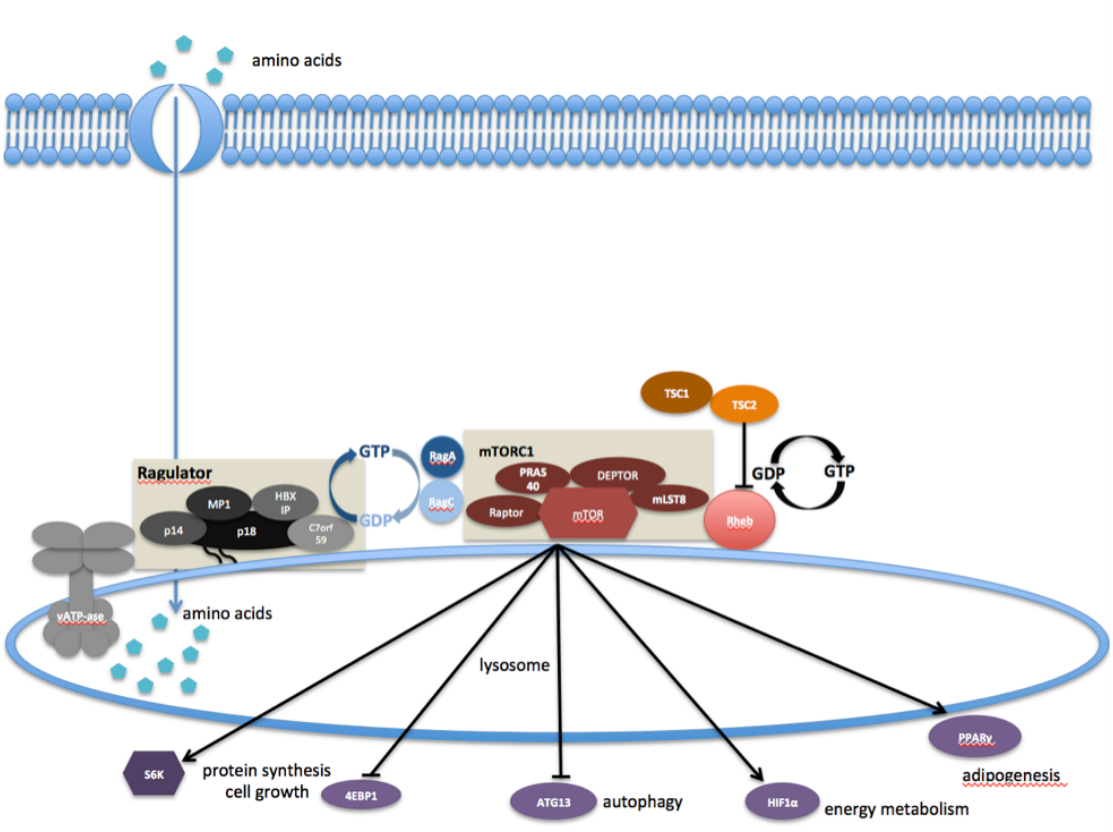

Figure 4. mTORC1 activation via amino acids

Extracellular amino acids cross the plasma membrane to create an intracellular pool, which can activate mTORC1 from lysosomal lumen. This results in conformational change of v-ATPase, which enables pentameric complex Ragulator to exert its function to Rag A and B GTPases. Active RagA/B recruits cytosolic mTORC1 to the lysosomal surface and releases lysosomal TSC, Rheb GAP, to the cytosol. This enables guanine nucleotide exchange on Rheb, which now, in GTP-bound state can bind to and activate mTOR at the lysosomal surface.

1.2.4. Small GTPase Rheb

The small GTPase Rheb represents a unique protein within the Ras family. It shares several structural and functional characteristics with the other members of the group.

There are two characterized Rheb proteins: Rheb and Rheb L1, with their respective genes localized on chromosome 7 (7q36) and 12 (12q13). Both *Rheb* genes share 51% amino acid identity (**Gromov et al. 1995; Mizuki et al. 1996; Patel et al. 2003**). Three main features characterize Rheb proteins: arginine (R) residue corresponding to glycine (G) at the position 12 for Ras proteins, conserved effector domain sequences and the C-terminal CAAX motif (C-cysteine, A-aliphatic amino acids, X-any amino acid, methionine (M) for Rheb), required for irreversible posttranslational modification, farnesylation (**Urano et al. 2001**).

The work presented in this thesis focuses on the original protein, Rheb. Rheb is a 21-kDa protein, consisting of 184 amino acids. Almost all of them form the highly conserved G-domain, while the last C-terminal 20 amino acids form hypervariable region (HVR) ending in CAAX box (**Yu et al. 2005**). Rheb G-domain contains G1-G5 boxes, features responsible for recognition of guanine ring and phosphates of guanine nucleotides **(Bourne, Wrischnik, and Kenyon 1990**). During GDP/GTP cycle, only switch I undergoes conformational change, while switch II remains stable, unlike switch II of other small GTPases. This process of GTP binding and hydrolysis is determining the protein activity and thereby, its function. The hydrolysis is facilitated by action of GAP TSC (discussed in section **1.3.2**.). GEF is promoting GTP binding to small GTPases, thereby activating them. However, GEF for Rheb is still unknown. Due to high activation state of Rheb even in cells deprived of nutrients or growth factors, existence of GEF is suspicious (**Inoki et al. 2003**) (discussed in section **1.3.1.**).

The functional role of Rheb is activation of the mTORC1, which results in promotion of anabolic (protein synthesis, cell growth), and inhibition of catabolic processes (autophagy). mTORC1 is activated by various upstream stimuli, but the crucial event is binding to Rheb-GTP and activation, which is the bottleneck for all the inputs.

1.3. Regulation of Rheb activity

The cycling of GTPases between active GTP-bound, regulated by GEFs, and inactive, GDP-bound state, regulated by GAPs, is necessary for them to exert their role as molecular switches and participate in the signaling cascades. GTP-hydrolysis is a rate-limiting step in proper regulation of activity of Ras GTPases. In hydrolysis, electronegative group is used for stabilization of hydrolytic water for nucleophillic attack of the γ-phosphate **(Li and Zhang 2004; Maegley, Admiraal, and Herschlag 1996**). In Ras subfamily, the carboxyamide oxygen of Gln in switch II, stabilized by GAP activity, achieves this, while 'arginine finger' neutralizes developing negative charge on α- and β-phosphates of GTP. As all other small GTPases, Rheb has a low intrinsic GTPase activity, but the mechanism of GTP-hydrolysis differs than the one in other Ras isoforms.

1.3.1. Positive regulation of Rheb

Positive regulation of Rheb activity is largely unknown. It was reported that translationally controlled tumor protein (TCTP) acts as a putative GEF fo*r* Rheb in both *Drosophila* and human cell lines, as it directly associated with Rheb and displayed guanine nucleotide exchange activity with it *in vitro* and *in vivo (***Hsu et al. 2007***)*. However, additional study disputed these results as it was found that no guanine nucleotide exchange activity of TCTP towards Rheb was detected *in vitro*, no direct interaction between Rheb and TCTP was detected by use of nuclear magnetic resonance (NMR) and depletion of TCTP showed no effect on activity of downstream effectors of Rheb (**Rehmann et al. 2008**).

Unlike other Ras isoforms, Rheb has an auto-inhibited mechanism of GTP-hydrolysis that involves Asp65 in switch II and Thr38 in switch I. Hydrolysis is inhibited by Tyr35, which constrains active site conformation, restricting the access of catalytic Asp65 to the nucleotide-binding pocket. This inhibitory effect is lowered upon binding to GAP TSC2, whose 'asparagine thumb' (Asn1643) promotes catalysis in synergy with Asp65. Tyr35 is necessary to maintain responsiveness to growth factors and for regulation of the activity, as mutants cannot bind TSC2, but as well to keep Rheb in highly active state.

(**Mazhab-Jafari et al. 2012**).

Rheb is usually found in high activation state in the cells; where more than 20% of the protein is still found in GTP-bound state in serum-starved cells (**Im et al. 2002**). For other Ras proteins, this percentage in serum starvation conditions is around 0.5-8% (**Satoh et al. 1990; Scheele, Rhee, and Boss 1995**). It was reported that Rheb has a higher affinity to bind GTP than GDP, and that this binding occurs preferably in solution, rather than bilayer membranes (**Mazhab-Jafari et al. 2013**). Additionally, cytosolic levels of GTP in cells are 10-fold higher than GDP (**Ahearn et al. 2012**), which would indicate that the guanine nucleotide exchange on Rheb does not require a positive regulator, but occurs rather spontaneously, in the absence or inhibition of negative regulator, TSC2.

1.3.2. Tuberous sclerosis complex negatively regulates Rheb activity

TSC is a protein complex formed of 130-kDa hamartin (TSC1) and 200-kDa TSC2, and recently discovered 35 kDa Tre2-Bub2-Cdc16 1 domain family, member 7 (TBC1D7) (**Dibble et al. 2012**). The complex acts as a tumor suppressor by regulating activation of mTORC1 complex through integration of the environmental cues (energy, oxygen, stress levels) and availability of nutrients and growth factors. Abundance of growth factors leads to inactivation of the complex resulting in guanine nucleotide exchange on Rheb and mTORC1 activation (**Huang and Manning 2008**).

The *TSC1* gene is located at chromosome 9 (9q34) (**van Slegtenhorst et al. 1997**), while *TSC2* is on the chromosome 16 (16p13.3) (**Kandt et al. 1992**) and *TBC1D7* on chromosome 6 (6p24.1). Defects in these genes result in a loss of control over cell growth and cause a disease called tuberous sclerosis complex (TSC). It is manifested in growth of benign tumors, seizures, developmental delay, skin abnormalities and lung and kidney disease (**Northrup et al. 1993**). The main function of the complex in the cell is its role as a GAP for small GTPase Rheb (**Inoki et al. 2003; Tee et al. 2003**). Only TSC2 possesses a GAP domain, unlike TSC1, which serves as a stabilizer of the complex, protecting TSC2 from ubiquitination and degradation (**Benvenuto et al. 2000**) and TBC1D7 stabilizes TSC1 dimerization (**Qin et**

al. 2016; Gai et al. 2016).

The GAP activity of TSC2 increases the low intrinsic activity of Rheb. This results in GTP hydrolysis and inactivation of mTORC1, as the conformation of GDP-bound Rheb cannot activate mTORC1 (**Patel et al. 2003; Inoki et al. 2003; Tee et al. 2003**).

Besides Erk activated ribosomal S6 kinase (RSK), which inactivates TSC2 by phosphorylating it at Ser 1798, the main regulator of TSC2 GAP activity is Akt. This was the first kinase demonstrated to phosphorylate TSC2 at Ser 939 and Thr 1462, thereby inactivating it. However, the molecular mechanism underlying this event is still largely unknown. One of the hypotheses suggests that the disruption of TSC is responsible for its inactivation, as the insulin stimulation promotes Akt phosphorylation-dependent TSC dissociation in *Drosophila* Schneider 2 (S2) cells (**Potter, Pedraza, and Xu 2002**). This has been disproven, as another study did not detect any effect on TSC complex integrity upon insulin stimulation and Akt activation (**Manning et al. 2002; Inoki et al. 2002**).

The last hypothesis suggested that the TSC2 GAP activity is spatially regulated. Subcellular fractionation revealed that TSC2 levels are elevated in the cytosol after insulin stimulation, whereas Rheb and TSC1 were exclusively found in the membrane fraction, and their levels remained unchanged, regardless of the growth factor stimulation. From these findings, it was concluded that phosphorylation of TSC2 by Akt triggers the release of TSC2 from TSC1, thereby changing its localization, resulting in impaired TSC2 GAP activity towards Rheb (**Menon et al. 2014; Demetriades, Doumpas, and Teleman 2014**).

Additional studies have proven that the mechanism of TSC2 activity is indeed spatially regulated. In cells deprived of nutrients and growth factors, TSC2 showed high perinuclear localization, co-localizing with the lysosomal marker lysosome-associated membrane protein 2 (LAMP2). In amino acid starved condition, TSC is recruited to the lysosomal surface via the activity of Rag GTPases. Upon stimulation with both nutrients and amino acids, TSC2 has a

diffuse, cytosolic pattern and does not associate with lysosomal membranes, abolishing the negative effect of it on mTORC1 activation **(Demetriades, Doumpas, and Teleman 2014; Demetriades, Plescher, and Teleman 2016; Menon et al. 2014**).

Besides Akt, the main negative regulator of TSC2, there are several upstream positive regulators of its activity. The activating role of AMPK and HIFα to TSC is a result of low energy and oxygen levels, respectively. AMPK phosphorylates TSC2 ant Thr 1227 and Ser 1345 (**Inoki et al. 2003; Shaw et al. 2004**), while HIFα induces REDD1 to neutralize AKT dependent inhibition of TSC2 (**DeYoung et al. 2008**).

Altogether, TSC serves as a bottleneck for the variety of upstream stimuli sensed by mTORC1. Its role as a negative regulator for Rheb acts as a final checkpoint before the cell decides to promote anabolic processes as cell growth, protein synthesis or inhibition of autophagy.

1.4. Localization is necessary for function of small GTPases

Ras protein can be divided into three separate parts. First one, N-terminal conserved G-domain determines activity state of the protein. It is similar amongst all members of the superfamily, and it possesses motifs necessary for guanine nucleotide binding. Second part is HVR, representing last 20 C-terminal amino acids. This part possesses several features determining localization of the protein, and highly varies from one member to another. At the C-terminal end, the third part, -CAAX box serves as a substrate for posttranslational modification, prenylation (**Lowy and Willumsen 1993**). Depending on the X in the CAAX box, either a farnesyl or a geranylgeranyl group is added. Enzyme farnesyltransferase recognizes methionine (M), serine (S), glutamine (Q), alanine (A) or cysteine (C), while geranylgeranyltransferase I recognizes leucine (L) or glutamate (E) (**Maurer-Stroh and Eisenhaber 2005; Taylor et al. 2003**). Additionally, three C-terminal amino acids (-AAX) are removed by RAS converting enzyme 1 (RCE1) and isoprenylcysteine o-methyltransferase methyl esterifies the

carboxyl group of prenylated cysteine (**Winter-Vann and Casey 2005**). Farnesylation, which occurs in Ras proteins, mediates protein-protein interactions and increases association of these proteins with membranes

H-, N- and K-Ras have additional localization feature(s) immediately upstream of farnesylated cysteine. In N- and H-Ras, the second signals are one or two palmitoylated cysteins, immediately upstream of the –CAAX box, respectively (**Figure 5., 1st and 2nd row**). K-Ras relies on polybasic stretch consisting of 9 positively charged lysines (**Figure 5., 3rd row**), which electrostatically interact with negatively charged phospholipids in the inner leaflet of the plasma membrane of the cell. Rheb lacks any of these features in the HVR, which has a net neutral charge (**Figure 5., 4th row**); therefore, its localization relies solely on farnesylation (**Hancock et al. 1989; Hancock et al. 1991; Rocks et al. 2010; Michaelson et al. 2005; Schmick et al. 2014**). This is why Rheb is associated with all endomembranes of the cell, and significant plasma membrane enrichment, visible for other Ras proteins, is lacking. It was reported that farnesylation of Rheb is required for full activation of mTOR *in vivo*, as the non-farnesylated mutant (-SAAX) was not able to induce S6K phosphorylation (**Hanker et al. 2010**).

Since many of Ras proteins are involved in oncogenic transformation of the cells, a lot of therapeutical approaches rely on targeting prenylation enzymes, thereby disrupting their subcellular localization. It was reported that phosphodiesterase 6D (PDEδ) is necessary in maintaining localization of prenylated Ras proteins, as its knockdown resulted in relocalization of plasma-membrane Ras proteins to membranes in the cell (**Chandra et al. 2012; Zimmermann et al. 2013; Schmick et al. 2014**). The role of solubilizing factor maintaining membrane localization is counterintuitive, however, solubilization is one in the chain of events necessary for proper localization of Ras proteins, forming a mechanism that will be discussed in the following chapters.

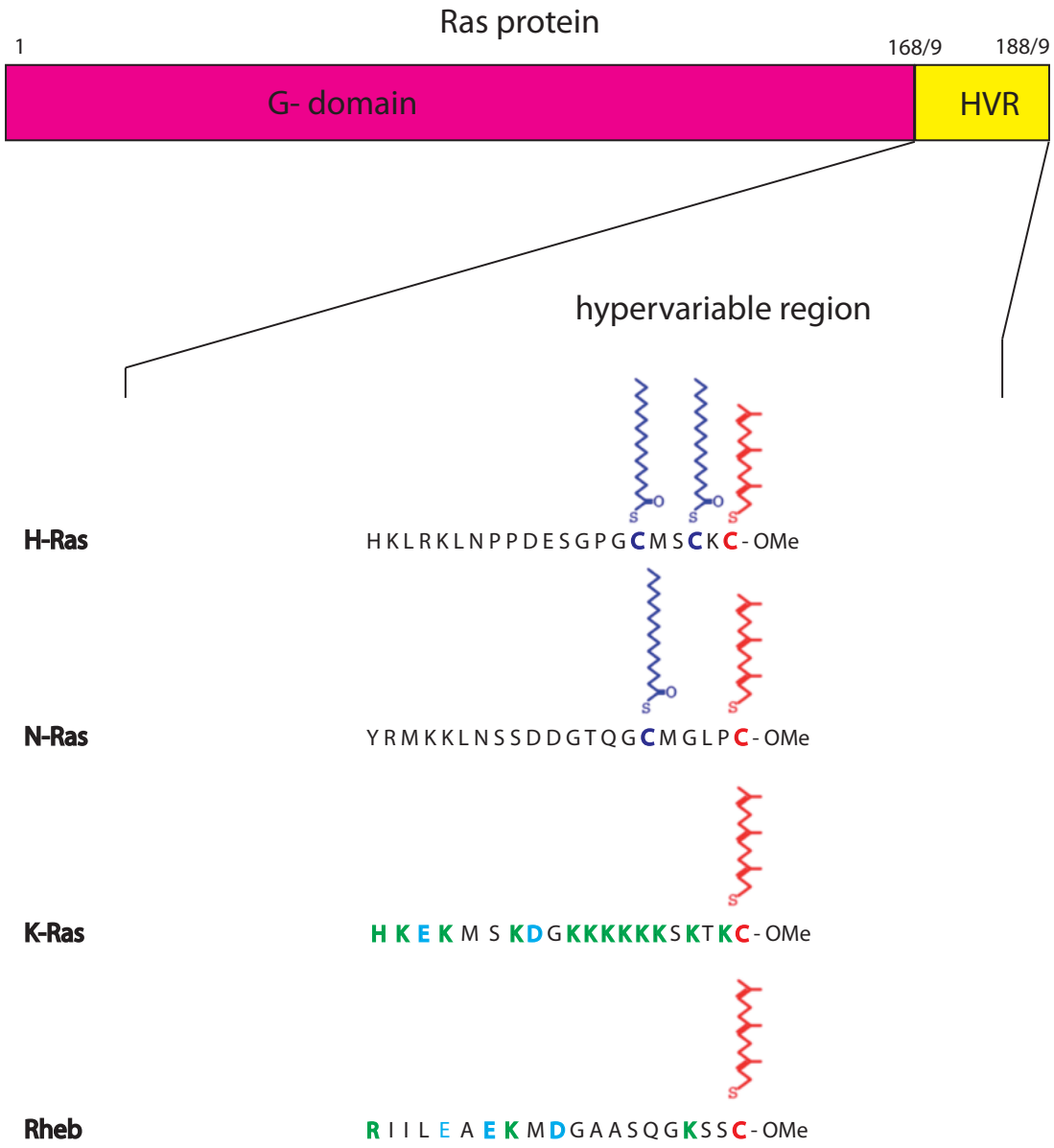

Figure 5. Hypervariable region (HVR) of Ras proteins mediates their membrane localization (based on (Bar-Sagi 2001)

Ras proteins are on average up to 189 amino acids long. N-terminal end consists of catalytic subunit- G domain, responsible for binding of guanine nucleotides and activity state of the GTPase. Last C-terminal 20 amino acids form hypervariable domain (HVR) that possesses features responsible for localization of the protein. All Ras proteins (H-, N-, K-Ras and Rheb) end in a common –CAAX motif, where the last cysteine undergoes irreversible posttranslational modification, farnesylation (in red), while the last three amino acids are methylated (OMe). H-Ras and N-Ras undergo additional reversible modification, palmitoylation, on either two (H-Ras) or one (N-Ras) cysteines in HVR. This increases their hydrophobicity, and they mostly associate with plasma membrane of the cell. K-Ras has a polybasic stretch consisting of multiple lysines (K) which through electrostatic interaction associate with negatively charged lipid bilayer of the plasma membrane. Rheb is solely farnesylated protein, with a net neutral charge in the HVR, therefore it associates mostly with endomembranes of the cell.

1.4.1. The GDI-like solubilization factor PDEδ prevents equilibration of prenylated Ras proteins on endomembranes

PDEδ has been identified as the fourth subunit of rod-specific cGMP phosphodiesterase, PDE6 (**Gillespie et al. 1989; Florio, Prusti, and Beavo 1996**). Holoenzyme PDE 6 is a heterodimer made of PDEα and PDEβ, regulated by two inhibitory γ subunits (**Gillespie et al. 1989**). Prenylation allows both PDEα and PDEβ to associate with membranes, with PDEα undergoing farnesylation and PDEβ geranylgeranylation (**Qin, Pittler, and Baehr 1992**). On the other hand, PDEδ is found exclusively in the soluble, cytosolic fraction of the cell. It was shown that PDEδ binds to the prenylated C-terminus of PDEα and β, resulting in a translocation of the holoenzyme PDE6 from membranes to cytosol (**Florio, Prusti, and Beavo 1996**). The specific residues on the inner surface of the lipid-binding pocket are identical to the ones from Rho GDIs. These proteins sequester and bury the lipid moiety (**DerMardirossian and Bokoch 2005; Goody, Rak, and Alexandrov 2005**). The core domain of PDEδ is made of an immunoglobulin-like β-sandwich fold with two β-sheets, followed by an N-terminal α-helix (**Hanzal-Bayer et al. 2002**). However, it lacks the N-terminal helix-loop-helix motif, which allows for interaction with the G domain of GTPases (position of the switch regions), which indicates that PDEδ binds the C-terminal part of GTPases, and that this interaction is nucleotide-independent **(Nancy et al. 2002; Hanzal-Bayer et al. 2002**). Additionally, PDEδ was identified as a solubilizer for prenylated proteins, with a stronger preference to farnesyl, rather that geranylgeranyl moiety, although it was reported to solubilize small GTPase Rab 13 (**Marzesco et al. 1998**). The similarity of the three-dimensional structure to Rho-GDI and all the described findings combined, established PDEδ as a GDI-like solubilizing factor for prenylated proteins, with a role similar to the Rho GDIs.

PDEδ has been shown to have an essential role in maintaining spatial organization of K-, N- and H-Ras proteins. Due to spontaneous dissociation from the membranes and endocytosis, these plasma membrane-bound proteins are internalized. By passively sequestering these proteins in the

cytosol, PDEδ enhances their effective diffusion speed and allows for faster exploration of the interior of the cell. The formation of PDEδ-Ras complex is necessary to counter the entropic tendencies arising from the structure of Ras proteins. As farnesylated proteins, they associate with any membrane in the cell, and in the absence of PDEδ, they tend to equilibrate to abundant surface of the endomembranes, resulting not only in mislocalization from the plasma membrane, but as well in their impaired signaling activity **(Chandra et al. 2012; Zimmermann et al. 2013; Schmick et al. 2014**). In addition to prenylated Ras proteins, PDEδ binds two small GTPases, Arl2 and Arl3 in a lipid independent, but nucleotide dependent manner, and serves as the effector for these two GTPases (**Hanzal-Bayer et al. 2002**). The fast diffusion of PDEδ-Ras complex in the cell enhances the speed of encountering perinuclear region of the cell. In this particular region, small GTPase Arl2 is active, GTP-bound and can bind to PDEδ. If it binds, this will result in a "closed" conformation of PDEδ, and displacement of farnesylated cargo (**Ismail et al. 2011; Schmick et al. 2014**). This event is essential for maintaining the localization of the Ras proteins, including Rheb. Arl2-Gpp-NHp and Arl2-GDP in complex with PDEδ and F-Rheb showed that PDEδ conformation is different in either of them. When bound to Arl2-GDP the hydrophobic pocket is open, resulting in a cavity of 581 Å and this conformation is called open conformation. In complex with Arl2-GTP, residues of PDEδ's hydrophobic pocket such as Met20, Ile129 and Arg61 are shifted toward the inside of the pocket and clash with the farnesyl group, and this conformation is called closed conformation (**Figure 6.**). To see how this PDEδ-Arl2-GTP interaction clashes with PDEδ-Rheb interaction, fluorescence correlation spectroscopy (FCS) with Rheb and PDEδ was done in cells. When Arl2GppNhp was added, the soluble fraction of Rheb was decreased, unlike when Arl2-GDP was added. This was confirmed with fluorescence polarization experiments as well. This showed that PDEδ in closed conformation cannot bind farnesyl group of Ras proteins and that Arl2 only in GTP-bound state can displace this cargo (**Ismail et al. 2011**). This placed Arl2 to have a role of GDI-displacement factor (GDF), a class of protein that unloads Rab and Rho proteins from their cognate GDI's to their respective destinations **(Dirac-Svejstrup et al. 2000; DerMardirossian and Bokoch**

2005; Dransart et al. 2005; Goody, Rak, and Alexandrov 2005).

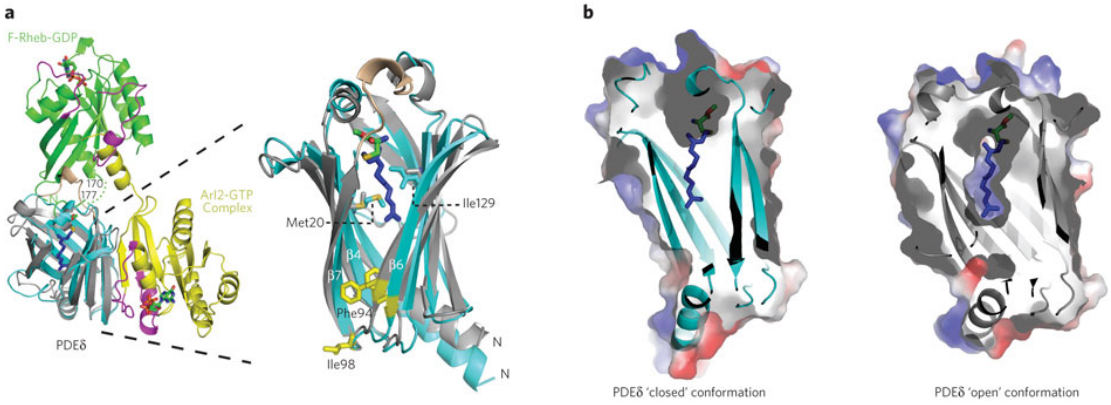

Figure 6. Mechanism of allosteric release of farnesylated cargo from PDEδ (adapted from: Ismail *et al*., 2011)

(**a**) Superimposition of F-Rheb–PDEδ, on the PDEδ–Arl2-GTP complex with PDEδ in cyan and Arl2 in yellow and switches in purple. Right-hand side shows an enlargement, with a rotation of ∼180° along the y-axis, of the two PDEδ conformations highlighting the conformational change involving movements of beta sheets. PDEδ amino acid residues shifting to closed conformation highlighted in the image. (**b**) Hydrophobic pocket of PDEδ and F-cysteine in the closed (left) and open (right) conformation, with farnesyl (blue) modeled into the Arl2 complex, shown as electrostatic surface presentation.

1.4.2. The PDEδ-Arl2 mediated spatial cycle maintains localization of prenylated Ras proteins

The hypervariable region of the Ras family of proteins is a crucial factor in determining their localization. All of these proteins undergo irreversible farnesylation in the CAAX box, enhancing their affinity for membranes. However, there are some different features in the HVR that target Ras proteins to specific membrane compartments. Although all of the proteins are subjected to a spatial cycle mediated by PDEδ and Arl2-GTP, their HVR features determine their steady state localization.

1.4.2.1. K-Ras spatial cycle

K-Ras possesses polybasic stretch consisting of 10 lysines in the HVR. The inner leaflet of phospholipids at the plasma membrane is negatively charged, therefore electrostatic interaction, combined with farnesylation localizes it at the plasma membrane of the cell. However, due to endocytic processes, but as well spontaneous dissociation of the protein itself from the plasma membrane (fulltime 8 min), K-Ras is eventually internalized and lost from the plasma membrane on the abundant surface of endomembranes (**Schmick et**

al. 2014). During endocytosis, plasma membrane undergoes through changes in the curvature. The positive (convex) curvature is imposed on inner leaflet of the plasma membrane during the formation of the vesicle, while the outer leaflet is negatively (concave) curved and borders lumen of the vesicle. The change in curvature is accompanied with the functional changes as well. It was observed that the phosphoinositide composition decreases upon membrane scission and that phosphatidinyl serine is excluded from the endosomes. Therefore, this net loss of negative charge will result in different association/dissociation rates to/from the proteins bound to them **(McMahon and Boucrot 2015; Sigismund et al. 2012)**. As endomembranes have an overwhelming surface area (200x more) compared to plasma membrane, internalized K-Ras will have a tendency to equilibrate on them inside the cell. However, the partitioning of K-Ras from endomembranes to cytosol is 2:1, unlike plasma membrane-endomembrane, which is 10:1. Therefore, once internalized majority of K-Ras will be found in the cytosol. Here, PDEδ passively sequesters it by binding to the farnesyl moiety, thereby enhancing its effective diffusion. It was shown that PDEδ is essential for localization of KRas, as the knockdown of it results in equilibration of K-Ras to all membranes. This paradox of passive solubilizing activity contributing to localization points to the existence of the energy-driven, additional component in this spatial cycle of K-Ras. The energy is provided in a form of small GTPase Arl2 (**Ismail et al. 2011**). This protein is active, GTP-bound in the perinuclear area of the cell. In its active form, it binds to PDEδ, causing an allosteric change resulting in displacement of the farnesylated cargo, allowing it to bind to membranes again. In this cellular region, recycling endosome, negatively charged on its cytoplasmic leaflet, serves as an electrostatic trap for K-Ras released from PDEδ via Arl2 activity. Fluorescence recovery after photobleaching (FRAP) experiments with mCitrine K-Ras and mTFP Arl2 wt or constitutively active form, Arl2 Q70L, showed that this recovery is normal and complete only with wt-form present, rather than constitutively active Arl2 Q70L, showing that this release mechanism indeed must be local otherwise the whole cycle would not be efficient. In the perinuclear area, recycling endosome-associated K-Ras is transported back to the plasma membrane via vesicular recycling (**Schmick et al. 2014; Schmick, Kraemer, and**

Bastiaens 2015) (**Figure 7, left**).

1.4.2.2. Acylation cycle H-Ras and N-Ras

H-Ras and N-Ras undergo additional lipidation on the two cysteins in their HVR. This reversible modification, palmitoylation, together with irreversible, farnesylation, makes a protein more hydrophobic and more susceptible to localize to plasma membrane of the cell. The non-palmitoylated mutant of H-Ras, H-Ras C181/184S, therefore localizes to endomembranes (**Misaki et al. 2010**). The cycles of depalmitoylation and palmitoylation are essential to counter endocytosis and spontaneous dissociation of the proteins, which would cause equilibration of H- and N-Ras on the endomembranes. The activity of acyl protein thioesterases (APTs) in the cytoplasm removes the palmitoyl moiety, reducing hydrophobicity and causing H- or N-Ras to partition between endomembranes and cytosol. In the cytosol, now solely farnesylated H- and N-Ras, are sequestered by farnesyl binding to hydrophobic pocket of PDEδ. This complex has a very high effective diffusion throughout the cell. Perinuclear activity of Arl2 GTPase releases it from PDEδ, enabling association with the membranes in this area. Additional localized activity of palmitoyltransferases (PATs) at the Golgi results in repalmitoylation and concentration of H- and N-Ras at this organelle. Both the H- and N-Ras then can be recycled to the plasma membrane by directed vesicular transport from the Golgi apparatus (**Figure 7, middle**).

Unlike H-Ras, which possesses two cysteins in the HVR and undergoes double palmitoylation, N-Ras has only one (**Rocks et al. 2010**). This makes it less hydrophobic compared to H-Ras, and at the steady state, in addition to plasma membrane, it is found in the interior of the cell, where, in the cytosol, it can bind to PDEδ. Additionally, since it loses the only palmitoyl moiety due to APT activity in the cytoplasm, it is always free to bind to PDEδ, and be released in the perinuclear area of the cell. Here, PATs can repalmitoylate and it can be recycled to the plasma membrane. This results in higher Golgi localization of N-Ras compared to H-Ras. As H-Ras is more hydrophobic, the spontaneous dissociation from the plasma membrane is slower compared to N-Ras, therefore, at the steady state, it is mostly found at the plasma

membrane with a very small fraction at the Golgi apparatus (**Vartak et al. 2014**).

1.4.2.3. Rheb spatial cycle

Farnesylation, together with additional membrane targeting motifs associates Ras proteins to membranes (**Welman, Burger, and Hagmann 2000**). As mentioned previously, K-, H- and N-Ras possess additional targeting features that enable association with the plasma membrane. Rheb, however, lacks any of these additional targeting features in the HVR, and is solely farnesylated (**Hancock, Paterson, and Marshall 1990**). Therefore, Rheb associates with the abundant surface of the endomembranes, rather than the plasma membrane exclusively. This was proven by changing Rheb HVR with H-Ras HVR, resulting in plasma membrane localization of Rheb (**Takahashi et al. 2005**).

Besides associating with the endomembranes, Rheb distinctly concentrates in the perinuclear region of the cell. Co-localization with Rab 7 and LAMP2 placed it at the late endosomal/lysosomal structures (**Sancak et al. 2008**). However, the correct mechanism of maintaining the localization of this protein is still unknown. It was shown that Rheb interacts with PDEδ and due to high spontaneous dissociation rate from the membranes, upon ectopic expression of PDEδ displays homogenous fluorescence intensity pattern in the cell. Additionally, it was corroborated that the Arl2-GTP-mediated release mechanism of farnesylated cargo from PDEδ was corroborated to occur in the perinuclear region of the cell (**Schmick et al. 2014**). Based on these observations, Rheb served as a candidate for PDEδ/Arl2-GTP system for maintainance of localization of prenylated Ras proteins. Due to its structure and the lack of secondary membrane-targeting feature, it dissociates faster (compared to K-, N- and H-Ras) from membranes to the cytosol. Here it is solubilized by PDEδ, and once the complex reaches perinuclear area, Arl2-GTP activity displaces it from PDEδ onto these membranes (**Schmick, Kraemer, and Bastiaens 2015**) (**Figure 7, right**).

In this thesis, we demonstrate that the PDEδ/Arl2-GTP driven spatial cycle is coupled to a GTPase cycle of Rheb. In this cycle, Rheb-GTP associates with

PDEδ in the cytosol, and through localized Arl2-GTP activity is displaced and concentrated onto perinuclear membranes. This drives its interaction with mTOR and its subsequent activation. In the absence of growth factors, perinuclear TSC2 activity promotes rapid GTP-hydrolysis on Rheb. This loosens Rheb-mTOR, interaction, resulting in enhanced dissociation of Rheb-GDP from perinuclear membranes and its resolubilization by PDEδ. Excess of GTP in the cytoplasm of cells **(Ahearn et al. 2012)**, together with the higher GTP-binding affinity of Rheb **(Patel et al. 2003; Im et al. 2002; Tabancay et al. 2003)** and the lack of GAP activity in the cytosol **(Demetriades, Doumpas, and Teleman 2014; Demetriades, Plescher, and Teleman 2016; Menon et al. 2014)**, causes efficient GDP/GTP exchange on soluble Rheb, switching it back into an active state. Growth factor stimuli (e.g. insulin) inactivate the GAP TSC2; effectively stopping the PDEδ/Arl2-GTP mediated spatial cycle by tight association of Rheb-GTP with mTORC1, which is not anymore available for (re) solubilization by PDEδ. The PDEδ/Arl2-GTP spatial cycle thus enhances responsiveness to growth factors by providing an energy-driven mechanism for the enrichment of Rheb-GTP on perinuclear membranes that thermodynamically favors its interaction with mTORC1.

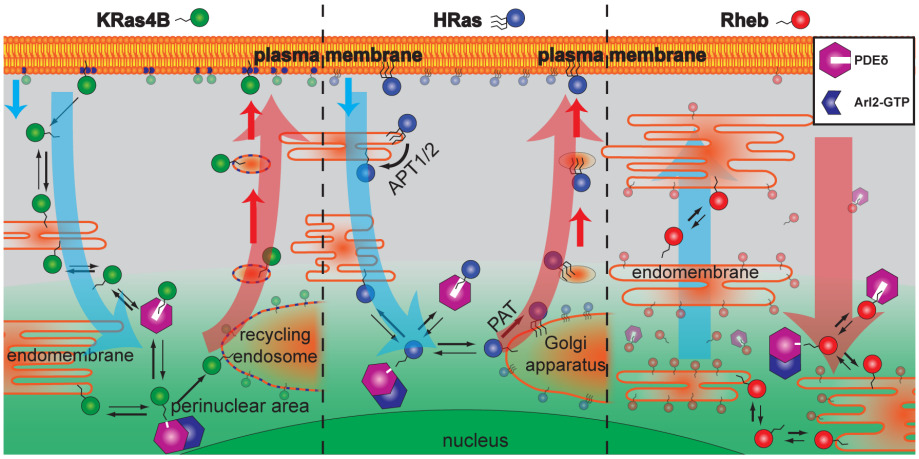

Figure 7. Spatial cycles of prenylated Ras proteins (adapted from Schmick *et al.*, 2015)

Due to spontaneous dissociation and processes such as endocytosis prenylated Ras proteins are displaced from the plasma membrane to the interior of the cell. Due to the farnesyl moiety in the HVR, they have a tendency to equilibrate to the abundant surface of the endomembranes. Upon dissociation from the membranes, KRas4B (green) is solubilized by binding to PDEδ. Once the complex reaches perinuclear area of the cell, Arl2-GTP binds to PDEδ, causing a conformational change resulting in displacement of KRas4B on perinuclear membranes. Here, negatively charged recycling endosome (RE) serves as an electrostatic trap for released KRas4B, which upon association with RE is transported to the plasma membrane of the cell. Upon dissociation from the plasma membrane, palmitoyl

moiety is cleaved from HRas (blue) via activity of acyl protein thyoesterases (APT1/2). This enables HRas to bind to PDEδ and once th complex reaches perinuclear area to be displaced by Arl2-GTP activity. Here, it associates with Golgi apparatus, where palmitoyltransferases re-palmitoylate HRas, which is then via vesicular transport recycled to the plasma membrane. As a solely farnesylated protein, Rheb (red) has a high partitioning rate from the endomembranes to the cytosol. In the cytosol, it is solubilized by PDEδ. Once the complex reaches the perinuclear area of the cell, Rheb is displaced from PDEδ via Arl2-GTP activity, maintaining its out-of-equilibrium enrichment at the perinuclear membranes of the cell.

1.5. Objectives

The main aim of this thesis was to determine whether Rheb localization is mediated by spatial cycle involving PDEδ/Arl2 system. Additionally, how this spatial cycle regulates subcellular Rheb localization and what are the implications on the signaling output of Rheb? The final question was to resolve whether the activity of Rheb has any effect on its localization, and in the end, what are the implications on cell physiology, which could arise as a consequence of this crosstalk?

In order to answer this, we have applied the previous knowledge known of the PDEδ/Arl2 spatial cycle and resolved how this mechanism is involved in maintenance of Rheb localization in the cell. Additionally, we have experimentally resolved cellular locus of PDEδ/Arl2 interaction, which, combined with previous knowledge, resulted in understanding how this release mechanism maintains localization of all prenylated Ras proteins.

We used cells with constitutively active Rheb to examine whether GTPase and spatial cycle are coupled and what are the implications of this coupling on signal propagation and processes regulated by Rheb/mTORC1.

This thesis is divided in four parts. The first part focuses on concept of cell-environmental communication and represents an overview of current knowledge on spatial cycles, regulation of Rheb activity and characteristics of the protein family it belongs to.

The second part covers methods that were used in order to resolve the mentioned questions, and overview of Crispr-CAS method for gene editing and FRET-FLIM, both used in different experimental setups.

The third part presents results obtained during the work, and the final part discusses the results and based on them, presents the model of coupling of GTPase and spatial cycle of Rheb.

2. MATERIALS AND METHODS

2.1. Materials

2.1.1. Chemicals

Acetic acid	Baker
30 % Acrylamide/Bis solution	Bio-Rad laboratories, Inc
Ammonium persulfate (APS)	SERVAElectrophoresis GmbH
Bromophenolblue	Sigma Aldrich®
Complete Mini EDTA-free protease inhibitor tablets	Roche Applied Science
Crystal Violet	Life Science
2´-deoxyadenosine-5´-triphosphate (dATP)	Invitrogen™ Life Technologies
2´-deoxythymidine-5´-triphosphate (dTTP)	Invitrogen™ Life Technologies
2´-deoxycitosine-5´-triphosphate (dCTP)	Invitrogen™ Life Technologies
2´-deoxyguanosine-5´-triphosphate (dATP)	Invitrogen™ Life Technologies
Dimethyl sulfoxyde (DMSO)	SERVAElectrophoresis GmbH
Disodium hydrogen phosphate (Na_2HPO_4)	Merck KG
Ethanol	J.T.Baker
Ethydium Bromide (EtBr) (10mg/mL)	Fisher Scientific
Ethylene diamine tetracetic acid (EDTA)	Fluka® Analytical
Ethylene glycol tetraacetic acid (EGTA)	Life Science
Glycerol	Gerbu Biotechnik GmbH
Glycine	Carl Roth GmbH
Roti®-Histofix 4%	Carl Roth GmbH
Hoechst 33258	Sigma

IGEPAL® CA-630	Sigma Aldrich®
Kanamycin sulfate	Gerbu Biotechnik GmbH
Magnesium chloride ($MgCl_2$)	Merck KG
Methanol	AppliChem GmbH
2-Mercaptoethanol	SERVAElectrophoresis GmbH
Monopotassium phosphate (KH_2PO_4)	J.T.Baker
Paraformaldehyde	Fluka
Phosphatase Inhibitor Cocktail 2	Sigma Aldrich®
Phosphatase Inhibitor Cocktail 3	Sigma Aldrich®
Potassium chloride (KCL)	J.T. Baker
Sodium chloride (NaCl)	SERVAElectrophoresis GmbH
Sodium deoxycholate (NaDOC)	Sigma Aldrich®
Sodium dodecyl sulfate	Carl Roth GmbH
Sodium pyrophosphate ($Na_4O_7P_2$)	J.T. Baker
N,N,N',N'-Tetramethylene-diamine (TEMED)	Sigma Aldrich®
Tris-Base	Carl Roth GmbH
Tris-HCl	J.T. Baker
Triton X-1000	SERVAElectrophoresis GmbH
Tween 20	SERVAElectrophoresis GmbH
Ultra-Pure™ Agarose	Invitrogen™ Life Technologies
Xylen cyanole	Sigma

2.1.2. Enzymes and proteins

AccuPrime™ *Pfx* DNA polymerase	Invitrogen™ Life Technologies
Age-I-HF (10 000 U/mL)	New England Biolabs Inc.
*Bam*HI (20 000 U/mL)	New England Biolabs Inc.
Bovine Serum Albumine (BSA)	New England Biolabs Inc.
*Bsr*GI (20 000 U/mL)	New England Biolabs Inc.
Calf Intestinal Phosphatase (10 000 U/mL)	New England Biolabs Inc.
*Dpn*I	New England Biolabs Inc.
*Eco*RI-HF	New England Biolabs Inc.
FastDigest *Bbs*I (BpiI) #FD1014	Fermentas/Thermo Scientific
Insulin solution human (I9278)	Sigma Aldrich®
PfuUltra High-fidelity DNA polymerase AD	Stratagene
PlasmidSafe ATP-dependent DNase #E3101K	Epicentre
T4 DNA-ligase #15224-017	Invitrogen™ Life Technologies
T4 polynucleotide kinase #M0201S	New England BioLabs
T7 DNA ligase #L602L	Enzymatics

2.1.3. Plasmids

mCherry-N1	Clontech Laboratories Inc.
mCitrine-N1	Clontech Laboratories Inc.
mTFP-N1	Clontech Laboratories Inc.
mCherry-Arl2 wt	generated by inserting cDNA encoding for human Arl2 to mCherry-N1 vector.
mCherry-Arl2 Q70L	generated by inserting cDNA encoding for human Arl2 to mCherry-N1 vector, then mutating glutamine (Q) at position 70 to leucine (L) to generate constitutively active mutant.
mCherry-PDEδ	generated by inserting cDNA encoding for human PDE6δ to mCherry-N1 vector.

mCherry-Rheb	generated by inserting cDNA encoding for human Rheb1 to mCherry-N1 vector.
mCitrine-Rheb	generated by inserting cDNA encoding for human Rheb1 to mCitrine-N1 vector.
mCitrine-Rheb HVR	generated by inserting cDNA encoding for hypervariable region (HVR) with CAAX-box of human Rheb1 to mCitrine-N1 vector.
mTFP-Arl2 wt	generated by inserting cDNA encoding for human Arl2 to mTFP-N1 vector.
mTFP-Arl2 Q70L	generated by inserting cDNA encoding for human Arl2 to mTFP-N1 vector, then mutating glutamine (Q) at position 70 to leucine (L) to generate constitutively active mutant.
Psp-Cas9-E (BB)-2A-puro #48139	Addgene

2.1.4. Oligonucleotides

1)
3’**ctcagatctcgagcc**aggataattttggaggcagaaaaaatggacggggcagcttcacaaggcaag tcttcatgctcggtgatgtga**gaattctgcagtcga** 5’ (Rheb-HVR with overhang in bold)
2) 3’ctcagatctcgagccaggataat 5’ (FW primer for mCitrine-RhebHVR)
3) 5’ gactgcagaattctcacatcacc 3’ (REV primer for mCitrine-RhebHVR)
4) 3’-CACCATCCCTGGCCCGCTCGTCCT-5’ (FW primer for sgRNA PDEδ)
5) 5’-AAACAGGACGAGCGGGCCAGGGAT-3’ (REV primer for sgRNA PDEδ)
6) 3’-catggtcctgctggagttcgtg-5’ (sequencing FW primer for pECFP-C1 vector (Clontech Laboratories Inc.))

7) 5’-gtttattgcagcttataatggttac-3’ (sequencing REV primer for pECFP-C1 vector (Clontech Laboratories Inc.))

8) 3’- cgggactttccaaaatgtcg-5’ (sequencing FW primer for pECFP-N1 vector (Clontech Laboratories Inc.))

9) 5’- gccacaagttcagcgtgtcc-5’ (sequencing REV primer for pECFP-N1 vector (Clontech Laboratories Inc.))

2.1.5. Antibodies

Table 1. List of primary antibodies

Antibody	Number of product	Manufacturer	Dilutions
Phospho-4E-BP1 (Thr37/46) Antibody	#9459	Cell Signaling Technology	1:500 (Western blot)
4E-BP1 Antibody	#9452	Cell Signaling Technology	1:500 (Western blot)
Phospho-S6 Ribosomal Protein (Ser235/236) (2F9)	#4856	Cell Signaling Technology	1:1000 (Western blot)
S6 Ribosomal Protein (54D2)	#2317	Cell Signaling Technology	1:500 (Western blot)
Rheb (E1G1R)	#13879	Cell Signaling Technology	1:500 (Western blot); 1:100 for IF
Tuberin (TSC2)	#4308	Cell Signaling Technology	1:200 for IF
TOR	#2983	Cell Signaling Technology	1:100 for IF
Rabbit monoclonal (IgG) (EPR14436) to Arl2	Ab183510	Abcam	1:3000 (Western blot) 1:2000 (PLA)

Mouse monoclonal (IgG1) (H4A3) to LAMP1	Ab25630	Abcam	1:50 for IF
PDE6D monoclonal antibody (M06), clone 5C7	H00005147-M06	Novus Biologicals	1:1000 (PLA)
Rheb monoclonal antibody (M01), clone 2C11	H00006009-M01	Novus Biologicals	1:100 for IF
PDE6D (N-15)	Sc-50260	Santa Cruz Biotechnology	1:300 (Western blot)
mTOR antibody (215Q18)	AHO1232	Thermo Scientific	1:100 for IF
Arl3	10961-1-AP	ProteinTech	1:100 for IF; 1:300 for WB
Monoclonal anti-α tubulin	T9026	Sigma Aldrich®	1:3000 (Western blot)

Table 2. List of secondary antibodies

Antibody	**Number of product**	**Manufacturer**	**Dilutions**
IRDYE® 680RD Donkey anti-rabbit	C50821-05	LiCor® Biosciences	1:5000
IRDYE® 800CW Donkey anti-mouse	C50924-02	LiCor® Biosciences	1:5000
IRDYE® 800CW Donkey anti-goat	C50917-05	LiCor® Biosciences	1:5000
Alexa 488 donkey anti mouse	A-21202	Life Technologies	1:500
Alexa 647 donkey anti rabbit	A-31573	Life Technologies	1:500

2.1.6. Buffers and solutions

10% APS	100 mg APS in 1 mL ddH20
10x DNA sample buffer	5 mL 100% glycerol, 1 mL Bromphenolblue, 1.6 mL 2.5% Xylene cyanole, 2 mL EDTA (0.5M, pH=7.4), 0.4 mL H_2O
LB agar plates	add 15 g agar per liter LB medium, pour plates when the autoclaved medium has approximately 55°C, add antibiotic of choice at desired concentration
10x PBS (pH=7.4)	80g NaCl, 2.0g KCl, 14.4g Na_2HPO_4, 2.4g KH_2PO_4 (for 1L)
1xPBS (pH=7.4)	100 mL 10xPBS, 900 mL ddH_2O (for 1L)
1xPBS (0.01% Tween-20)	100 mL 10x PBS, 1 mL Tween-20, 899 mL dd H_2O (for 1L)
1xPBS (0.01% Triton-1000)	100 mL 10x PBS, 1 mL Triton-1000, 899 mL dd H_2O (for 1L)
4% PFA	4g paraformaldehyde, 100 mL 1xPBS (pH=7.4) (for 100mL)
RIPA buffer	1% NaDOC, 150 mM NaCl, 1 mM Na_2EDTA, 20 mM Tris-Cl (pH=7.5), 1 mM EGTA, 2.5 mM $Na_4O_7P_2$, 0.1% SDS, 0.1% IGEPAL, 100 µL Phosphatase inhibitor cocktail #2, 100 µL Phosphatase inhibitor cocktail #3, 1 tablet complete mini EDTA-free, adjust volume to 10 mL with ddH_20
5x sample buffer	0.6mL 1M Tris-HCl (pH=6.8), 5mL 50% glycerol, 2 mL 10% SDS, 0.5 mL 2- glycerol, 2 mL 10% SDS, 0.5 mL 2-mercaptoethanol, 1 mL 1%

	bromophenol blue, adjust volume to 10 mL with ddH20
10% SDS	10g SDS in 100 mL ddH_20
10x SDS running buffer	30g Tris-Base, 144 g Glycine, 10g SDS (for 1L)
1x SDS running buffer	100 mL 10x running buffer, 900 mL ddH_2O (for 1L)
Separating gel buffer	1.5 M Tris (pH=8.8) (18.17 g Tris-HCl in 100 mL)
SOC medium	20 g/l Bacto-Trypton, 5 g/L bacto-yeast extract, 0.5 g/l NaCl, 2.5 mM KCl, 10 mM $MgCl_2$ (SOB medium). Autoclave and before use add 20 mM glucose.
Stacking gel buffer	0.5 mM Tris (6.05 g Tris-HCL in 100 mL ddH_20)
1xTAE buffer	40mM Tris/Acetate, (pH=7.5) , 20mM NaOAc, 1mM EDTA
1x transfer buffer	100 mL 10x transfer buffer, 200 mL methanol, 700 mL ddH_2O (for 1L)
10x TBS (pH=7.6)	60.6 g Tris, 87.6g NaCl (for 1L)
1x TBST (0.01% Tween-20)	100 mL 10x TBS, 1 mL Tween-20, 989 mL dd H_2O (for 1L)

2.1.7. Commercial solutions and kits

Adenosine 5'- triphosphate, 10 mM #P0756S	New England BioLabs
BigDye® Terminator v3.1 cycle sequencing kit	Applied Biosystems
100xBSA	New England Biolabs Inc.
Deltarasin	Chemietek
100 mM dNTP kit	Invitrogen™ Life Technologies
1,4-Dithiothreitol (DTT)	Gerbu Biotechnik GmbH
2-log DNA ladder	New England Biolabs Inc.
DUOLINK in situ detection reagents (far red) (DUO92013-100RXN)	Sigma Aldrich®
DUOLINK in situ PLA probe anti-rabbit minus (DUO92005-100 RXN)	Sigma Aldrich®

DUOLINK in situ PLA probe anti-mouse plus (DUO92001-100 RXN)	Sigma Alrdich®
Fermentas Tango buffer #BY5	Fermentas/Thermo Scientific
50mM Magnesium Sulfate	Invitrogen™ Life Technologies
Micro BCA™ Protein Assay Kit (#23235)	Thermo Scientific
NucleoBond® Xtra Midi Plus EF	Macherey-Nagel
NucleoSEQ Columns (1604/002)	Macherey-Nagel
Odyssey Infrared Imaging System blocking buffer	LiCor® Biosciences
10x *Pfu* amplification buffer	Invitrogen™ Life Technologies
Precision Plus Protein™ standards	Bio-Rad Laboratories
QIAquick®Gel Extraction Kit	Qiagen
RedSafe nucleic acid staining solution #21141	iNtRON
10x Restriction Enzyme Buffer 1	New England Biolabs Inc
10x Restriction Enzyme Buffer 2	New England Biolabs Inc
10x Restriction Enzyme Buffer 3	New England Biolabs Inc
10x Restriction Enzyme Buffer 4	New England Biolabs Inc
Rheb activation assay kit (#81201)	New East Biosciences
Roti®-Prep Plasmid MINI (HP29.2)	Carl Roth GmbH
Stbl3 chemically competent *E. coli* #C737-03	Life Technologies
5x T4DNA ligation buffer #46300-018	Invitrogen™ Life Technologies
10x T4 DNA ligase reaction buffer #B0202S	New England BioLabs
XL10 Gold bacterial strain	Stratagene (regrown in house)
Zymoclean™ Gel DNA Recovery Kit (D4001)	Zymo Research

2.1.8. Cell lines and solutions for cell culture work

2.1.8.1. Cell lines

Table3. Cell lines used for experimental procedures

Cell line	Origin	Supplier	Reference
HeLa	Human cervical adenocarcinoma	ATCC	

TSC2+/+ p53-/- MEF	Mouse embryonic fibroblast	Kind gift of Prof. Dr. Aurelio Teleman (with permission of Dr. David Kwiatkowski)	Loss of Tsc1/Tsc2 activates mTOR and disrupts PI3K-Akt signaling through downregulation of PDGFR, JCI (2003)
TSC2+/+ p53-/- MEF psp-Cas9-E (BB)-2A-puro	Mouse embryonic fibroblast	Made in house by the use of Crispr-Cas system	
TSC2+/+ p53-/- MEF psp-Cas9-E (BB)-2A-puro-sgRNA PDEδ	Mouse embryonic fibroblast	Made in house by the use of Crispr-Cas system	
TSC2-/- p53-/- MEF	Mouse embryonic fibroblast	Kind gift of Prof. Dr. Aurelio Teleman (with permission of Prof. Dr. David Kwiatkowski)	
TSC2-/- p53-/- MEF sp-Cas9-E (BB)-2A-puro	Mouse embryonic fibroblast	Made in house by the use of Crispr-Cas system	
TSC2-/- p53-/- MEF psp-Cas9-E (BB)-2A-puro-sgRNA PDEδ	Mouse embryonic fibroblast	Made in house by the use of Crispr-Cas system	

2.1.8.2. Solutions for cell culture work

DPBS	PAN™ Biotech GmbH
Dulbecco´s Modified Eagle´s Medium (DMEM)	PAN™ Biotech GmbH
Effectene® transfection reagent	QIAGEN
Fetal calf serum (FCS)	PAN™ Biotech GmbH
Fugene® 6 transfection reagent	Roche Applied Scence
100x L-glutamine	GIBCO®/Invitrogen
Lipofectamine™ 2000	Invitrogen™ Life Technologies

100x Non-essential amino acids (NEAA)	PAN™ Biotech GmbH
Penicillin-Streptomycin	PAN™ Biotech GmbH
Sodium pyruvate (Na-pyruvate)	PAN™ Biotech GmbH
Trypsin/EDTA	PAN™ Biotech GmbH
100x vitamin solution	PAN™ Biotech GmbH

2.1.9. Materials and equipment

2.1.9.1. Centrifuges and rotors

Centrifuge 5415R	Eppendorf
Centrifuge 5417R	Eppendorf
Centrifuge 5810R	Eppendorf
Centrifuge RC 26 Plus	Sorvall®
Rotor SH-3000	Sorvall®
Rotor FA-45-24-11	Eppendorf
Rotor FL-064-04053	Eppendorf
Vacuum centrifuge	Eppendorf

2.1.9.2. DNA work

Gel Imaging Station	Bio-Rad Laboratories
Gene Pulser™	Bio-Rad Laboratories
Incubator Shaker Series I26	New Brunswick Scientific
Nanodrop® ND-1000 specrophotometer	Peqlab Biotechnologie GmbH
Mastercycler® pro	Eppendorf
Power Pac™ 1000	Bio-Rad Laboratories
PMR-30 shaker	Grant-bio

2.1.9.3. Protein work

1 mm cassetes for western blot	Invitrogen™ Life Technologies
1.5mm cassetes for western blot	Invitrogen™ Life Technologies
1 mm 10-well combs	Invitrogen™ Life Technologies
1.5 mm 10-well combs	Invitrogen™ Life Technologies
Incubation box	LiCor® Biosciences
96-well microplates (#655101)	Greiner Bio-one

Odyssey® CLx Imaging System	LiCor® Biosciences
PVDF membrane	Bio-Rad Laboratories
Sonicator needle (MS 73)	Bandelin Electronic GmbH
Ultraschall HD 2200	Bandelin Electronic GmbH
Test tube rotator	NeoLab
Multiskan Ascent 96/384 plate reader	Thermo Scientific

2.1.9.4. Cell culture work

Cell scraper	Falcon/Sarstedt
Easy Grip™ tissue culture dish	BD Falcon™
10 cm dish	Sarstedt
Tissue culture plate (6-well)	Sarstedt
E-Plate 16	ACEA Biosciences, Inc.
4-well LabTek® chambers No.1	Nunc®
8-well LabTek® chambers No.1	Nunc®
Imaging Chamber CG (8-well)	Miltenyl Biotec GmbH
Rapid Flow™ sterile disposable filter unit (75 mm)	Thermo Scientific
Glass Pasteur pipettes (150mm and 230 mm)	Brand GmbH & Co. KG
CoolCell® LX freezing container	BioCision
CryoPure Tube	Sarstedt
NUAIRE™ Cellgard class II biological safety cabinet	Integra Biosciences
Vacusafe comfort	Integra Biosciences
Laboratory CO_2 Incubator	NuAire
Vi-Cell™ XR cell viability analyzer	Beckman Coulter, Inc.
xCELLigence RTCA DP	ACEA Biosciences Inc.
Heracell CO_2 incubator	Thermo Fisher
Typhoon TRIO+ variable mode imager	Amersham Biosciences

2.1.9.5. Materials and equipment for general use

Magnetic stirrer “IKMAG®RCT”	IKA® Labortechnik
Pipettes	Eppendorf

Pipette tips	Eppendorf/Sarstedt
Safe lock tubes 0.5, 1.5 and 2 mL	Eppendorf
Falcon tubes (15 and 50 mL)	BD Falcon™
Heating block (QBD2)	Grant
Parafilm®	Pechiney Plastic Packaging
Nitrile examination gloves	Blossom®
Latex gloves	Kimtech
Pipetboy	INTEGRA Biosciences
Serological pipettes (5, 10 and 25 mL)	Sarstedt
Scale “Precisa 62 A”	Precisa Instruments AG
Scale “Precisa 620 C”	Precisa Instruments AG
Surgical disposable scalpel (No.11)	Braun Meslungen AG
“Vortex Genie 1” touch mixer	Scientific Industries
ThermoShaker (TS1)	Biometra

2.1.9.6. Microscopes

Leica TCS SP5	Leica Microsystems
AE31 trinocularAE30 Inverted Microscope	Motic
Olympus IX81	Olympus

2.1.9.7. Software

Adobe Illustrator® CS4 14.0.0.	Adobe Systems Inc.
ImageJ 1.47k	Research Services Branch
Lasergene 14.0.0.	DNA STAR
Microsoft Office 2011	Microsoft
Olympus Fluoview 4.1	Olympus Live Science
SymPhoTime 64	PicoQuant
Olympus Cell^R/scan^R system	Olympus Live Science
LAS AF 2.7.3.9723	Leica Microsystems
Image studio 5.2.	LiCor® Biosciences
Python 2.3.7.	Python™
Anaconda Python Distribution	Continuum analytics

EndNote X7	Thompson Reuters
Oracle VM VirtualBox 5.0.20	Oracle Corporation
OriginPro 9.0G 32Bit	OriginLab Corporation
Multiskan Ascent 2.6.	Ascent Software
Vi-Cell XR 2.04	Beckman Coulter
Quantity One® 1D Analysis Software	Bio-Rad Laboratories
RTCA software 1.2.1	rtca-software. software.informer.com/1.2
Typhoon Scanner Control v5.0	Amersham Biosciences

2.2. Methods

2.2.1. Cloning

2.2.1.1. Transformation of chemically competent *E. coli*

The tubes with 100 µL of frozen (-80 °C) *Escherichia coli* XL Gold stock were left on ice to thaw. Once thawed, 3.25 µL of 2.25 mM DTT was added. To each 25 µL aliquot, approximately 50 ng (1 µL) of plasmid DNA or ligation mix was added, and left on ice for 30 minutes. The tubes with transformation mix were heat-shocked for 30-60 seconds on 42°C and returned to ice for 5 minutes. To each tube 100 µL of SOC medium was added, and the mix was left on 37°C, 225 rpm for 60 minutes. 15-20 µL of the final mix was then added to LB agar plates containing appropriate antibiotic (kanamycin or ampicillin) and left overnight to grow on 37°C.

2.2.1.2. Preparation of bacterial culture

After 24 h of incubation at 37°C, LB agar plates with *E.coli* colonies were used for colony picking and preparation of bacterial culture to obtain plasmid DNA. Few colonies from the plate were picked with a sterile pipette tip, and placed into their respective falcon tubes containing 5 mL (for mini-prep) or Erlenmeyer flask with 50 mL LB medium (for midi-prep) supplemented with appropriate antibiotic. The bacterial cultures were incubated overnight (16-24 h) on 37°C, 200 rpm.

2.1.1.3. Preparation using Roti®-Prep Plasmid MINI kit

The QIAprep® Spin Miniprep Kit is used routinely to isolate up to 20 µg of high-purity plasmid for further use in molecular biology (PCR, cloning, restriction). The kit is based on alkaline analysis of bacterial cells and absorption of the plasmid DNA onto a silica membrane in the presence of high-salt buffers. DNA can be eluted from the membrane with ddH_2O or low-salt buffer. 4 mL of bacterial cell suspension (preparation described in **2.2.1.2.**) was centrifuged in 2 series (2x2mL) at 10 000rpm for 2 minutes, and then further steps were done as described in the manufacturer's protocol (Roti®-Prep Plasmid MINI). The DNA was eluted with 30 µL of Elution buffer provided in the kit.

2.2.1.4. Endotoxin-free Plasmid DNA Preparation Using NucleoBond® Xtra Midi EF Kit

Gram- negative bacteria (such as *E.coli*), unlike Gram-positive bacteria have a second membrane enclosing the inner membrane and a cell wall. The outer layer of this membrane consists of amphiphilic lipopolysaccharides (LPS), or endotoxins. They are released from cells in small amounts during cell growth, and in higher amounts upon cell death and lysis, hence, during plasmid purification. For this reason, they have to be removed during plasmid preparation to assure high transfection rates and viability of transfected cells. With NucleoBond® Xtra Midi EF Kit the endotoxin level is reduced to <0.05 EU/µg plasmid DNA for up to 1000 µg high-copy plasmid DNA. Endotoxin-free plasmid DNA was prepared following NucleoBond® Xtra Midi EF Kit user manual. 50 mL of bacterial culture (described in **2.2.1.2.**) was centrifuged for 20 min at 4500g, 4°C. Endotoxin-free plasmid DNA was eluted by using NucleoBond® finalizers with 300 µL of TE- EF buffer.

2.2.1.5. Agarose Gel Electrophoresis of DNA

Agarose gel electrophoresis is a method of gel electrophoresis used to separate DNA or proteins in an agarose matrix. An electric current to move the charged molecules through the agarose matrix separates biomolecules.

As DNA is negatively charged, it travels towards the positively charged anode. Polymerized agarose forms pores that depend on the concentration used, therefore the smallest fragments migrate faster and are closer to anode at the end of the when the current is stopped.

Agarose gels were prepared with 1x TAE buffer supplemented with RedSafe nucleic acid staining solution (5 µL/100 mL). RedSafe emits green fluorescence when bound to DNA (excitation peaks: 309 nm, 419 nm, emission peak: 537 nm). After the gel is polymerized, it is transferred to electrophoretic chamber filled with 1x TAE buffer. Electrophoresis is preformed at constant voltage of 100 V for 30 min. DNA samples were prepared by mixing the DNA samples with 5x DNA loading buffer (final volume depends on the comb size used for the gel). DNA marker was used to determine the size of the DNA fragments in the gel.

Table 4. Agarose concentration used for separation of different sized DNA fragments

Agarose concentration (%)	Size of DNA fragments
2.5	<100 bp
2	0.1 -1 kb
1.8	0.2 – 2kb
1.5	0.3 – 3 kb
1.2	0.5 – 5 kb
1	0.7 – 5 kb
0.8	0.8 – 12 kb
0.5	1 – 30 kb

2.2.1.6. Isolation of DNA fragments from agarose gels

The QIAquick® Gel Extraction Kit is used for gel extraction or cleanup of up to 10 µg of DNA (70 bp to 10 kb). It contains a silica membrane assembly for DNA binding in high-salt buffer and elution with low-salt buffer or water. With this procedure various impurities from DNA samples are removed (primers, enzymes, salts, agarose…) and DNA samples are eluted in the final step. After visualizing agarose gels for DNA fragments, the ones of interest are cut, put in eppendorf tube and weighed. The appropriate amount of buffer is added to the slices, which are subsequently left for dissolving at 50°C for 10 minutes. The purification is made according to the QIAquick® Gel Extraction Kit protocol.

2.2.1.7. Restriction digestion

Restriction digestion or DNA fragmentation is a procedure in molecular biology used for DNA preparation for further processing or analysis. With the help of restriction endonucleases, enzymes that bind and cleave DNA molecules, DNA is cleaved at the restriction site. This is a specific sequence of nucleotides (4 to 8 base pairs in length), which are recognized by restriction enzymes. Restriction digestion is most commonly used for molecular cloning of DNA fragment into a vector. Today, most of the artificial plasmids possess a segment called ´multiple cloning site' that contains various restriction sites, allowing insertion of almost any DNA into plasmid vectors.

For digestion of 1µg of DNA in a 30 µL reaction mix, 3 µL of appropriate 10x reaction buffer (depends on the enzymes used) 1 µL of 10 U restriction enzyme, 3µL of 10 x BSA and ddH_2O up to final volume was used. The reaction mix was then incubated at a temperature and time recommended by manufacturer (usually 37°C for 1h).

2.2.1.8. Dephosphorylation

Digested DNA possesses a 5´group that is necessary for proper ligation. However, the chance that the vector will relegate itself back, instead of

implementing DNA fragment of interest are very high, especially when a single restriction is preformed. To avoid the high fraction of empty vectors, it is necessary to dephosphorylate the 5´end. For this, 0.5 U/µg DNA of alkaline dephosphatase (calf intestinal phosphatase- CIP) is added to the reaction mix and the tubes were incubated for 30 minutes at 37°C. Agarose electrophoresis is preformed to visualize the results, and the fragments of interest are cut from the gel and purified by using Zymoclean™ Gel DNA Recovery Kit.

2.2.1.9. Ligation

Ligation is a procedure of creating recombinant DNA, by joining two DNA fragments from a different source together to a new DNA molecule. Ligation involves making a phosphodiester bond between the 3´hydroxyl of one nucleotide with 5´of another. This reaction requires two or more fragments of DNA that have blunt or compatible ´sticky' ends, a buffer that contains ATP and T4 DNA ligase that connects DNA fragments with overhanging ´sticky' or blunt ends. The ligation conditions require 50 ng of vector DNA and three-fold molar excess of insert DNA. The amount of insert is calculated according to the formula:

Equation 1.

$$insert\ (ng) = \frac{vector\ (ng) x\ insert\ size\ \ (bp)}{vector\ size\ (bp)}$$

The final ligation mix contains calculated amount of insert DNA, 5x T4 DNA ligase buffer, 1 U T4 ligase buffer and the final volume (20 µL) was adjusted with ddH_2O. The mix was incubated overnight at 16°C before transformation to chemically competent *E.coli* XL10 Gold.

2.2.2.10. Polymerase chain reaction (PCR)

Polymerase chain reaction (PCR) is a method used for amplification of DNA, usually between 0.1 and 10 kbp, generating up to millions of copies of DNA of interest. Today it has a wide application range, starting from molecular cloning

and sequencing, to diagnostic, genetic identification or functional analysis. The major factor in the reaction is DNA polymerase, an enzyme that is capable of producing complementary DNA strand from the template and as the PCR progresses, sets in mode a chain reaction, where this template is exponentially amplified. A typical PCR reaction needs to contain: DNA template- DNA of interest that is used for amplification, DNA polymerase, primers- short DNA sequences that are complementary to 3´ end of each DNA template strand (both sense and anti-sense), deoxynucleoside triphosphates (dNTPs)- all four nucleotides (A, T, G, CTP) used as building blocks for a new DNA strand and a buffer supplemented with ions (e.g. Mg^{2+}) to ensure optimal environment for the activity of the polymerase. PCR consists of four steps: denaturation, when double-stranded DNA helix is separated at a high temperature (> 90°C), annealing of primers to the separated DNA strand and extension of each strand through the activity of DNA polymerase at a lower temperature (50-70°C) and exponential amplification of the new DNA. The annealing temperature varies in different PCR reactions, as it depends on the T_m and the GC (usually 40-60%) percentage of the primer pair, which are specific for each DNA template. The final product is obtained after 25-30 cycles of the four steps, and can be visualized on an agarose gel.

2.2.2.11. Making mCitrine-Rheb HVR construct

mCitrine-C1 vector was generated by insertion of AgeI/BsrGI PCR fragments of mCitrine (gift from R.Tsien) cDNA into pEGFP-C1 vector. mCitrine-Rheb HVR was generated by creating oligonucleotide corresponding to the last C-terminal 20 amino acids +CAAX-box (72 nucleotides) of full-length Rheb with an overhang of 15 nucleotides upstream and downstream of it corresponding to XhoI and EcoRI cutting sites in pECFP-C1 vector (look at **2.1.4.** for sequences of the construct and primers). The PCR reaction consisted of initial denaturation at 95°C for 2 minutes, 25 cycles of denaturation (95°C for 15 s), annealing (51°C for 30 s) and extension (68°C for 30 s). The mCitrine-C1 vector was digested with XhoI and EcoRI, and ligated with Rheb-HVR amplified oligonucleotide using T4 ligase. After transformation of chemically

competent XL-10 bacteria with the ligation mix, positive clones were selected by seeding the bacterial culture on agar plate supplemented with 100 µg/mL Kanamycin. All constructs were verified by sequencing.

2.2.1.12. Sequencing

DNA sequencing was preformed following Sanger method (**Sanger and Coulson 1975**) or dideoxy chain terminating method (**Sanger, Nicklen, and Coulson 1977**). The method is based on incorporating dideoxynucleotides (ddNTPs) through action of DNA polymerase during i*n vitro* DNA replication. The ddNTPs lack a 3´-OH group, causing polymerase to stop the reaction when a certain ddNTP is incorporated, as it cannot form a phosphodiester bond. The method here described is based on dye-terminator sequencing, where each of the four ddNTPs is labeled with fluorescent dye, each of which emits light at a different wavelength. The nucleotides are detected by capillary gel electrophoresis. The in-house based Zentrale Einrichtung Biotechnologie provided the sequencing service.

The typical sequencing reaction was preformed by using the BigDye® Terminator v3.1 Cycle Sequencing Kit. In a 20 µL reaction, up to 300 ng DNA, 4µL BigDye® Terminator mix, 2 µL BigDye® Terminator 10x buffer, 0.5µL 10 mM primer of FW primer in one mix (**2.1.4.** section, number 6) or 8)) and the same volume of REV in another one (**2.1.4.** section, number 7) or 9)) and ddH_20 for reaching final volume were used. The PCR reaction consisted of initial denaturation at 96°C for 1 min, 25 cycles of denaturation (96°C for 10 s), annealing (50°C for 5 s) and extension (60°C for 4 min).

Sequencing mix was cleaned up from excess of ddNTPs by using NucleoSEq columns according to manufacturer's manual. Cleaned product was transferred to 0.5 ml Eppendorf tube, dried in a vacuum centrifuge and sent for analysis.

2.2.2. Biochemistry

2.2.2.1. Whole cell lysates preparation

After aspiration of medium, cells were once washed with ice-cold PBS, and

lysed with ice-cold RIPA buffer supplemented with 1 tablet Complete Mini EDTA free protease inhibitor and 100 µL of phosphatase inhibitor cocktail 2 and 3. After 10 minutes of incubation on ice, cells were scraped and the lysate was transferred to a pre-cooled 1.5 mL Eppendorf tube. Samples were then sonicated for 12 s, cycle 3, with 30% power and centrifuged at 14 000 rpm, 4°C for 15 minutes. Supernatant was transferred to a fresh pre-cooled 1.5 mL Eppendorf tube. The samples could be snap-frozen in liquid nitrogen and stored at -80°C until further use, or continued to be used for determination of protein concentration. In a last step, a proper amount of 5x loading buffer was added to each sample, which was then boiled for 5-10 minutes at 95°C, and shortly centrifuged before loading on the gel.

2.2.2.2. Determining protein concentration

Total protein concentration was determined by bicinchoninic acid (BCA) assay. The method is based on the reduction of Cu^{2+} to Cu^{+} by protein in an alkaline medium, where Cu^{+} is colorimetrically detected using a reagent containing bicinchoninic acid. The final product of the reaction is purple colored and is formed by chelation of two molecules of BCA with one cuprous ion. The diluted BSA samples (range from 100-20000 ng/µL) were used as standards, while three reagents available from the kit (A, B and C) were mixed in a 25: 24: 1 dilution to make working solution. 4 µL of standards or total cell lysate were mixed with 80 µL of the prepared working solution and left for incubation at 37°C for 30 min-1h. The samples were afterwards read in a spectrophotometer on 562 nM wavelength to determine their protein concentration.

2.2.2.3. SDS denaturing gel electrophoresis

Western blot is a technique used to detect proteins in a tissue homogenate or extract. It is based on a gel electrophoresis to separate proteins by 3D structure in a native condition or denaturated proteins by size. The SDS denaturing gel electrophoresis was preformed with 1.5 mm gels, and each sample was loaded into its respective well. The samples were run at 80 V until the samples passed stacking gel, and 130 V while at the separating gel.

Following electrophoresis, electroblotting through Invitrogen system, following manufacturer's manual, was preformed. The proteins were transferred to a polyvinyldene difluoride (PVDF) membrane, which was pre-activated with methanol for 5 minutes. After this, membrane, gel and two pieces of filter paper were left to equilibrate in a 1x transfer buffer before forming a ´sandwich´ in a following sequence: filter paper, gel, membrane, filter paper, and placing it in chamber so that the proteins are traveling towards the positively charged cathode. In this method, transfer is preformed at 35 V, for 1.5 h. After the finished transfer, the membrane was placed in a LiCor® incubation box with Odyssey Infrared Imaging System blocking buffer for 1h at RT. The antibodies were diluted in the fresh blocking buffer (for antibody list and dilutions see table 1.) and incubated on 4°C overnight. The next day, membranes were washed 3x5minutes with 1xTBST (0.1% Tween-20), which was followed by secondary antibodies incubation (diluted in blocking buffer) for 1h at RT. The membranes were again washed 3x5 minutes with 1x TBST (0.1% Tween) and the protein detection was done with Odyssey Imaging System. Western blots were quantified using ImageJ 1.47k (Java). The background of the blots was subtracted by applying the rolling ball substraction with a radius of 50 px. Afterwards the integrated intensity of the bands was measured and used for quantification.

2.2.3. Cell culture work

2.2.3.1. Subculturing of adherent cells

Cells were maintained in Dulbecco's Modified Eagle's Medium (DMEM) supplemented with 10% fetal bovine serum (FBS), 1% L-glutamine and 1% non- essential amino acids (NEAA) (v/v), grown at 37 °C in a 90% humidified incubator with 5% CO_2. DMEM without any supplements was used for starvation purposes.

Cells are harvested in exponentially growth phase where approximately 70-80% of the substrate of the culture is occupied. Cells were washed once with PBS to remove residues of the serum and incubated for 1 minute with 2 mL Trypsin/EDTA solution for detachment. Once detached, trypsin was deactivated and cells were resuspended in a 1:6 ratio in the new growth

medium and transferred to an appropriate Falcon tube. 500 µL of total cell suspension was used for determining final number and viability in Vi-CellTM XR cell viability analyzer and the desired number of cells was seeded in new cell culture dishes.

2.2.3.2. Cryopreservation and storage of cells

Sub-confluent cells from a T75 flask were splitted as described above and chosen for a storage when the total number was between 800 000 and 1 500 000 cells/mL. The cell suspension was centrifuged for 3 min on 200 rpm, and upon removal of the medium, the cells were resuspended in a growth medium containing 10% (v/v) DMSO. For cryopreservation purposes, cryoprotectants such as DMSO are essential to block the formation of intracellular ice crystals during freezing and thawing procedures. The cells in a cryo-medium were aliquoted in cryo-vials and transferred to CoolCell® LX freezing container. The boxes have control freezing rates of 1°C per minute to avoid cell damage. They were left on -80°C overnight and finally the cells were moved to -150°C freezer for long-term storage.

Thawing procedure needs to be fast to avoid damaging ice crystals which form in temperatures from -120°C up to 0°C. DMSO exhibits toxic effects on cells on 37°C, therefore thawed cells were quickly resuspended in at least 10 mL of growth medium and seeded in a T75 flask. After the cells attached, the medium was exchanged to remove any residual DMSO and the cells were cultured as described above.

2.2.3.3. DNA transfection

Transfection is a process of deliberately introducing nucleic acids in eukaryotic cells by non-viral methods. This method typically involves opening of transient pores in a cell membrane to allow the uptake of the DNA or RNA. Transfection methods can be chemically based, such as calcium phosphate precipitation, or the material can enter the cells by electroporation, cell squeezing or by production of liposomes, which fuse with the membrane and release the cargo inside the cell.

In this study, the latter approach, lipofection, was used for transfection of DNA in the cells. The transfection ragents Lipofectamine ™ 2000 and Fugene ®6

were used, and the transfection was performed according to the manufacturer's guidelines (Lipofectamine™2000: https://tools.thermofisher.com/content/sfs/manuals/Lipofectamine_2000_Reag_protocol.pdf

Fugene®6: https://www.promega.de/~/media/files/resources/protocols/technical%20manuals/101/fugene%206%20transfection%20reagent%20protocol.pdf).

Cells were plated in a 6-well or a 4 –well LabTek dish a day prior to transfection. For Fugene®6, the DNA: transfection reagent ratio was always 1:3 (1µg: 3µL) and for Lipofectamine ™2000 2:1.

Table 5. Transfection procedures for Fugene®6

Vessel	Surface area (cm^2)	Fugene®6 (µL)/well	DNA (µg)/well	Serum-free medium (µL)/well
10 cm	55	18	6	600
6 well	9,4	3	1	100
4 well LabTek	1,8	0,75	0,25	25

Table 6. Transfection procedures for Lipofectamine™2000

Vessel	Surface area	Lipofectamine™2000 (µL)/well	DNA (µg)/well	Serum-free medium (µL)/well
6 well	9,4 cm^2	5-12,5	2,5	250
4 well LabTek	1,8 cm^2	1-2,5	0,5	50

After the transfection, the cells were cultured in a humidified incubator with 5% CO_2, on 37°C, and the medium was changed after 7-8 hours to avoid cell toxicity. The cells were lysed or imaged a day post-transfection.

2.2.3.4. siRNA transfection

100 000 cells /well and 10 000 cells/well were seeded in full DMEM in a 6-well plate or 4-well Labtek dish, respectively. The following day, the cells were

transiently transfected with control siRNA, siRNA targeting Arl2 and Arl3 by using Dharmafect transfection reagent in a final concentration of 50 nM following manufacturer's guidelines. After 48 hours, cells from a 6-well plate were lysed and effect on signaling was examined via Western blot and cells from a 4-well plate were used for immunofluorescence.

2.2.3.5. Immunofluorescence

Day after transfection with mCitrine Rheb, the medium was aspirated from the wells and cells were washed once with PBS. After that, the cells were fixed for 10 minutes at RT with Histofix and, after 3x5 minutes of rinsing with PBS, permeabilized for 10 minutes with PBS+0.1% Triton X-100. After another 3x5minutes washing step with PBS, the blocking was preformed by applying Odyssey Blocking Buffer for 1h at RT. Primary antibodies were diluted in recommended ratio (see table 1.) in Odyssey Blocking Buffer and incubated overnight at 4°C. The next day, the antibody solution was aspirated and the cells were rinsed with PBS+0.1% Tween-20 3x5 minutes. Secondary antibodies were prepared in Odyssey Blocking Buffer (see table 2.), and incubated for 1h at RT. After removing the secondary antibody solution and final washing step with PBS+ 0.1% Tween-20 3x5 minutes, PBS was added to cells and the cells were stored at 4°C until imaging.

2.2.3.6. Proximity ligation assay

8000 cells/well were seeded in an 8-well Labtek. The next day, the cells were once washed with PBS and fixed with Histofix for 10 minutes, permeabilized with PBS+0.1% Triton X-100 for 10 minutes and blocked with a blocking solution (DUO92005-100RXN, Sigma-Aldrich) for 1 h at RT. Antibodies were diluted in experimentally determined, suitable ration (see table 1.) in Antibody diluent (DUO92005-100RXN), Sigma-Aldrich, and applied separately (negative control) and together in individual wells, and incubated overnight at 4°C. The next day, the assay was performed according to manufacturer's instructions: https://www.sigmaaldrich.com/content/dam/sigma-aldrich/docs/SigmaAldrich/Instructions/1/duolink-fluorescence-user-

manual.pdf. The nuclei were stained with Hoechst dye diluted 1:500 in PBS for 15 minutes. The cells were stored at 4°C in PBS until imaging.

2.2.3.7. Colony formation assay

Clonogenic assay is a cell-survival assay based on the ability of a single cell to grow into a colony. 100 of all cells per well were seeded in 6-well plate in full DMEM and incubated in a humidified incubator with 5% CO_2 at 37°C for 10 days. The medium was changed every 2 to 3 days to avoid deprivation of nutrients. At the day of experiment, cells were once washed with PBS, fixed with Histofix for 10 minutes at RT, washed 3x with PBS and incubated with 0.01% (v/v) Crystal Violet solution. After 1 hour incubation at room temperature, Crystal Violet was aspirated; the wells were washed 2-3 times with ddH_2O and left for drying. The plates were scanned with Typhoon TRIO + scanner (Amersham Biosciences) and analyzed using a script from **(Guzman et al. 2014)**.

2.2.3.8. Real-Time Cell Analysis (RTCA)

Real-time cell analysis (RTCA) is a system that enables real-time monitoring of cell proliferation, cellular morphology and attachment quality. An electrode-covered surface detects electronic impedance, which increases proportionally with the number of cells attached. Experiments were performed by using 16-well E-plate on the Dual Plate xCelligence instrument (Roche Applied Science, Indianapolis, IN). 5000 cells of TSC2 +/+, TSC2 +/+ -/-E.V. and TSC2 +/+ sg RNA PDEδ MEFs and 3500 of TSC2 -/-, TSC2 -/- E.V. and TSC2 -/- sg RNA PDEδ MEFs were plated in each well in 200 µL of full DMEM. Cells were allowed to settle for 30 min at room temperature before being inserted into the xCELLigence instrument in a humidified incubator at 37°C with 5% CO_2. Impedance measurements were monitored every 15 min up to 200 hours. All assays were performed in duplicates. The growth rate was analyzed by calculating slope of the curve between 40 and 60 hours by using the following formula:

Equation 2.

$$y = \frac{y2 - y1}{x2 - x1}$$

where y represents the average growth rate (slope), y2 growth rate at 60 hour time point, y1 growth rate at 40 hour time point, x2 is 60 hours and x1 40 hour time point.

2.2.3.9. CRISPR-Cas9 system for genome engineering

CRISPR (Clustered regularly interspaced short palindromic repeats) are segments of prokaryotic DNA containing repetitions of base sequences. Each repetition is followed by a 'spacer DNA' of viral origin, result of a previous exposure to bacteriophages or any foreign DNA. This system represents a form of an acquired immunity used by bacteria and archeae, as the spacers are recognized and cut in a manner analogous to RNA interference in eukaryotic cells. This interference principle is used as a technique for genomic manipulation and editing of mammalian and other eukaryotic cells. The CRISPR/Cas9 technique for genomic editing, based on *Streptococcus pyogenes* immune system, relies on two main components: a CRISPR-associated 9 endonuclease (Cas 9) and a single guide RNA (sgRNA) that recognizes spacer region, and directs nuclease activity.

sgRNA consists of two elements: trans-activating RNA (tracrRNA) that makes a complex with Cas9 and Crispr RNA (crRNA) that recognizes the region of interest and binds tracrRNA. Cas9 has two active cutting domains: homing endonuclease (HNH), that cleaves the target DNA strand and RuvC domain, that cleaves non-targeting DNA strand, resulting in double strand DNA break (DSB). Protospacer adjacent motif (PAM) sequence (5'-NGG-3' in *S.pyogenes*) provides additional specificity for Cas9 nuclease activity as it immediately follows the sequence recognized by Cas9. While sgRNAs can transport Cas9 anywhere in the cell, the editing itself occurs only at the place where Cas9 recognizes PAM. DSB's are repaired by non-homologous end joining (NHEJ), which can result in insertion/deletion (INDEL) mutations in a coding exon, leading to frame shift mutation and premature stop codons, silencing the gene (**Figure 8. a)-c)**).

2.2.3.9.1. Generation of stable cell lines by using Crispr-Cas9 system

The protocol for creating PDEδ knockout was described in (**Ran et al. 2013**). sgRNA used for knockdown are described in 2.1.4. (4) and 5)). and were generated by using online CRISPR Design Tool (http://tools.genome-engeneering.org). The plasmid used for delivery was pSpCas9 (BB)-2A-Puro (PX4599), Addgene number: 48139 (**Figure 8. d**). Double stranded break in plasmid was repaired by use of non-homologous end joining (NHEJ). The ligated sgRNA-pSpCas9 (BB)-2A-Puro plasmid was treated with PlasmidSafe and transformed in Stbl3 chemically competent bacterial strain on an agar plate supplemented 100-µg/mL ampicillin. We performed mini and midi-preps from bacterial cultures that grew overnight at 37°C. TSC2+/+ p53-/- and TSC2-/-p53-/- MEFs were seeded in $1*10^6$density in a 6-cm dish, and sgRNA-pSpCas9 (BB)-2A-Puro plasmid or pSpCas9 (BB)-2A-Puro (empty vector) were transfected by using Fugene®HD transfection reagent, according to manufacturer's instructions. The next day 2µg/mL of puromycin was applied for selection of transfected cells. The media (full DMEM supplemented with puromycin) was exchanged every 2-3 days until single colonies could be selected for subculturing and cryopreservation.

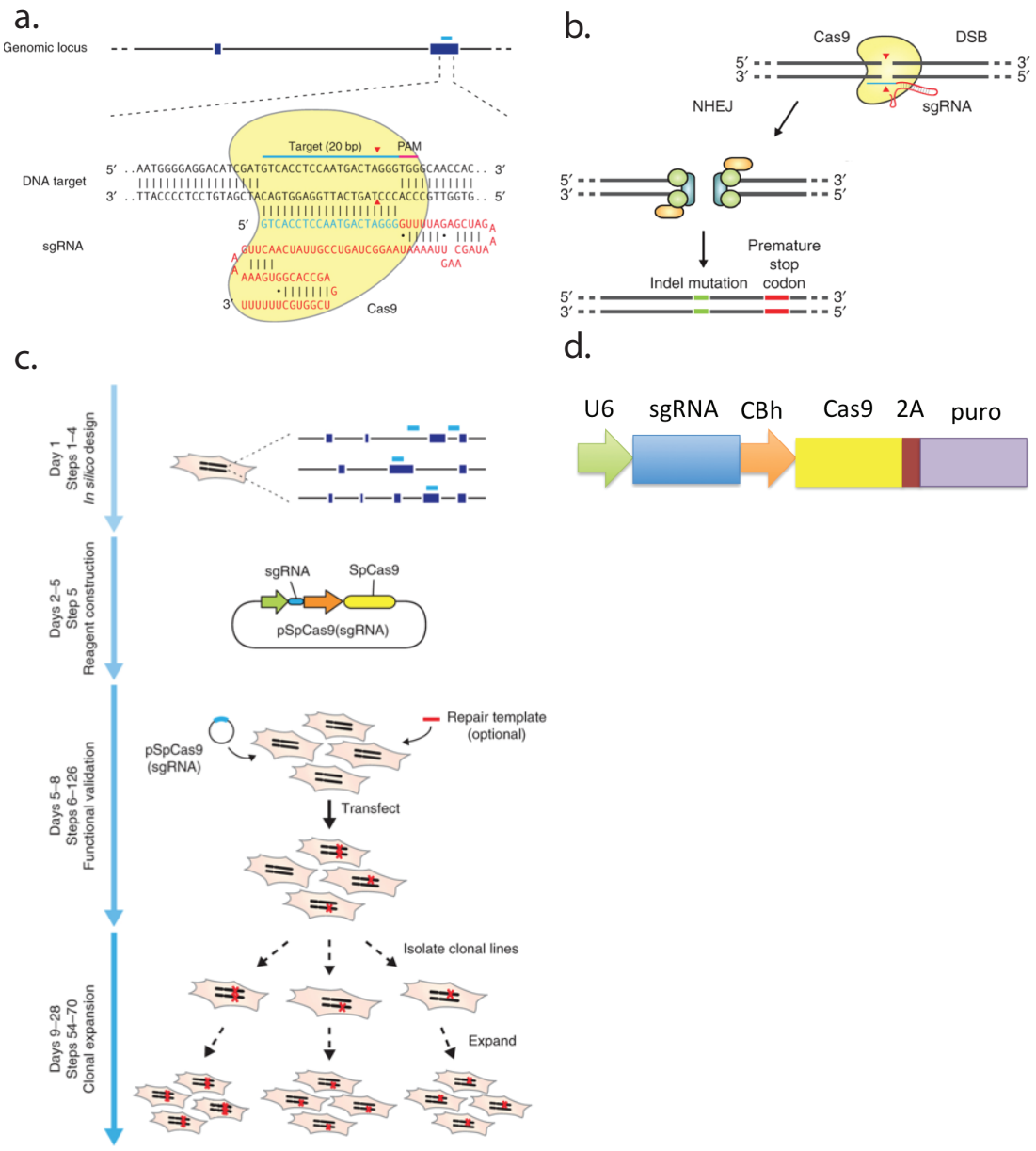

Figure 8. Creating cells with PDEδ knockout via Crispr-Cas system (adapted from Ran *et al.*, 2013)

a. The Cas9 nuclease from *S. pyogenes* (in yellow) is targeted to genomic DNA (shown for example is the human *EMX1* locus) by an sgRNA consisting of a 20-nt guide sequence (blue) and a scaffold (red). The guide sequence pairs with the DNA target (blue bar on top strand), directly upstream of a requisite 5′-NGG adjacent motif (PAM; pink). Cas9 mediates a DSB (double stranded break) ~3 bp upstream of the PAM (red triangle). **b.** DSBs induced by Cas9 (yellow) were repaired by using NHEJ (non-homologous end-joining) pathway: the ends of a DSB are processed by endogenous DNA repair machinery and rejoined, which can result in random indel mutations at the site of junction. Indel (INDEL- INsertion or DELetion of DNA bases in an organism) mutations occurring within the coding region of a gene can result in frame shifts and the creation of a premature stop codon, resulting in gene knockout. **c.** Steps for reagent design, construction, validation and cell line expansion are depicted. sgRNA guide sequences can be cloned into an expression plasmid bearing both sgRNA scaffold backbone (BB) and Cas9, pSpCas9(BB). The resulting plasmid is annotated as pSpCas9 (sgRNA). Completed and sequence-verified pSpCas9 (sgRNA) plasmids are then transfected into cells and assayed for their ability to mediate targeted cleavage. Finally, transfected cells can be clonally expanded to derive isogenic cell lines with defined mutations. **c.** Vector with sgRNA against PDEδ; U6 promotor for guide RNA expression, sgRNA against PDEδ, CBh promotor for Cas9, 2A peptide and puromycin expression (the cells are selected based on their puromycin resistance).

2.2.4. Microscopy

2.2.4.1. Laser scanning confocal microscopy

Images of live or fixed cells were obtained by using Olympus FluoroView FV1000 confocal laser-scanning microscope. DAPI/Hoechst was excited with 405 nm, mTFP with 458 nm, mCitrine and Alexa 488 with 488 nm line of Argon laser. mCherry was excited with 561 nm line of DPSS laser, and Alexa 647 with 633 nm HeNe laser. The objectives used were air objective 40x /0.9 N.A. for PLA experiments and immersion oil objective 60x 1.2 N.A. for the rest of the experiments. The dichroic mirrors DM 458/515 and DM 405/488/561/633 nm HeNe laser. The objectives used were air objective 40x /0.9 N.A. for PLA experiments and immersion oil objective 60x 1.2 N.A. for the rest of the experiments. The dichroic mirrors DM 458/515 and DM 405/488/561/633 were used to detect the fluorescence, with 250 μM pinhole width. Fluorescence detection was done by acusto-optic tunable filter (AOTF) and SIM scanner. Bandwidth 420-460 nm was used for DAPI detection, through SDM 490 emission beam splitter (also separated blue from green/yellow fluorophores), 498-552 nm for Alexa 488 and mCitrine, through a SDM 560 (also separated yellow and red fluorophores), 571-650 nM for mCherry and BP from 655-755 nm for Alexa 647 (**Figure 9.**). Sequential imaging was performed with 3 averaged frames and by application of Kalman filter. Live cell imaging was performed on 37°C and fixed samples were imaged on room temperature.

2.2.4.2. Fluorescence Lifetime Imaging Microscopy (FLIM)

Fluorescence Lifetime Imaging (FLIM) is a technique based on the differences between the exponential decay rates of the fluorescence from the fluorescent sample. Fluorescent lifetime of the fluorophore is used to produce the image, as it does not depend on concentration, photo bleaching, sample thickness etc., therefore is more robust than other intensity based methods. However, it depends on pH, ion or oxygen concentration or the proximity of the energy acceptor molecules, which makes FLIM a technique of choice for imaging in cells. Usually, FLIM is applied to measure protein-protein interaction of

fluorescently tagged proteins by means of Förster resonance energy transfer (FRET).

2.2.4.2.1. Fluorescence lifetime

The emission of fluorescent light consists of three stages. In the first, a single fluorophore molecule absorbs the energy and the electron from the ground state (S_0) is promoted to a higher excited singlet state (S_1, S_2, S3…). If any of excited states higher than S1 are involved, the electron relaxes within a few picoseconds (ps) to the S1 state. This is a process of non-radiative relaxation or internal conversion. From S1 state, the electron relaxes back to the ground state by internal conversion or radiatively upon emitting a photon. This process occurs usually in a nanosecond (ns) range (**Figure 10**).

The fluorescence lifetime (τ) is the period of time in which that electron stays in an excited state before emitting a photon, consequence of relaxation to ground state. It is defined as the inverse of the sum of the emissive (Γ) rate and the non-radiative decay state (k_{nr}) (**Equation 3.**) (**Lakowicz et al. 1992; Bastiaens and Squire 1999; Ng et al. 1999; Wouters and Bastiaens 1999**).

Equation 3.

$$\tau = \frac{1}{\Gamma + k_{nr}}$$

2.2.4.2.2. FLIM methods

There are two distinct methods employed to resolve fluorescent lifetime of a specific compnonet in a mixture: time-domain and frequency-domain FLIM.

Time-domain, method of choice presented in this work, relies on use of pulsed source to determine fluorescent lifetime. When an ultrashort pulse of light excites a sample, the fluorescence decays exponentially. If the pulse or detection response is too wide, the fluorescence (d) is not exponential.

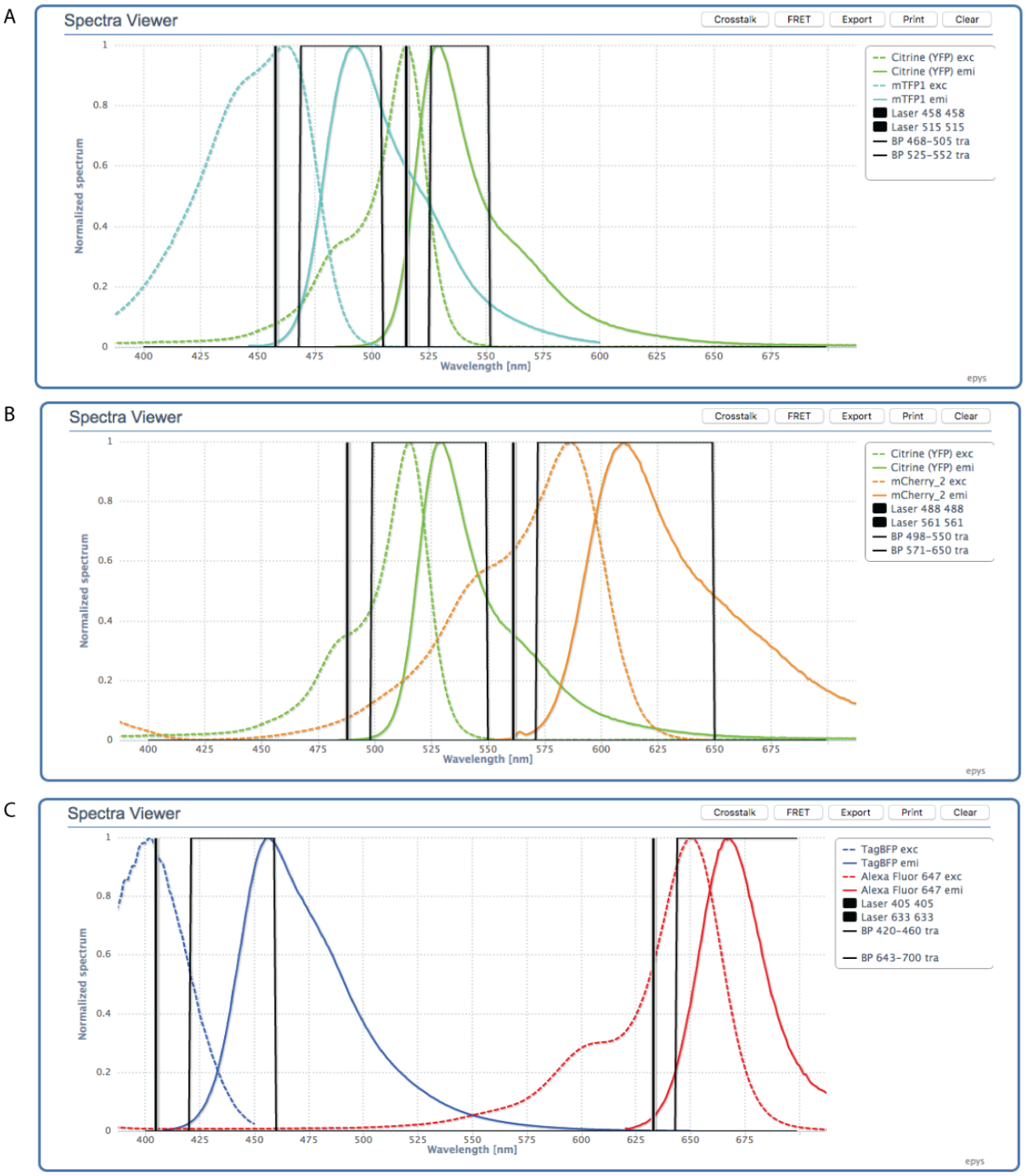

Figure 9. Instumental setting for imaging fluorescent proteins

Excitation (dotted line) and emmission spectra (full line) of mTFP and mCitrine (**A**), mCitrine and mCherry (**B**) and Alexa 405 and Alexa 647 (**C**) with corresponding excitation laser line (black vertical line in graph) for each fluorophore (458 for mTFP, 515 for mCitrine (**A**), 488 for mCitrine, 561 for mCherry (**B**), 405 for Alexa 405 and 633 for Alexa 647 (**C**)). Collection channel bandwidth for each fluorophore represented as a rectangle in the graph (468-505nM for mTFP, 525-552nM for mCitrine (**A**), 498-552 nM for mCitrine, 571-650 nM for mCherry (**B**), 420-460 nM for Alexa 405, 643-700 nM for Alexa 647 (**C**)). Spectra obtained from: http://epys.df.uba.ar/

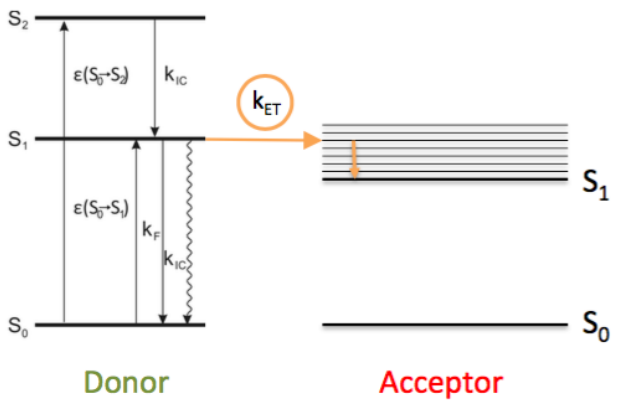

Figure 10. Jablonski diagram (made by: K.C. Schürmann)

explains how electrons in common fluorophores are excited from the ground state into higher energy states, and how these excited molecules relax by photon emission and other mechanisms to fall back into the ground-level energy state. S0-ground state; S1-S2- excited states.

Therefore, the instrument response function (IRF) is convolved with the decay function (F) (**Equation 4.**). IRF is usually measured by use of scattered excitation light or measuring a sample with an extremely short lifetime (rose-bengal solution).

Equation 4.

$$d = IRF * F$$

The correct contribution of each fluorophore in a mixture can be determined by fitting the decay to biexponential function if both fluorophores have a monoexponential lifetime (**Lakowicz 1988**).

Frequency-domain FLIM uses a phase-modulation method to determine fluorescence lifetime. Light source is pulsed or modulated at high frequency (i.e. continuous wave source combined with a modulator) and the fluorescence is demodulated and phase shifted, which is related to decay of the fluorophore (**Lakowicz 1988; French, Gratton, and Maier 1992**).

2.2.4.2.3. Time-Correlated Single-Photon Counting (TCSPC)

Since variations in source intensity and photoelectron amplitudes are ignored, the time correlated single photon counting (TCSPC) is applied to measure fluorescence lifetimes in time-domain FLIM.

TCSPC records times at which individual photons are detected by a photo-multiplier tube (PMT) or an avalanche photo diode (APD) after a single pulse. The recordings are repeated for additional pulses and after enough recorded events; one is able to build a histogram of the number of events across all of the recorded time points **(Lakowicz et al. 1992; O'Connor 1984)**. The histogram can be fitted to an exponential function that contains the exponential lifetime decay function of interest, and the lifetime parameter can accordingly be determined (**Figure 11.**). To obtain information of localization of the protein or the dye in the cell, TCSPC is combined with a scanning microscope.

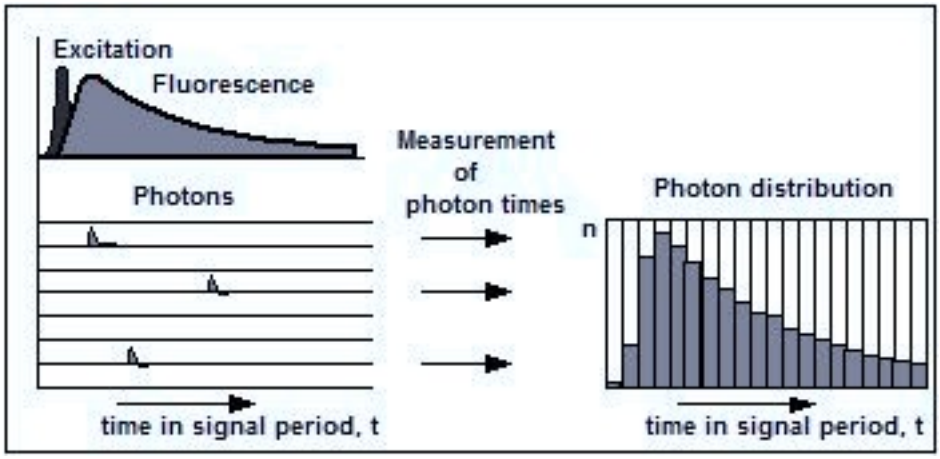

Figure 11. Principles of time-correlated single-photon counting (TCSPC) (adapted from: (Becker 2015)

TCSPC repetitively and precisely registers single photons in a sample. Pulsed laser source repetitively excites the sample, and emitted photons are detected with a photomultiplier, which acts as a stopwatch, as it measures arrival time of a photon in respect to the excitation pulse. By counting many events, histogram of arrival times of excited photons is built up. This histogram can be fitted to an exponential function, from which a lifetime of a sample can be determined.

2.2.4.2.4. Förster resonance energy transfer (FRET)

FRET is a mechanism describing energy transfer between two light-sensitive molecules (fluorophores). Donor fluorophore, in the excited state, transfers energy to an acceptor fluorophore through non-radiative dipole-dipole coupling, thereby relaxing back to the ground state. The efficiency of this

process is inversely proportional to the sixth power of the distance between donor and acceptor (typically 1-10nm), making FRET extremely sensitive to small changes in distance (**Equation 5.**).

Equation 5.

$$E_T = \frac{R_0^6}{R^6 + R_O^6}$$

ET= energy transfer

R= donor-acceptor distance

Ro= donor acceptor distance when FRET efficiency is 50% (Förster radius)

Equation 6.

$$R_0 = [2{,}8 * 10^{17} * \kappa^2 * \Phi_D * \eta^{-4} * J(\lambda)]^{16}$$

The Förster radius depends on the orientation factor of the transition dipoles of the fluorophores (κ), the donor quantum yield (Φ_D) (**Equation 7.**), the refractive index of the medium (η), and the integral of the overlap- ping spectra (J(λ)) (**Equation 6.**).

Equation 7.

$$\Phi = \frac{number\ of\ emitted\ photons}{number\ of\ absorbed\ photons}$$

The refractive index, the overlap integral, and the orientation of the dipoles should be constant for each specific FRET pair. Therefore, the FRET efficiency is only governed by the change in distance, and it can occur only between two interacting proteins (**Förster 1948; Clegg 1992**).

2.2.4.2.5. Global analysis

In samples with multiple lifetime components, it is very difficult to determine the contribution of each species in the mixture. A biexponential fitting in each pixel requires a large amount of collected photons in each pixel, which is unfeasible due to long acquisition times and excessive photobleaching. An

alternative method is global analysis of data sets, which assumes the lifetimes to be spatially invariant. This allows decoupling the determination of the lifetimes (global) from the relative contributions of the species in each pixel (local). It relies on a Fourier transform of the fluorescence decay curve that is calculated for each pixel and representation of the complex Fourier components on a phasor plot where the x-axis is the real, and the y-axis the imaginary component. The global lifetimes are calculated from the distribution of phasors. In FRET-FLIM only the lifetime of the donor is measured. If the donor molecule interacts with the acceptor molecule, the energy transfer occurs and the donor fluorescence decays faster, shifting its lifetime to lower values. If these two lifetimes are constant across the sample, global analysis is applicable and the relative contributions of each species, the interacting fraction of the proteins (α) (**Equation 8.**), can be calculated for each pixel. (**Grecco, Roda-Navarro, and Verveer 2009**).

Equation 8.

$$\alpha = \frac{[DA]}{[D] + [DA]}$$

Additionally, the donor only average lifetime (τ_D) and FRET lifetime (τ_F) can be used to calculate the FRET efficiency (**Equation 9.**)

Equation 9.

$$E = 1 - \frac{\tau_F}{\tau_D}$$

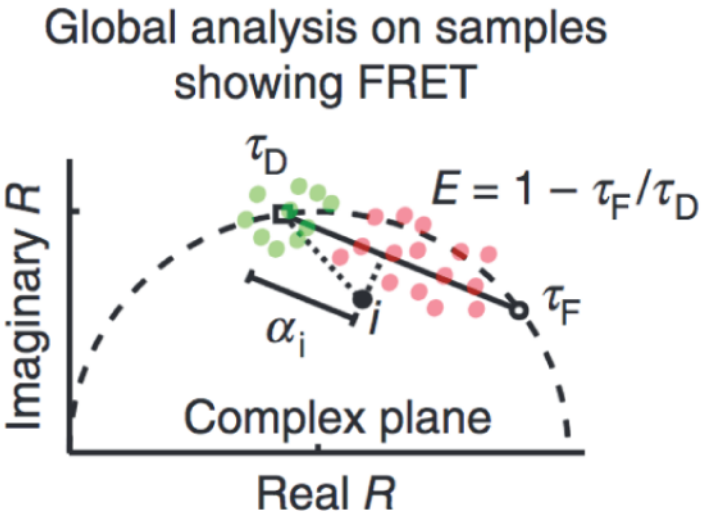

Figure 12. Global analysis and phasor plot (adapted from Grecco et al., 2010)

2D plot where the x-axis is the real component and the y-axis the imaginary component of the complex Fourier coefficients; values on the semicircle correspond to monoexponential lifetimes. The fluorescent decay of each pixel is transformed into a unique position on a phasor plot. The resulting distribution is used to fit a straight line, whose intersects with the semi-circle constitute the values of τ_D (donor lifetime) and τ_F (FRET lifetime). The values for interacting fraction of the proteins (α) in each pixel of the sample are calculated from the projection of the respective phasors onto the line.

2.2.4.2.6. Acquisition and analysis of the FRET-FLIM data

FLIM measurments were made in a setup composed of Olympus FluoroView FV1000 laser scanning confocal microscope equipped with time-correlated single-photon counting module (TCSPC) (LSM Upgrade Kit, Picoquant). Photons were detected by using a single-photon counting avalanche photodiode (PDM Series, MPD) and the signal was transferred to digitally modulated driver (PicoHarp 300). For mCitrine detection, the sample was excited using a 510 nm diode laser (64%) (LDH510, Picoquant) at a 40 MHz frequency by APD equipped with bandpass filter 530/11 nm. The fluorescence was collected through an oil immersion microscope (60x/1.35 UPlanSAPO, Olympus) and filtered by using the dichroic mirror DM 405-442/510. For mTFP, 470nM pulsed laser (36%) and filter 480/20 nm was used, and the dichroic mirror used for detection of the fluorescence was 458/515 nm (**Figure 13**).

The lasers were controlled with the SymPhoTime software (PicoQuant GmbH) with pulse repetition every 25 ns. The resulting .pt3 or .ptu files were subjected to MatLab (Mathworks) based autoglobal analysis (see global analysis). Donor count (DC) image was used to create masks for raw lifetime (lt) and alpha (α) images in ImageJ 1.47k (Java).

2.2.5. Analysis

2.2.5.1. PLA distribution analysis

Angel Stanoev performed analysis for PLA according to the instructions: for the estimation of PLA punctae localization relative to the nucleus, we calculated the distance between each punctum and the nuclear center. Cell shape affects this distribution; therefore, every measured cell was compared to a random distribution of PLA punctae to nuclear center, as a reference. This random distribution was generated by measuring the distances of each cell pixel to the nuclear center for each individual cell mask. Averaging these distributions across all the cells produced the average random distribution of PLA punctae distances to the nuclear center. This approach is equivalent to calculating the randomized distributions in a Monte Carlo fashion.

2.2.5.2. Analysis of protein intensity distribution

The experiments were done in Anaconda Python (2.7) software by using segmentor tool. For each pixel in the cell, the distance to nucleus and plasma membrane was determined. The cells were divided to 3 spatial bins (1=closest to the plasma membrane, 3= closest to the nuclear membrane), with equal radius between them (segment thickness identical across the cell). For angular masking, the center of the nucleus was determined and the intensity weighted ‘center of the cell’ and a central axis was fitted to these two points. 60° around the axis was used for the analysis of intensity distribution, and in the WT image section the image used for the weighting was typed in. Images for segmentation were defined to appear in a designated order, with a corresponding intensity profile. Each value of the segment was normalized to the sum of intensity in all segments, and the resulting mean value with the standard deviation was plotted in the graph. P values were determined by a

Student's unpaired t-test. All values <0.05 were determined as not significant.

A

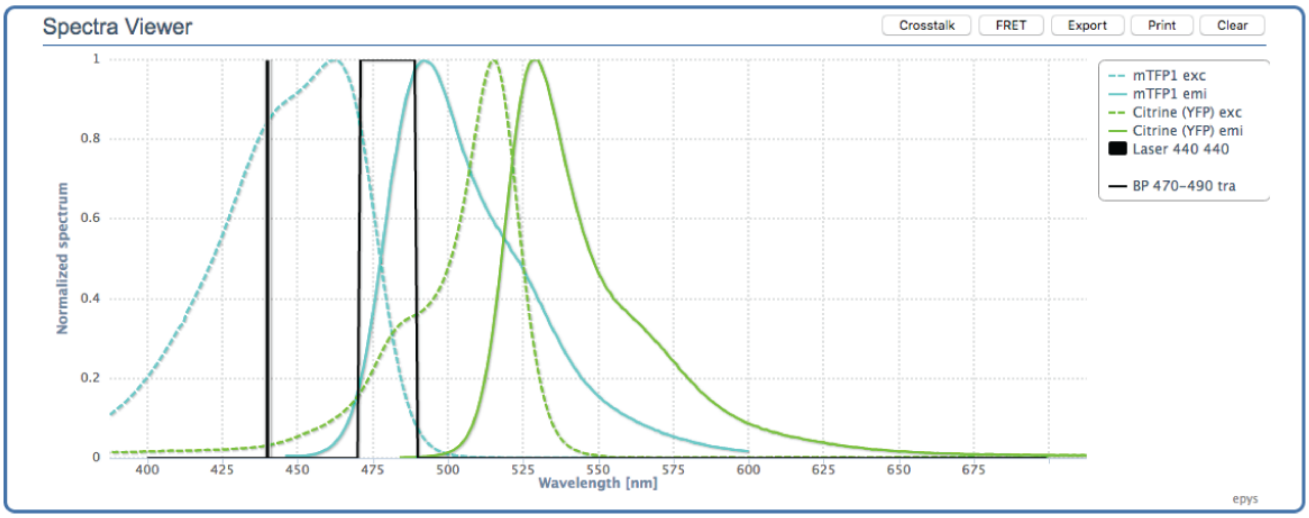

B

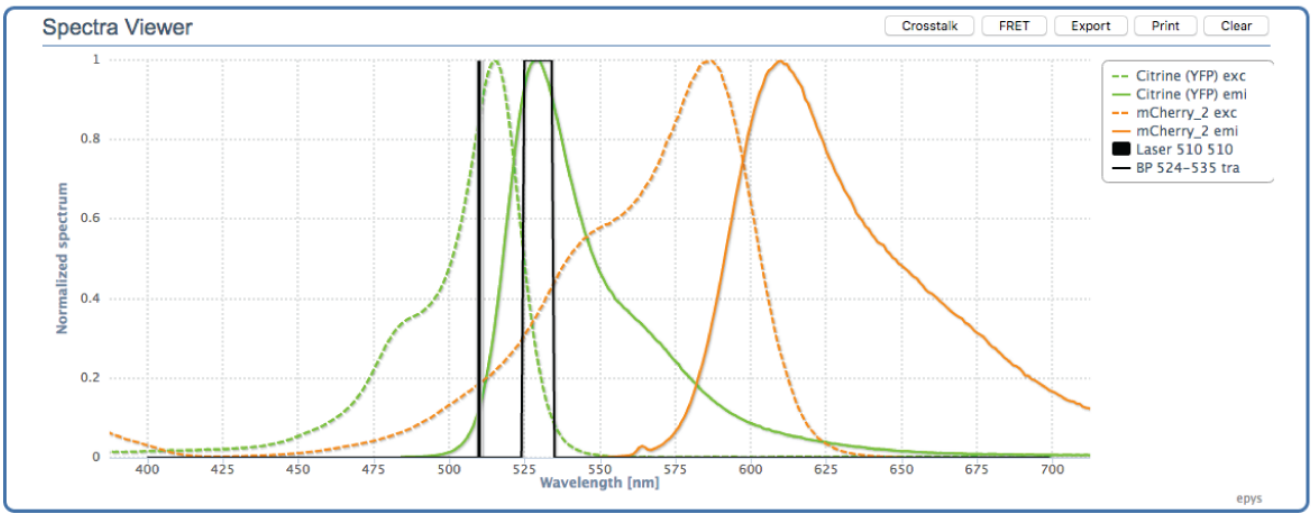

Figure 13. Instrumental setting for FLIM

Spectra of used FRET pairs (mTFP as donor and mCitrine as an acceptor in **A**, mCitrine as donor and mCherry as an acceptor in **B**). Pulsed lasers used for excitation of donors are represented as vertical lines in the graph (440 nM for mTFP (**A**) and 510 nM for mCitrine (**B**)). Detection bandwidth for donor mTFP is from 470-490 nM (**A**) and mCitrine from 524-535 nM (**B**), represented as rectangle in the graph. Spectra from: http://epys.df.uba.ar/

3.RESULTS

3.1. Rheb is localized in the perinuclear region of the cell due to PDEδ-Arl2 interaction

3.1.1. Rheb and mTOR are localized in the perinucelar area of the cell

In order to determine the localization of Rheb in the cell, we ectopically expressed mCitrine-Rheb and performed immunofluorescence (IF) on endogenous Rheb in mouse embryonic fibroblasts immortalized through p53 knockout (TSC2+/+ p53-/- MEFs, in the remaining text TSC2+/+ MEFs). Both endogenous and fluorescently tagged protein displayed a significant enrichment in the perinuclear area of the cell, with the majority of this intensity co-localizing with the lysosomal marker, Lamp1 (**Figure 14. a.)**. This is the reported organelle where the interaction of Rheb with its effector, mTOR occurs (**Sancak et al. 2008**).

In order to examine whether mTOR and Rheb are found in the same area of the cell, we performed IF on endogenous Rheb and mTOR in TSC2+/+ MEFs. To quantify the spatial distribution of proteins, cells were divided in 3 segments with equal radius (1- closest to the plasma membrane, 3-closest to the nuclear membrane), and the 60° angle around the longitudinal cellular axis was used to determine the distribution of mCitrine-Rheb ('segmenting analysis' in the remaining text) in each cell line. Both proteins displayed high co-localizing perinuclear concentration (**Figure 14. b**.), which indicated that the wider perinuclear area of the cell is the region where the interaction between Rheb and mTOR occurs.

In order to investigate whether Rheb localization is influenced by interaction with mTOR, we ectopically expressed mCitrine-Rheb in serum-starved TSC2+/+ MEFs and monitored its perinuclear enrichment after stimulation with insulin. We observed an increase in perinuclear intensity of mCitrine-Rheb, suggesting that active Rheb is recruited in the perinucelar area through interaction with effector mTOR (**Figure 14. c.**).

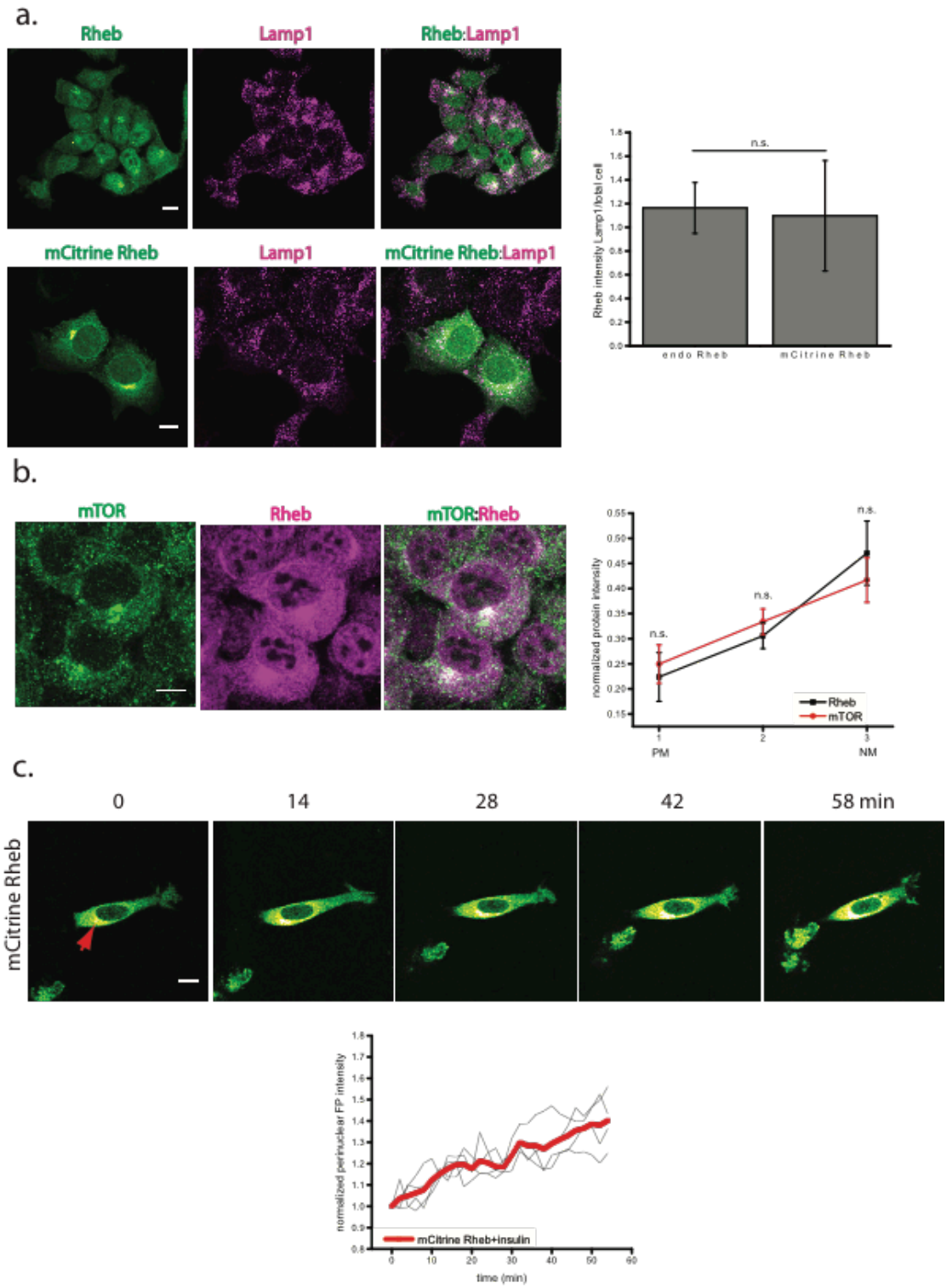

Figure 14. Rheb and mTOR localize at the perinuclear area of the cell

a. Representative (immuno) fluorescence micrographs of endogenous Rheb (upper image), mCitrine-Rheb (lower image) (first column) and Lamp1 (second column) in TSC2+/+ MEFs. Overlay of Rheb and mCitrine-Rheb with Lamp1 (third column). Graph: Ratio of mean Rheb or mCitrine Rheb intensity co-localizing with Lamp1 versus total cell intensity ± s.d. n>20 for both. **b.** Representative immunofluorescence micrograph of mTOR (green) and Rheb (magenta), with their overlay (third image) in TSC2+/+ MEFs.). Graphs: quantification of mCitrine-Rheb intensity in

three separate cell segments (1-closest to plasma membrane (PM), 3-closest to nuclear membrane (NM)) using a 60° angle around an intensity weighted cellular axis. n> 20. **c.** Serum-starved TSC2+/+ MEFs expressing mCitrine-Rheb. Stimulation with 300 nM insulin after 1 min of imaging. Red arrow indicates perinuclear area used for quantification. Graph: quantification of perinuclear mCitrine-Rheb fluorescence intensity, normalized to pre-insulin addition value (y-axis), time in minutes (x-axis). Red thick curve: average of all mCitrine-Rheb curves. n=4. Scale bars= 10µm.

3.1.2. PDEδ interacts with Rheb and is essential for its perinuclear enrichment

Endogenous Rheb displayed higher intensity level in the nucleus, compared to mCitrine-Rheb. This indicated that a substantial soluble fraction of Rheb exists at the endogenous level. When mCitrine-Rheb was co-expressed with red fluorescent protein tagged PDEδ (mCherry-PDEδ), its nuclear, soluble fraction was increased proportionally to the expression of the solubilizer, mCherry-PDEδ. This indicated that PDEδ acts as a solubilizing factor for Rheb (**Figure 15. a.**).

To observe the interaction between PDEδ and Rheb in live cells, we performed fluorescence lifetime imaging microscopy of Förster resonance energy transfer (FLIM-FRET) in transiently co-transfected MEFs with mCitrine-Rheb and mCherry-PDEδ (**Figure 15.b.**). The homogenous fluorescence patterns of both mCitrine-Rheb and mCherry-PDEδ indicated that Rheb is indeed solubilized by PDEδ, which was confirmed by the decrease in donor (mCitrine) lifetime (τ_{av}) from approximately 3 ns to 2.85 ns (upper graph) and computed molar fraction of interacting proteins (α), which increased proportionally to expression of the acceptor (lower graph). After addition of 3 µM of the small-molecule PDEδ inhibitor, Deltarasin (**Zimmermann et al. 2013**) the loss of mCitrine-Rheb soluble state was immediate and this was reflected in increase of donor lifetime comparable to donor-only control and decrease of α (see graphs).

Since the treatment with Deltarasin resulted in loss of PDEδ-Rheb interaction, we used it to determine whether the perinuclear Rheb localization is generated by action of PDEδ. For this, we transiently co-expressed the mCitrine-tagged hypervariable region of Rheb (mCitrine-Rheb HVR) and full-length mCherry-Rheb and monitored perinuclear localization of both after

addition of 3 μM of Deltarasin (**Figure 15.c.**). We observed a gradual decrease of perinuclear enrichment for both proteins over the course of approximately 15 minutes. This showed that perinuclear localization of Rheb is maintained through the interaction of its farnesyl group in the HVR with PDEδ.

Quantitative Western blot analysis, examining phosphorylation of mTORC1 downstream effectors S6P and 4EBP1 was performed to examine the role of this perinuclear Rheb localization on the activity of its main effector, mTORC1. Treatment with increasing concentration of Deltarasin decreased the phosphorylation of mTORC1 effector, ribosomal protein S6 (S6P) and eukaryotic translation initiation factor 4E-binding protein 1 (4EBP1) (**Figure 16.**), indicating that the perinuclear concentration of Rheb, maintained by PDEδ-mediated solubilization, is necessary to maintain proper mTORC1 signaling in cells.

3.2. TSC2 GAP activity is coupled to the PDEδ/Arl2 mediated spatial cycle of Rheb

3.2.1. TSC2 co-localizes with Rheb

The only known regulatory protein, determining the guanine nucleotide loading of Rheb is its GAP, TSC2. It is active and promotes hydrolysis on Rheb in cells deprived of growth factors and nutrients. . In serum-starved TSC2+/+ p53-/- MEFs, TSC2 displayed higher perinuclear localization compared to the cells grown in full medium (**Figure 17.a.**). Interestingly, TSC2 localization is not completely perinuclear in serum starved conditions, which confirms the previous reports that in order to completely recruit TSC2 to the lysosomal surface, the lack of both growth factors and amino acids must be present (**Demetriades, Doumpas, and Teleman 2014**). Additionally, Rheb and TSC2 displayed high co-localization in the perinuclear area of the cell, as analyzed by segmenting analysis (**Figure 17.b.**). This indicated that the perinuclear region of the cell is as well the area of activity regulation of Rheb, as it is the area of Arl2-GTP mediated release of Rheb from PDEδ, resulting in Rheb enrichment on membranes in this area of the cell.

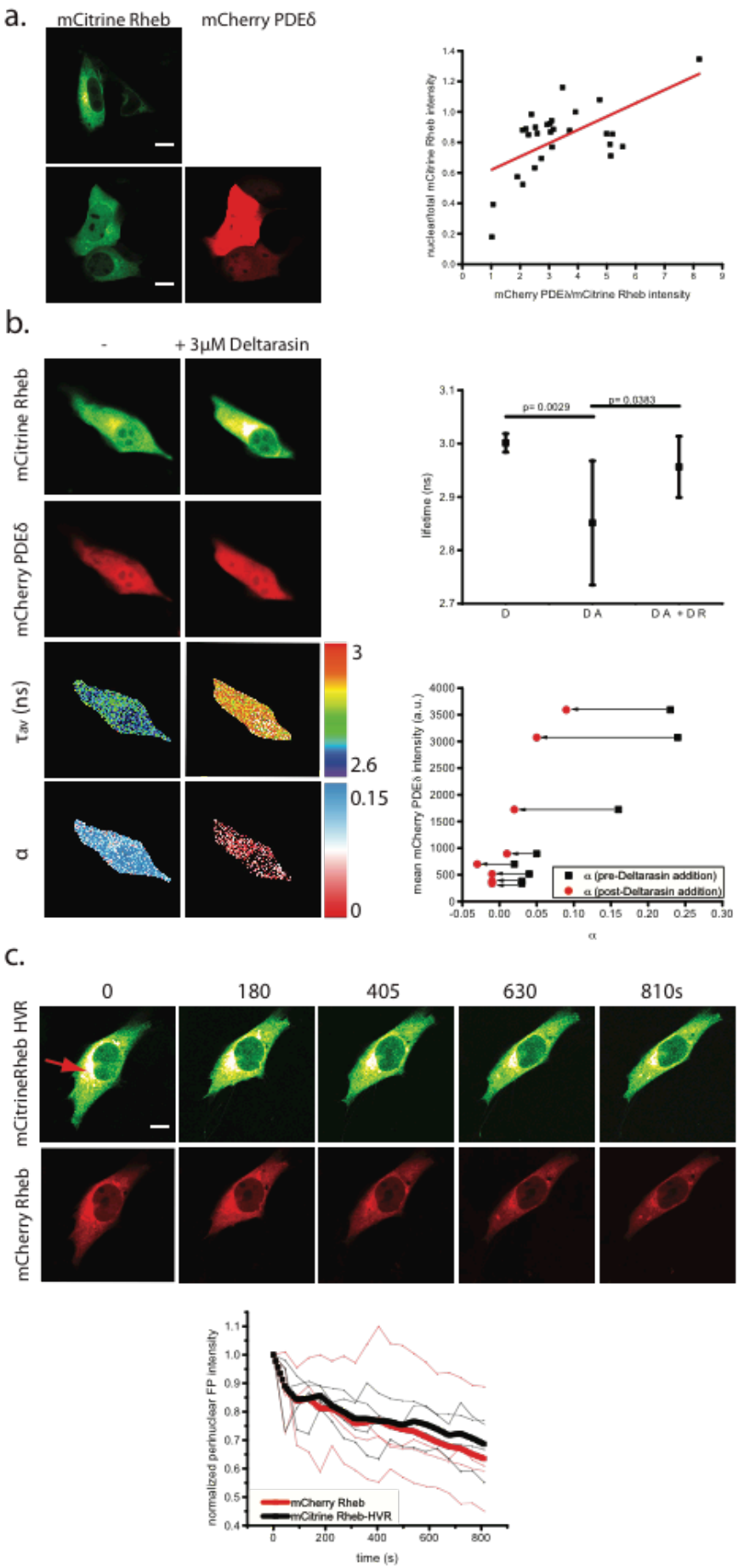
a.
mCitrine Rheb
mCherry PDEδ
nuclear/total mCitrine Rheb intensity
mCherry PDEδ/mCitrine Rheb intensity
b.
-
+ 3μM Deltarasin
mCitrine Rheb
mCherry PDEδ
τav (ns)
α
3
2.6
0.15
0
p= 0.0029
p= 0.0383
lifetime (ns)
D
DA
DA + DR
mean mCherry PDEδ intensity (a.u.)
α (pre-Deltarasin addition)
α (post-Deltarasin addition)
α
c.
0
180
405
630
810s
mCitrineRheb HVR
mCherry Rheb
normalized perinuclear FP intensity
mCherry Rheb
mCitrine Rheb-HVR
time (s)

Figure 15. PDEδ is necessary for perinuclear enrichment of Rheb and mTOR signaling

a. Representative fluorescence micrographs of endogenous Rheb (left), mCitrine Rheb (middle) and mCherry PDEδ (right) in TSC2+/+ MEFs. Graphs: Ratio of mean nuclear Rheb, mCitrine Rheb and mCitrine Rheb co-expressed with mCherry PDEδ intensity versus total cell intensity ± s.d. (left). Nuclear versus total cell mCitrine Rheb intensity in single cells (x-axis) as a function of mCherry PDEδ expression (y-axis). Red line represents linear fit for the entire dataset. n>20 for both.

b. FRET-FLIM measurements of the interaction of mCitrine-Rheb and mCherry-PDEδ before (-) and after addition of Deltarasin (+3 μM Deltarasin). For each sample, the fluorescence intensity of the indicated proteins (upper two rows), the spatial distribution of the mean fluorescence lifetime (τ_{av}) in nanoseconds (third row) and the molar fraction of interacting molecules (α) (fourth row) are shown according to the false-color look-up tables. Left graph: quantification of average lifetimes of donor only (D), donor-acceptor complex (DA) and donor acceptor complex after Deltarasin addition (DA+DR) ± s.d. Right graph: quantification of interacting fraction α before and after Deltarasin addition as a function of mCherry-PDEδ expression. Black arrows indicate decrease in α after Deltarasin addition for all cells. n=8.

c. Time series of mCitrine-Rheb-HVR (upper row) and mCherry-Rheb (lower row) relocalization after application of 3μM Deltarasin. Perinuclear fluorescence intensity was used for quantification (red arrow). Graph: quantification of perinuclear mCitrine-Rheb HVR (black) and mCherry-Rheb (red) fluorescence intensity, normalized to pre-Deltarasin addition value (y-axis), time in seconds (x-axis). Black thick curve: average of all mCitrine-Rheb HVR curves, red thick curve: average of all mCherry-Rheb curves. n=4. All p-values were obtained by unpaired t-test. All scale bars=10 μM.

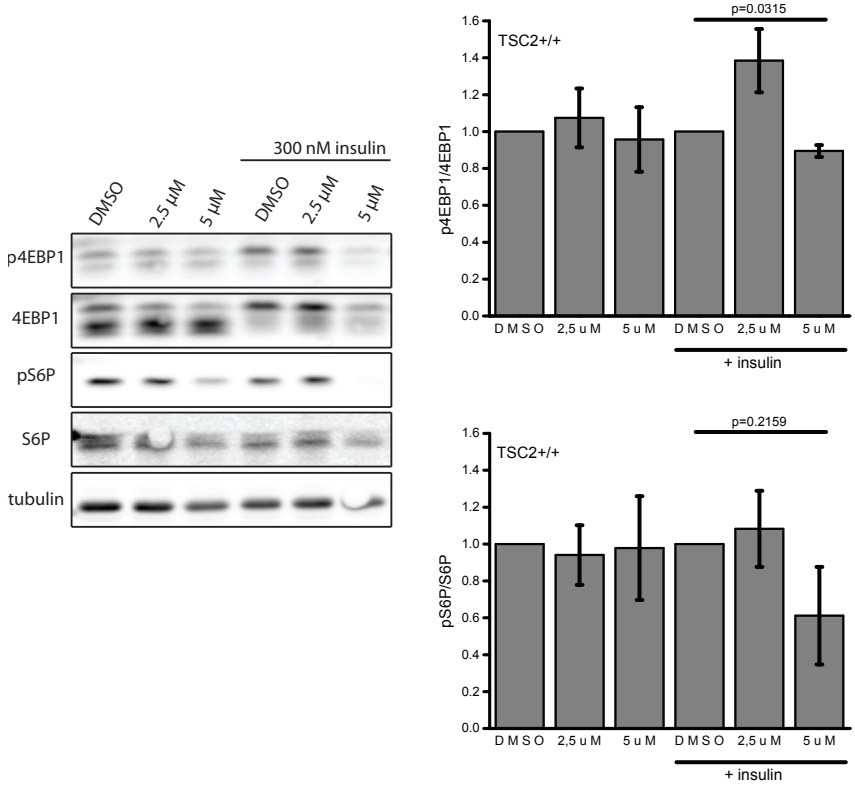

Figure 16. PDEδ inhibition impairs mTORC1 signaling

Western blot analysis of TSC2+/+ MEFs. Phosphorylation levels determined before and after 15-minute stimulation with 300 nM insulin. Left panels: representative western blots of (top to bottom) p4EBP1, 4EBP1, pS6P, S6P and loading control, and tubulin. Graphs: quantification of p4EBP1/4EBP1 (left) and pS6P/S6P (right) normalized to insulin-stimulated control.

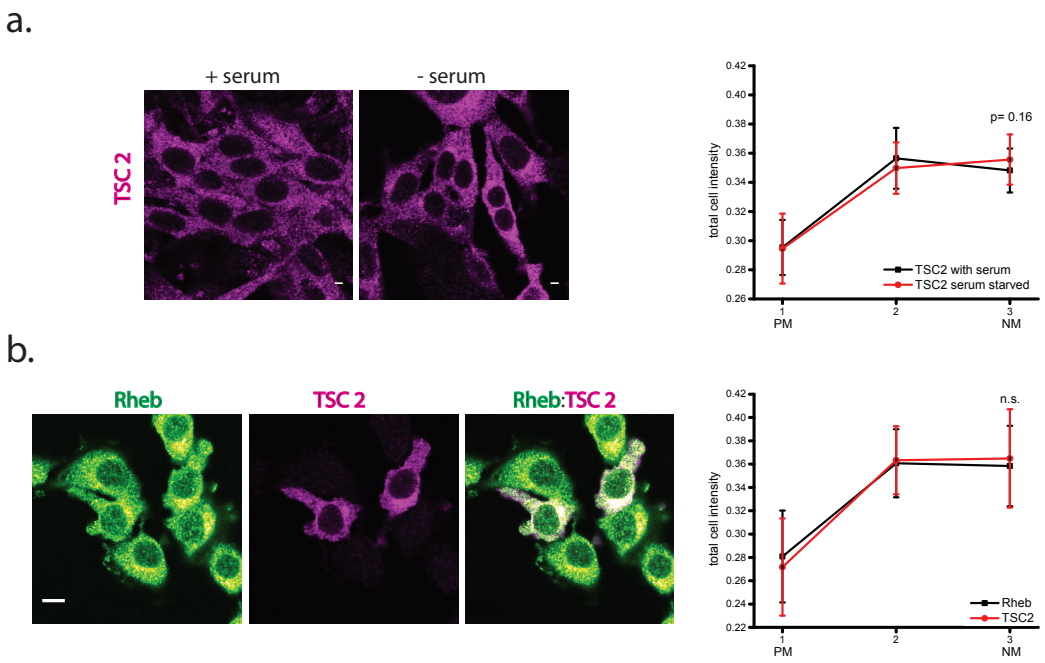

Figure 17. TSC2 is perinuclear and co-localizes with Rheb

a. Representative immunofluorescence micrographs of TSC2 with (left) and without (right) serum. Graph represents quantification of TSC2 intensity in three separate cell segments (PM-plasma membrane, NM- nuclear membrane). **b.** Immunofluorescence micrographs of Rheb (green) and TSC2 (magenta) and their overlay (third image) IN TSC2+/+ cells. Graph: quantification of protein intensity in three cellular segments.

3.2.1. Solubilization by PDEδ is necessary to maintain Rheb localization and mTORC1 signaling in growth factor responsive cells

In order to investigate the contribution of PDEδ-mediated solubilization of Rheb and its own activity state, mediated by the GAP TSC2, on Rheb localization and mTOR signaling, we generated TSC2+/+ and TSC2-/- MEFs with PDEδ knockout via Crispr-Cas system **(Jinek et al. 2012; Ran et al. 2013)**. TSC2-/- MEFs have a knockout of Rheb GAP, TSC2, which results in constitutively active Rheb-GTP and constant activation of mTORC1 (**Zhang et al. 2003**). The intensity distribution of mCitrine-Rheb was quantified by dividing the cells into three segments with equal radius (1-closest to the plasma membrane, 3-closest to the nuclear membrane), and the values within 60° angle around the longitudinal intensity weighted cellular axis taken into account. The distribution of mCitrine-Rheb in TSC2+/+ E.V. (empty vector) control cells increased towards the 3rd cellular segment, while in TSC2+/+

MEFs with PDEδ knockout (sgRNA PDEδ) the intensity profile was significantly flatter (**Figure 18.a.**). We also performed Western blot analysis on S6P phosphorylation in TSC2+/+ E.V. and sgRNA PDEδ MEFs before and after 15-minute stimulation with insulin, to determine the effect of perinuclear Rheb concentration, mediated by PDEδ solubilization, on mTOR activation.
S6P phosphorylation was significantly reduced as compared to the control in unstimulated TSC2+/+ sgRNA PDEδ MEFs. These cells maintained responsiveness to insulin, as apparent from the increased S6P phosphorylation, albeit to a significantly lower extent than the control TSC2+/+ E.V. cells (**Figure 18.b.**).

3.2.3. Rheb solubilization depends on its nucleotide-bound state

In contrast to previous results, TSC2-/- MEFs displayed no mislocalization of mCitrine-Rheb nor inhibitory effect on mTORC1 signaling, as determined by S6P phosphorylation levels, regardless of the presence of PDEδ (**Figure 18. c.-d.**).
Interestingly, the distribution of mCitrine-Rheb HVR in both TSC2 +/+ and TSC2 -/- sgRNA PDEδ MEFs decreased significantly in the 3rd cellular segment compared to their respective E. V. controls (**Figure 19. a., b.**). This indicates that the perinuclear concentration of Rheb depends not only on the PDEδ- mediated solubilization, but as well its own activity state.
This was additionally confirmed by expressing mCitrine-Rheb in parental TSC2+/+ and TSC2-/- MEFs, where its measured perinuclear fraction was significantly higher in TSC2-/- MEFs, compared to TSC2+/+ MEF (**Figure 20.a.**).
The co-expression of mCherry-PDEδ resulted in reduced mCitrine-Rheb perinuclear fraction in both cell lines, albeit to a lower extent in TSC2-/- MEFs. Single cell analysis uncovered that the gradual decrease of perinuclear mCitrine-Rheb fraction occurs with increasing expression of mCherry-PDEδ, while only at the very high levels of mCherry-PDEδ, a minor loss of perinuclear mCitrine-Rheb in TSC2-/- MEFs was observed (**Figure 20. b.**)

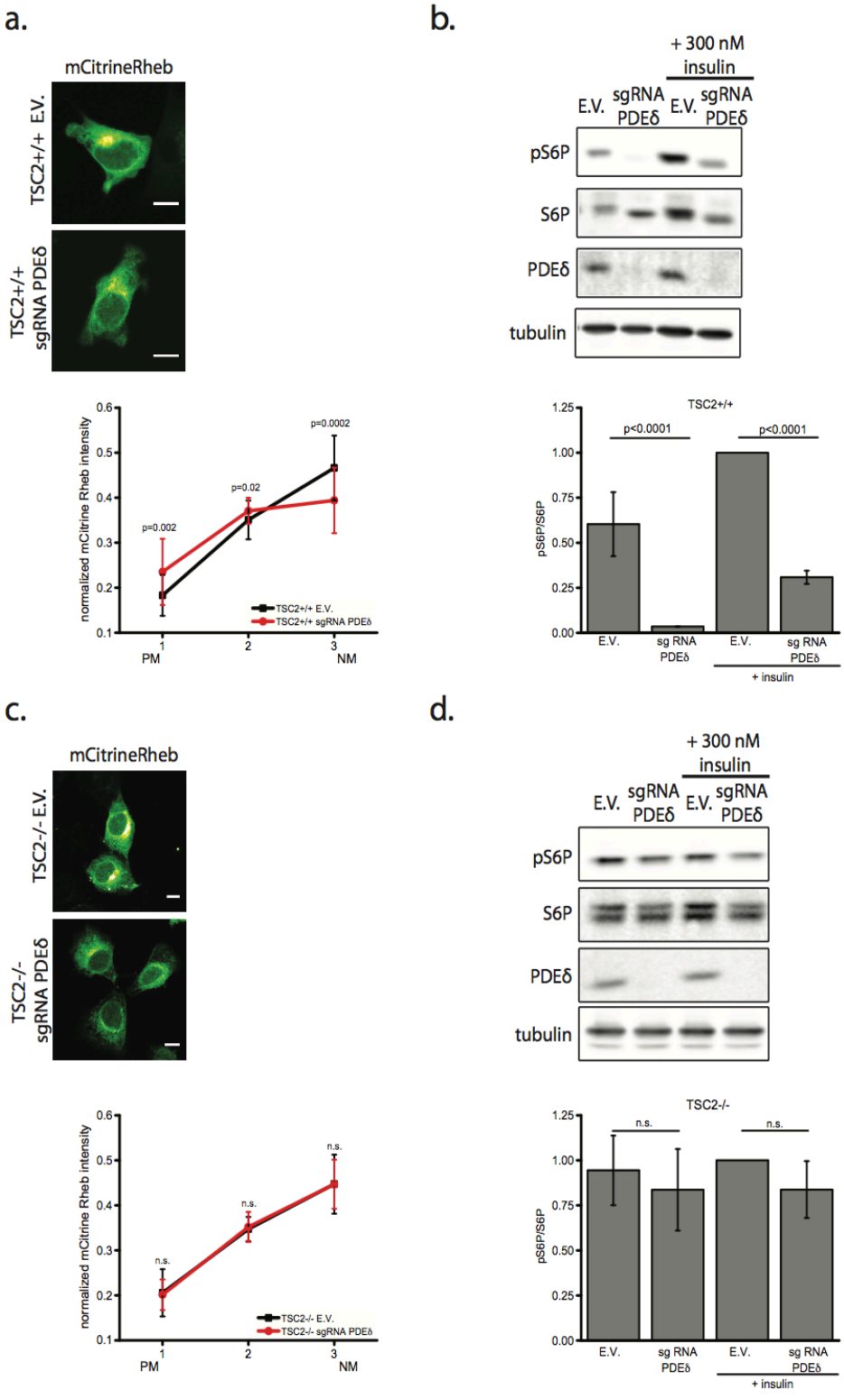

Figure 18. Solubilization by PDEδ is necessary to maintain Rheb localization and mTORC1 signaling in growth-factor responsive cells

(**a.**,**c.**) Fluorescence intensity patterns of mCitrine-Rheb in TSC2+/+ (**a.**) and TSC2-/- MEFs (**c.**) stably expressing empty vector (E.V., upper images) and guide RNA for silencing PDEδ (sgRNA PDEδ, lower images). Graphs: quantification of mCitrine-Rheb intensity in three separate cell segments (1-closest to plasma membrane (PM), 3-closest to nuclear membrane (NM)) using a 60° angle around an intensity weighted cellular axis. n> 20 for each

condition. Scale bars= 10µm. (**b.,d.**) Western blot analysis of S6P phosphorylation in TSC2+/+ E.V. MEF and TSC2+/+ sgRNA PDEδ MEF (**b.**) and TSC2-/- E.V. MEF and TSC2-/- sgRNA PDEδ MEF (**d.**). Phosphorylation levels were determined prior and post-stimulation with 300 nM insulin for 15 minutes. Left panels: representative western blots of five independent experiments for each cell line. From top to bottom row: phosphorylation of S6P (pS6P), total levels of S6P (S6P), PDEδ and loading control (tubulin). Graphs: quantification of pS6P/S6P normalized to insulin-stimulated control cell line (E.V. + insulin).

In order to investigate whether this perinuclear Rheb concentration is necessary for mTORC1 activation, we analyzed the level of S6P phosphorylation in cells as a function of ectopic mCherry-PDEδ expression via Western blot analysis. Compatible with the results described above, we observed decrease in S6P phosphorylation with increased level of mCherry-PDEδ expression, while it remained unchanged in TSC2-/- MEFs (**Figure 20.c.**).

Altogether, these results show that solubilization by PDEδ is an essential step in generating high enough perinuclear concentration of Rheb to engage and activate mTOR. The solubilization is superseded in TSC2-/- MEFs, due to stable interaction of constitutively active Rheb-GTP with mTOR, resulting in increased perinuclear fraction of Rheb-GTP, impaired solubilization and unhampered mTORC1 signaling.

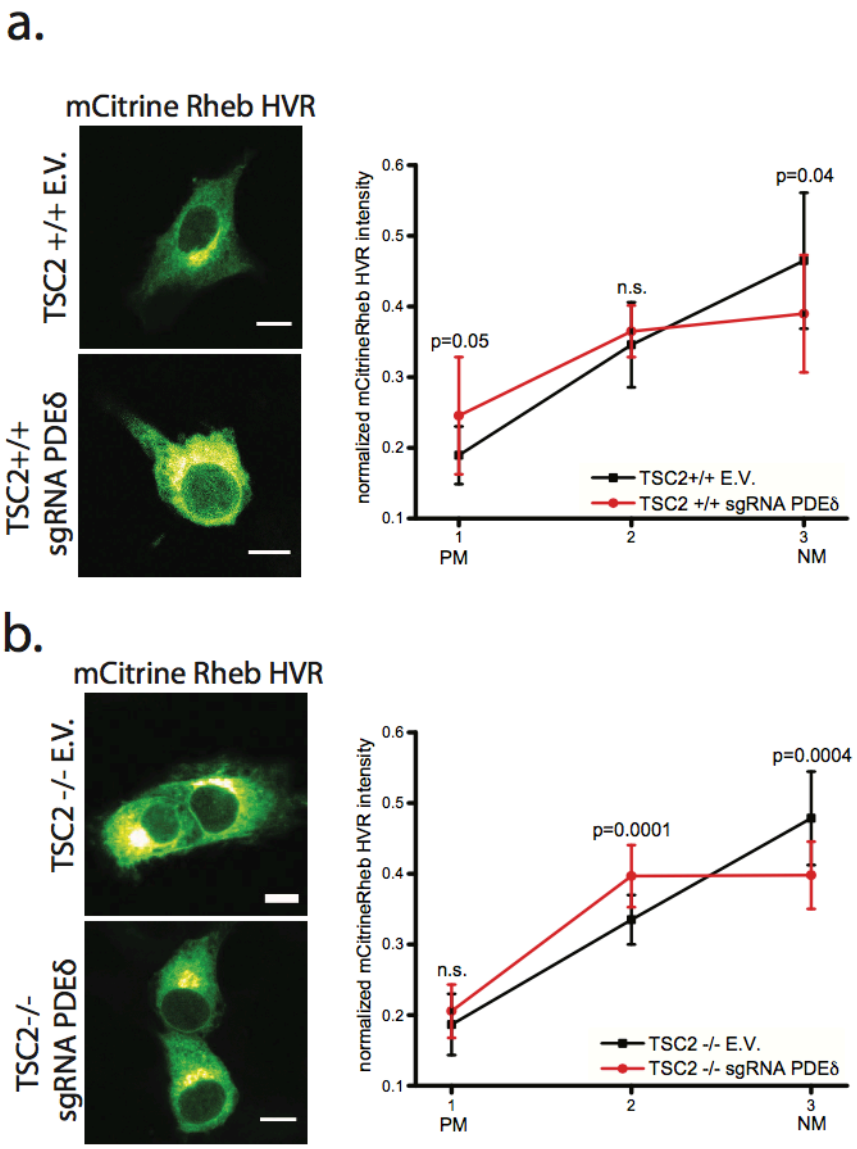

Figure 19.

(**a., b.**) Fluorescence intensity patterns of mCitrine-Rheb HVR in TSC2+/+ (**a.**) and TSC2-/- MEFs (**b.**) stably expressing empty vector (E.V., upper images) and guide RNA for silencing PDEδ (sgRNA PDEδ, lower images). Graphs: quantification of mCitrine-Rheb HVR intensity in three separate cell segments (1-closest to plasma membrane (PM), 3-closest to nuclear membrane (NM)) using a 60° angle around an intensity weighted cellular axis. n> 20 for each condition.

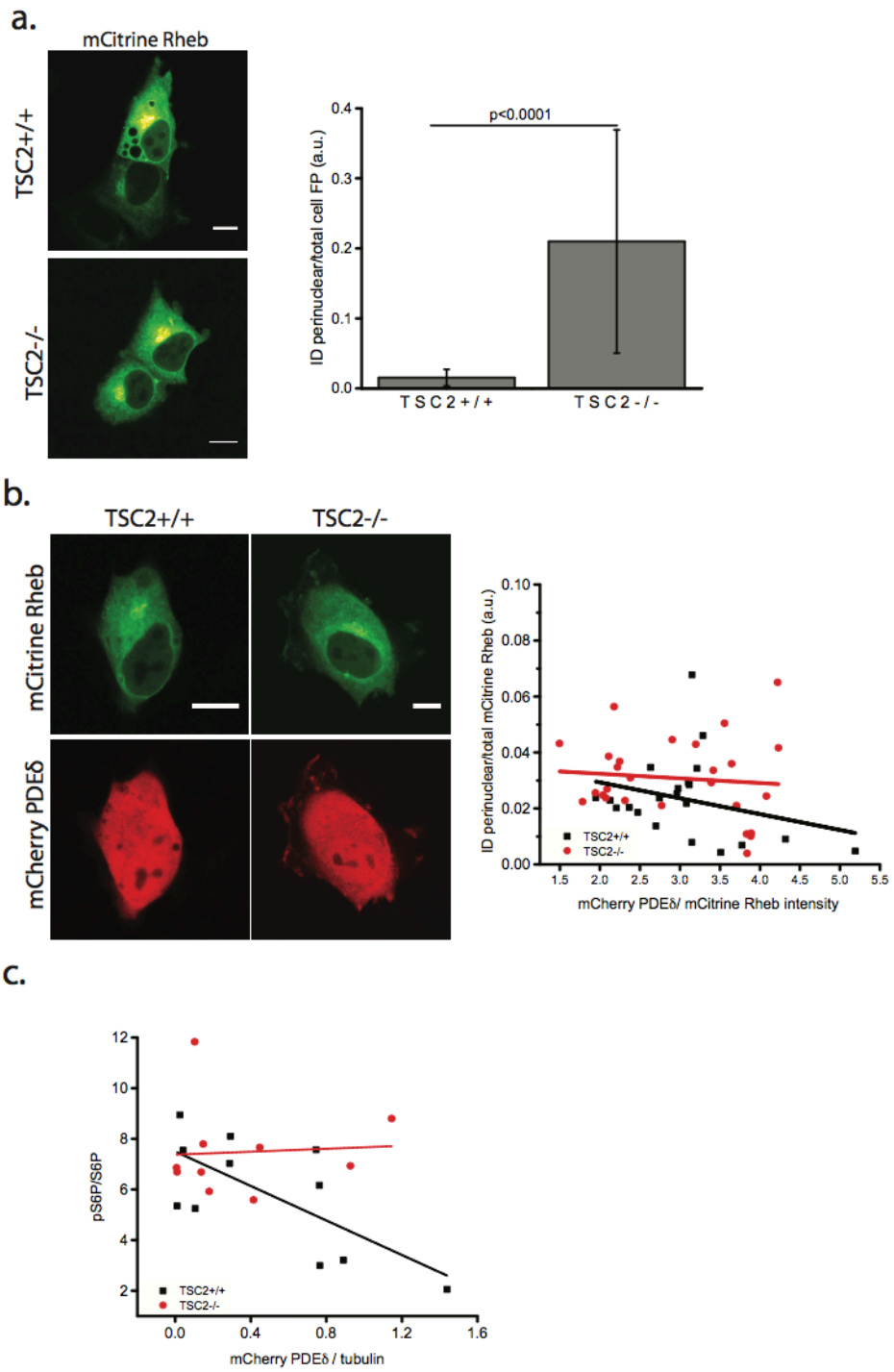

Figure 20. mTOR signaling and perinuclear enrichment of Rheb depends on nucleotide bound state of Rheb

a. Images of TSC2+/+ (left) and TSC2-/- MEFs (right) ectopically expressing mCitrine-Rheb. Graph: quantification of perinuclear mCitrine-Rheb integrated intensity vs. total cell intensity in both cell lines.

b. Representative fluorescence micrographs of mCitrine Rheb fluorescence intensity in TSC2+/+ MEFs (left, n=28) and TSC2-/- MEFs(right, n=34) with co-expression of mCherry-PDEδ (lower images). Graphs, left: Perinuclear mCitrine-Rheb intensity (y-axis) in dependence on mCherry-PDEδ expression level (x-axis) in both cell lines. Values on both axes are normalized to total mCitrine-Rheb intensity. Lines represent linear fit for each individual dataset (black=TSC2+/+; red= TSC2-/-). Statistical difference between two datasets determined by F-test with resulting p value of 0.2.

c. Representative expressing mCherry PDEδ. p value obtained by unpaired t-test. All scale bars= 10 μM. **c.** Left: Linear fit of western blot data on S6P phosphorylation as a function of ectopic mCherry-PDEδ expression level in TSC2+/+ MEFs (black) with a or TSC2-/- MEFs (red). n=3. p value obtained by unpaired t-test.

3.2.4. Arl2-mediated localized release generates perinuclear membrane-associated Rheb

Although it was reported that both Arl2 and Arl3 displace farnesylated Ras proteins from PDEδ, knockdown of Arl2 only, not Arl3 (**Figure 21. e.**) lead to increased solubilization of Rheb in TSC2+/+ MEFs (**Figure 21. a.**), effect observed in other Ras proteins as well (**Schmick et al. 2014**). Accordingly, knockdown of Arl2 lead to a decreased phosphorylation rate of S6 in these cells (**Figure 21. c.**). On the other hand, localization of mCitrine-Rheb in TSC2-/- MEFs with a Arl2 or Arl3 knockdown did not lead to any visible change (**Figure 21. b.**), and phosphorylation of S6 remained the same, regardless of the presence of Arl2 (**Figure 21. d.**). These results show that impairing the PDEδ/Arl2-GTP mediated spatial cycle of Rheb by removing either of the two factors results in mislocalization of Rheb in growth factor responsive cells only, while it has no effect in cells with constitutively active Rheb. This implies that the Rheb spatial cycle mediated by PDEδ/Arl2-GTP is coupled to the Rheb nucleotide bound state, as well that it is necessary for the perinuclear accumulation in growth factor-responsive cells.

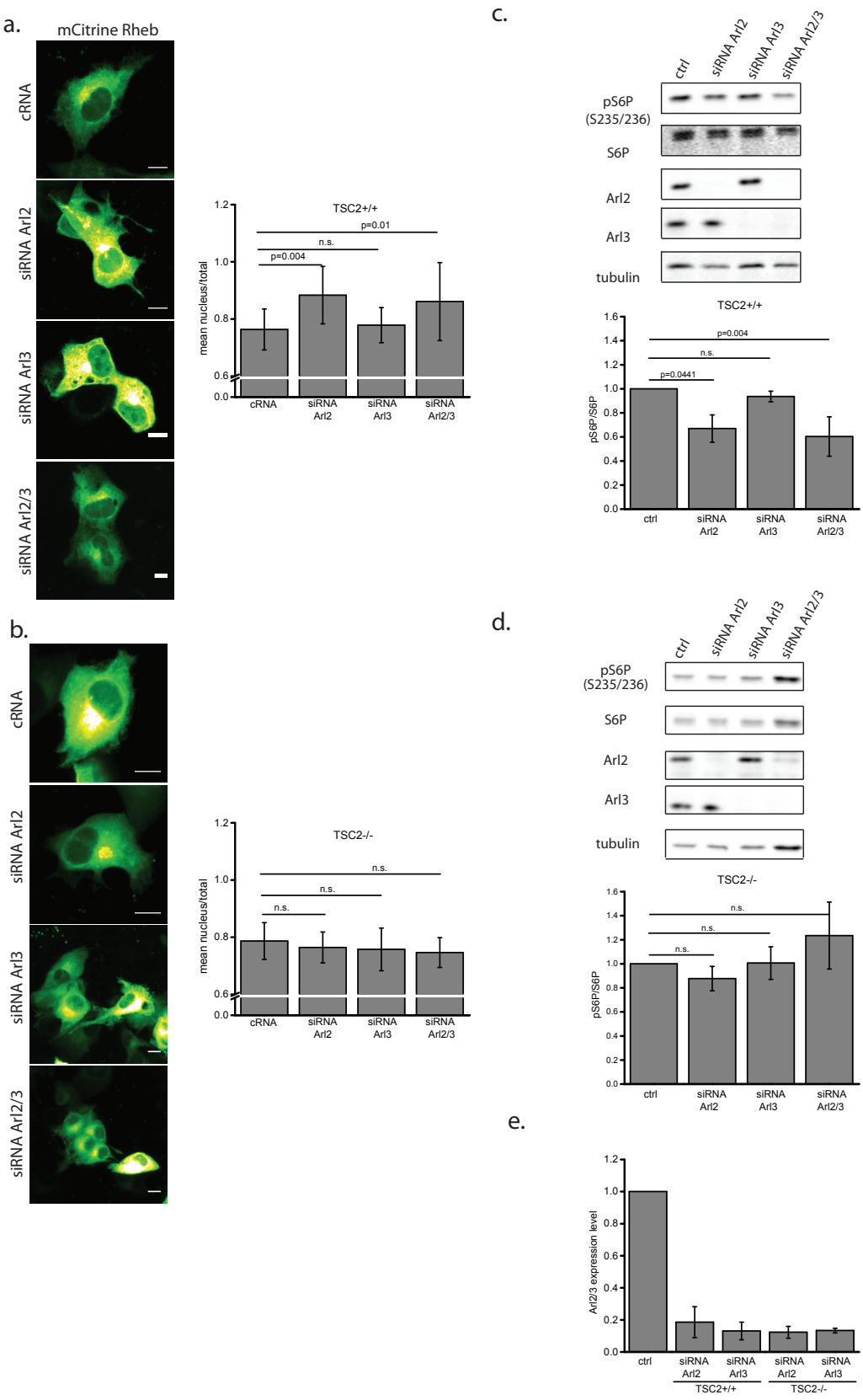

Figure 21. Arl2-mediated perinuclar enrichment of Rheb is necessary for mTORC1 signaling

(**a,b**) Representative maximal intensity projections of z-stacks of mCitrine-Rheb distribution in TSC2+/+ (**a.**) and TSC2-/- MEFs (**b.**) cells transfected with non-targeting siRNA (cRNA), siRNA against Arl2, Arl3 or both. Graphs:

mean nuclear/total cell intensity ± s.d. n> 16 for each condition. Scale bars=10µm. (**c,d**) Western blot analysis of S6P phosphorylation in TSC2+/+ (**c**) and TSC2-/- MEFs (**d**) with siRNA-mediated knockdown of Arl2 or Arl3 or both. Phosphorylation levels were determined 48h post siRNA transfection. Left panels: representative western blots of three independent experiments for each cell line. From top to bottom row: phosphorylation of S6P (pS6P), total levels of S6P (S6P), Arl2, Arl3 and loading control (tubulin). Graphs: quantification of pS6P/S6P normalized to control RNA transfected cells. **e.** Quantification of expression level of Arl2 or Arl3 from **c,d**. Data in c,d,e is shown as mean ± s.e.m. All p values were obtained by unpaired t-test. P values >0.05 labeled as not significant (n.s.).

3.3. Allosteric displacement of Rheb from PDEδ via Arl2-GTP activity occurs in the perinuclear area of the cell

3.3.1. Interacting proteins Arl2 and PDEδ

Arl2-GTP activity has been shown to displace farnesylated Ras proteins from PDEδ. It was shown that this activity needs to be restricted to a confined area of the cell, and the results above indicated that this is the perinuclear region.
In order to confirm the interaction between Arl2 and PDEδ we performed fluorescence lifetime imaging microscopy of Förster resonance energy transfer (FLIM-FRET) to determine the whether the interaction between PDEδ and Arl2 occurs in this area of the cell.
Ectopically expressed teal fluorescent protein-tagged Arl2 (mTFP-Arl2) and PDEδ fused to red fluorescent protein (mCherry-PDEδ) showed a homogenous distribution of interacting molecules (**Figure 22. a.**). However, immunofluorescence (IF) of endogenous Arl2 and PDEδ demonstrated that Arl2 is significantly enriched in the perinuclear region, compared to flatter PDEδ (**Figure 22. b.**), what was not observed in distribution of fluorescently tagged-Arl2. This indicated that the interaction of these proteins should take place mostly in this part of the cell. According to previously published data **(Schmick et al. 2014**), and the data presented here, the displacement of farnesylated cargo, therefore, the interaction between Arl2-GTP and PDEδ occurs in the locally, at the area of the cell.

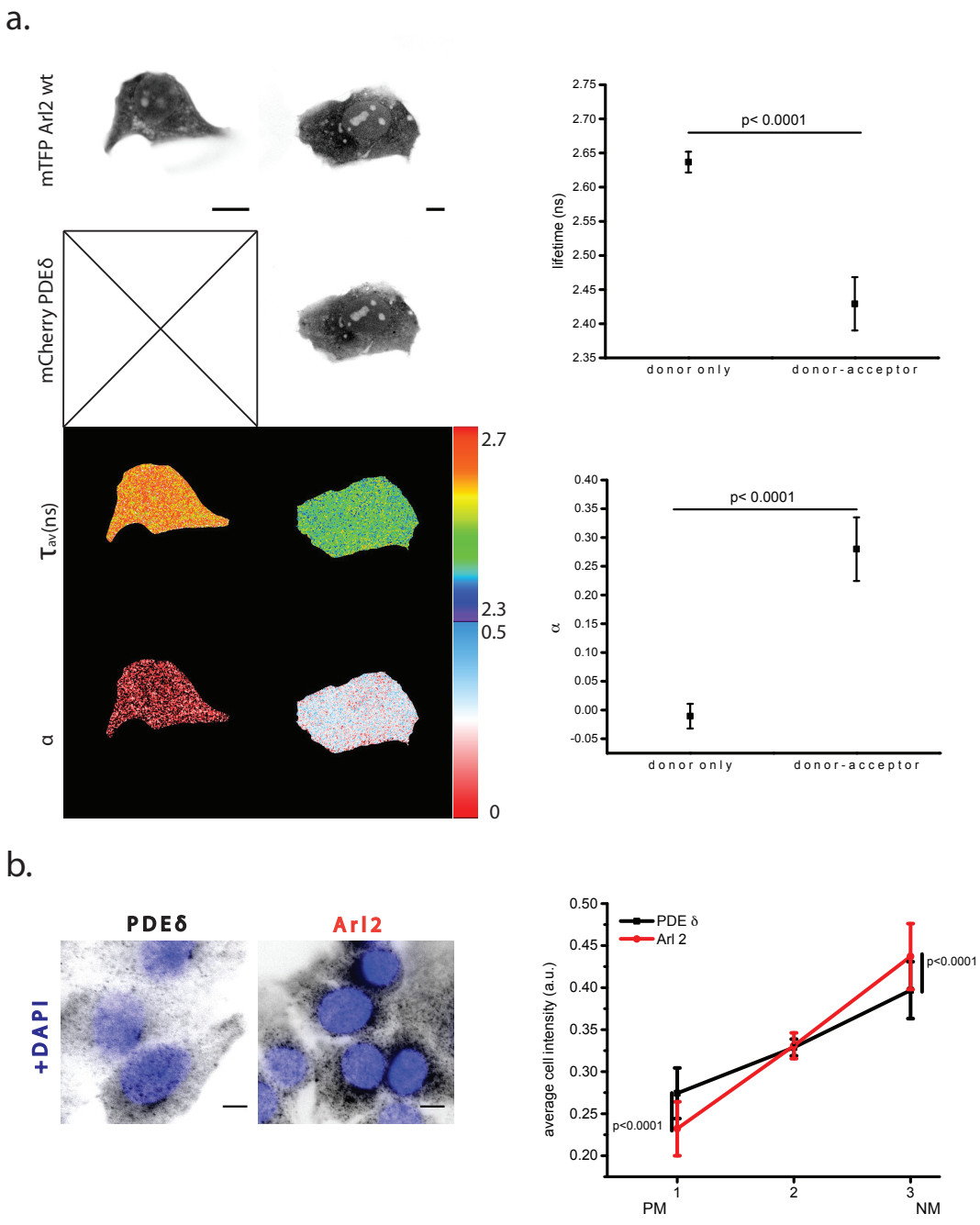

Figure 22. Interaction and localization of Arl2 and PDEδ

a. FRET-FLIM measurements of the interaction of mTFP-Arl2 and mCherry-PDEδ). For each sample, the fluorescence intensity of the indicated proteins (upper two rows), the spatial distribution of the mean fluorescence lifetime (τ_{av}) in nanoseconds (third row) and the molar fraction of interacting molecules (α) (fourth row) are shown according to the false-color look-up tables. Upper graph: quantification of average lifetimes of donor only (D) and donor-acceptor complex (DA) ± s.d. Lower graph: quantification of interacting fraction α. n=12.

b. Representative immunofluorescence micrographs of PDEδ (upper) and Arl2 (lower) in TSC2+/+ MEFs with DAPI stain for nucleus. Graph represents quantification of PDEδ (black line, n=55) and Arl2 (red line, n=43) fluorescence intensity distribution in three cellular segments (1- closest to the plasma membrane (PM), 3- closest to the nuclear membrane (NM)) ± s.d. P values were determined by unpaired t-test.

3.3.2. Arl2 and PDEδ interact in the perinuclear area of the cell

In order to determine the interaction between two proteins at the endogenous level we preformed *in situ* proximity ligation assay (PLA) (**Soderberg et al. 2006**) (**Figure 23.**). PLA results in fluorescent puncta in the areas where interaction between two proteins ocurrs (**Koos et al. 2014**). The release of the farnesylated cargo should be independent on its own nucleotide bound state, but dependent on GTP-loaded state of Arl2. Therefore, we examined interaction pattern of Arl2 and PDEδ in TSC2+/+, TSC2-/- and HeLa cells. To determine the distribution of Arl2-PDEδ interaction puncta in the cell, we computed the position of the nuclear membrane in the cell and the distance of each punctum to the center of the nucleus. The resulting distribution was compared to a calculated randomized puncta distribution, calculated by determining the distance of each cell pixel to the nuclear center (**Figure 23., Figure 24.).** The distance distribution of puncta depends on the cell shape; as can be seen from the randomized distributions that are shifted more to the perinuclear region in the spindle-shaped TSC2+/+ MEFs (**Figure 23.a., Figure 24.a.)**, than the more circular TSC2-/- MEFs (**Figure 23. b., Figure 24. b.**) and HeLa cells (**Figure 23. c., Figure 24. c.**). Yet, compared to the randomized distributions, most of the PDEδ-Arl2 interaction puncta were closer to the nuclear membrane, and became less frequent towards the outer regions of the cell in all examined cell types. This demonstrates that PDEδ-Arl2-GTP interaction preferentially occurs in the perinuclear region of the cell, where most of Arl2 is localized. This interaction results in displacement of the farnesylated cargo.

These results combined highlighted the essential role of PDEδ-Arl2GTP ‘pump’ on maintainance of Rheb localization by binding/localized release of farnesylated moiety to/from PDEδ.

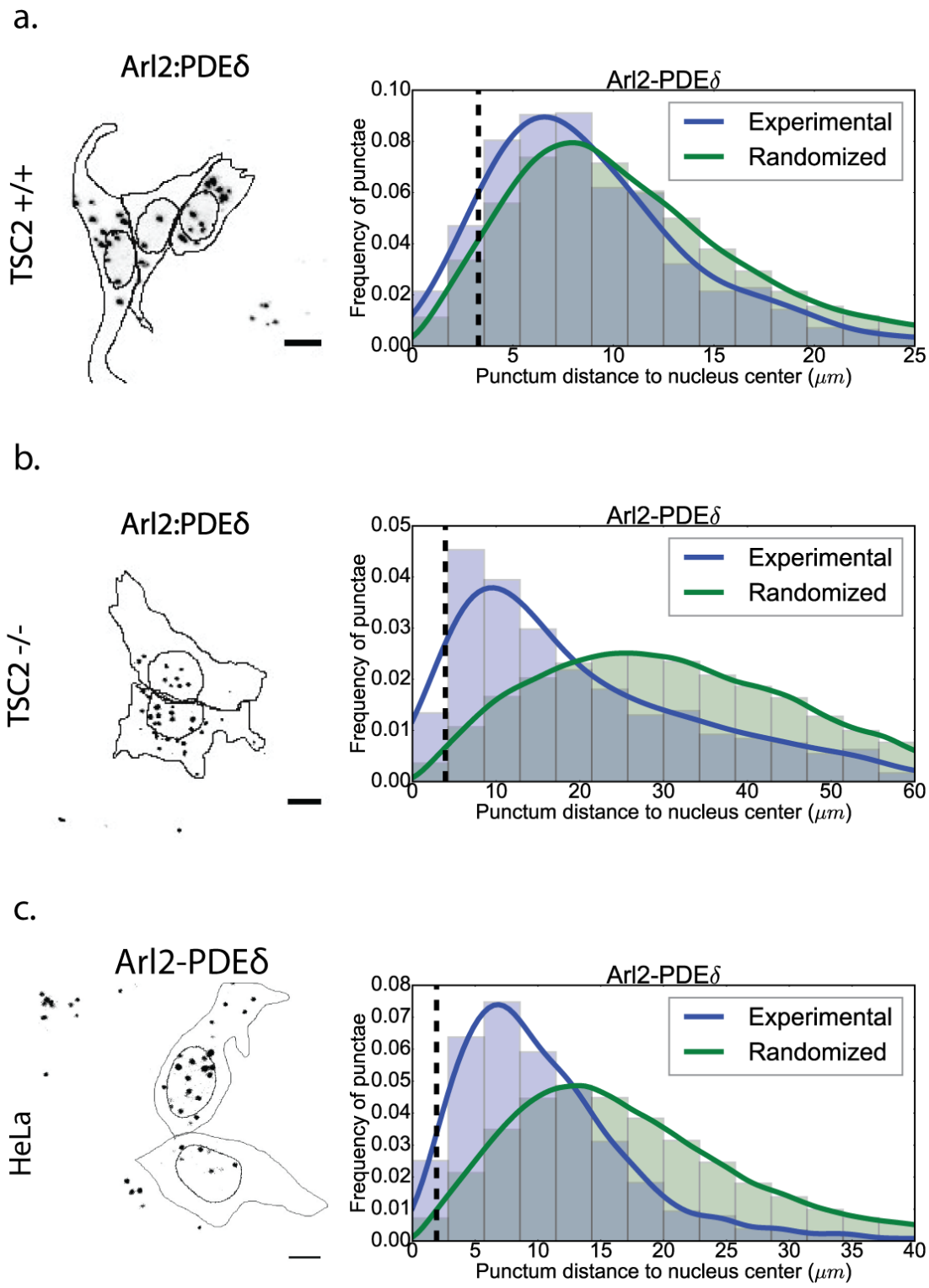

Figure 23. Arl2 and PDE δ interact in the perinuclear region of the cell

(a.-c.) Representative maximum intensity projection of a Z-stack depicting PLA interaction puncta between Arl2 and PDEδ in TSC2+/+ MEFs (**a.**, n=47 cells), TSC2-null MEFs (**b.,** n=31 cells) and HeLa cells (c., n=35). Graphs: Distribution of distances of PLA puncta to the nuclei of the cells. Green: histogram and profile of a calculated random distribution, blue: histogram and profile of the measured PLA interaction puncta, black line: nuclear membrane. X-axis: punctum distance from nuclear center (μm); y-axis: frequency of puncta. P values for individual cells determined by Kolmogorov-Smirnov test. P< 0.05: 19/47 cells for **a.** 24/31 for **b.** and 35/35 for **c.** All scale bars=10 μM.

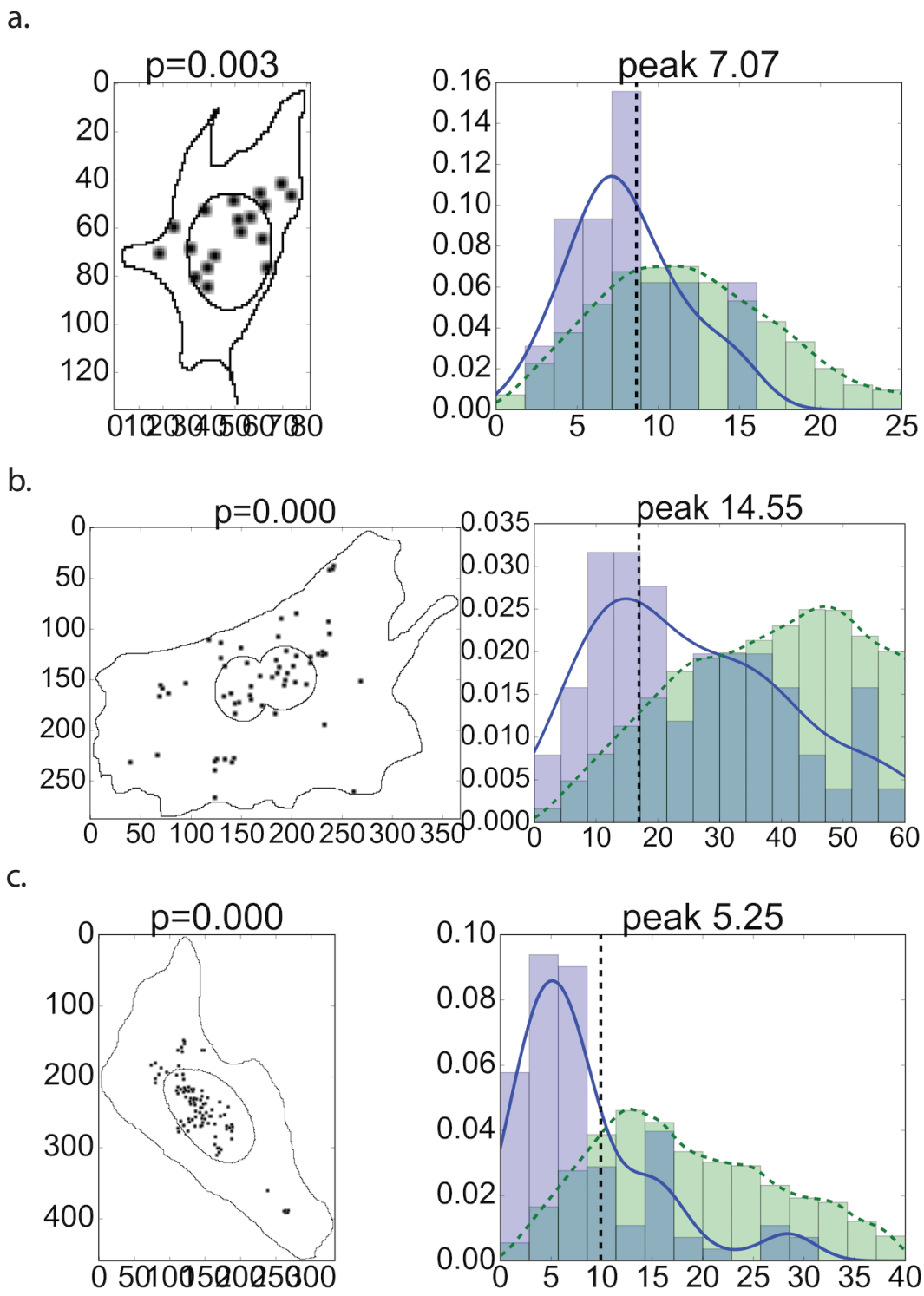

Figure 24. PLA analysis in single cells

(a.-c.) Examples of the analysis of PLA interaction puncta of Arl2 with PDEδ in TSC2+/+ MEF **(a.)**, TSC2-/- MEF **(b.)** and HeLa **cells (c.)** (see also PLA distribution analysis in Materials and Methods). Left: generated cell mask derived from maximal intensity projection where black dots represent PLA interaction puncta in a cell. Blue histogram: distribution of puncta relative to the nuclear center, green histogram: random distribution for the representative cell. X-axis: punctum distance from nuclear center (µm); y-axis: frequency of puncta.

3.4. Cell growth depends on perinuclear release of Rheb-GTP from PDEδ

Since PDEδ knockdown resulted in decreased activity of mTORC1 downstream effectoors in growh-factor responsive cells, we correlated this with cell growth and proliferation, processes highly regulated by mTOR.

For this, we performed impedance-based real-time cell analyzer (RTCA) measurements in TSC2+/+ and TSC2-null MEFs with and without PDEδ knockout.

A prominent growth inhibitory effect was observed in TSC2+/+ PDEδ-null MEFs (**Figure 25.a.)**. However, the TSC2, PDEδ-null MEFs exhibited a faster growth rate than the empty vector control (**Figure 25.b.)** corroborating the tight interaction of Rheb-GTP with mTORC1 that propagates growth signals. The reason why the TSC2, PDEδ-null cells grow faster as the parental TCS2 null cells is likely the increased amount of Rheb-GTP interacting with mTOR that cannot get solubilized by PDEδ.

To evaluate long-term effects of PDEδ knockout on cell growth and proliferation, we seeded the same number of TSC2+/+, TSC2+/+ E.V. and TSC2+/+ PDEδ-null MEFs, and monitored colony formation over the course of 10 days (**Figure 25.c.**). Colony formation completely reflected the RTCA growth profiles (**Figure 25.d.)**, where TSC2+/+, PDEδ-null cells generated only a few colonies while TSC2, PDEδ-null cells generated significantly more colonies as compared to the parental cell lines. These results show that the perinuclear concentration of Rheb as maintained by the PDEδ/Arl2 cycle is necessary for efficient mTOR engagement and activation of anabolic processes in growth-factor responsive cells.

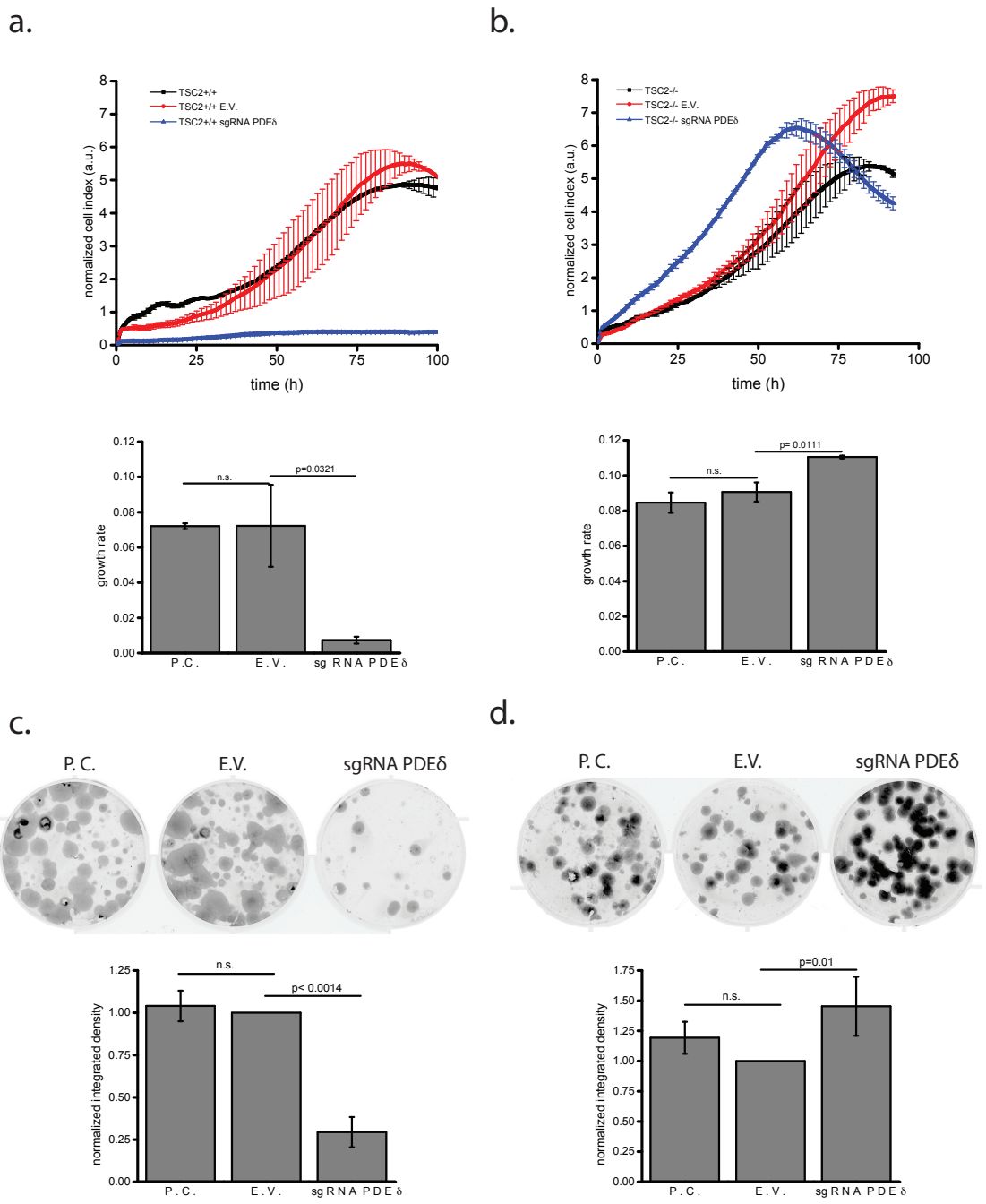

Figure 25. Cell growth depends on perinuclear release of Rheb-GTP from PDEδ

(**a.,b.**) Upper panels: Representative RTCA growth profiles of TSC2+/+ MEF (black), TSC2+/+ E.V. MEF (red) and TSC2+/+ sgRNA PDEδ MEF (blue) ± s.d. in **a.** and TSC2-/- MEF (black), TSC2-/- E.V. MEF (red) and TSC2-/- sgRNA PDEδ MEF (blue) ± s.d. in **b.**. Lower panels: Average growth rate ± s.e.m. between 40 and 60 hours from three independent experiments of all cell lines with corresponding p values. (**c.,d.**) Upper panels: Representative images of colony formation assay of TSC2+/+ MEF, TSC2+/+ E.V. MEF and TSC2+/+ sgRNA PDEδ MEF in **c.** and TSC2-/- MEF, TSC2-/- E.V. MEF and TSC2-/- sgRNA PDEδ MEF in **d.**. Cells were seeded at same density and grown for 10 days. Lower panels: Graphs represent quantification of area coverage for all cell lines ± s.e.m. based on three independent experiments, with corresponding p values. All p values were obtained by unpaired t-test. P values >0.05 labeled as not significant (n.s.).

4. DISCUSSION

Proper information processing is a complicated, yet necessary network of events taking place inside of the cell, responsible for maintaining its identity in the ever-changing surrounding environment. The cellular identity in this context does not refer to robust response, keeping the cell in one state upon one available stimulus, as the type, amount, even the combination of various stimuli drives different, fine-tuned responses appropriate for a certain condition. Cell growth and protein synthesis are predecessors for other, more complicated processes such as proliferation, differentiation, but as well, apoptosis. The response to various stimuli, such as growth factors, hormones, nutrients, energy and oxygen availability events has a crucial importance to maintain cell and organismal homeostasis. All of these inputs converge on a single protein kinase, mTOR, whose activation is the final checkpoint in driving these processes. mTOR kinase is the most important member of the multiprotein complex driving all anabolic processes in the cell. Interestingly, although the information from the cellular exterior finds its way to the mTOR through a red of different upstream proteins, the only direct activator that receives the signals is the small GTPase Rheb. This ubiquitously expressed protein has a nucleotide-dependent activating role towards mTOR kinase, as the activation and signal propagation occurs only when Rheb is GTP, rather than GDP-bound. However, the nucleotide-binding state depends on the balance of GAPs and GEFs, proteins that modulate the intrinsic hydrolytic state of all GTPases, by promoting the GTP hydrolysis or GTP binding, respectively. Small GTPases from a Ras family are included in various signal transduction processes activating different protein kinases, and this cycle of GDP/GTP binding marks their role as a ‘molecular switch’, as those processes are driven by their ‘on’ (GTP-bound) or ‘off’ (GDP-bound) state. Rheb differs from the other members of the Ras family as it is found in a very high activation state in the cells, even in those deprived of growth factors or nutrients. This implies two ways of regulation: either mTOR is constantly active, or the activity state of Rheb is depends mostly on negative regulation, through GAP. The latter one is more likely, as the permanent activation of cell

growth and protein synthesis are not sustainable solutions in cells that need to sense changes in the environment and accordingly formulate the strategy for response. The high activation state of Rheb implied that the GEF for it is not necessary, and that its activity is modulated purely by its GAP, TSC. In the absence of activating stimuli, TSC2 (member of the complex with the GAP domain) localizes to the lysosomes, where the reported interaction between Rheb-GTP and mTOR takes place. Growth factor or hormonal availability relocalizes TSC2 to the cytoplasm, which is additionally phosphorylated at different sites through PI3K/Akt action, resulting in its inactivation. Therefore, Rheb activity and mTOR activation are modulated by spatial segregation of active TSC2.

Rheb is an endomembrane bound protein, which undergoes irreversible posttranslational modification, farnesylation, and displays a high perinuclear concentration. It was reported that these characteristics are necessary for its signaling activity, however, why this is the case, it is unknown.

Additionally, Rheb binds to PDEδ, a GDI-like solubilizing factor for farnesylated Ras proteins, whose role was proven to be essential in maintaining their localization. Through Arl2-GTP mediated localized release, it was reported that K-Ras gets electrostatically trapped on the recycling endosome, from where its plasma-membrane association is reinstated by vesicular transport. However, role of Arl2-GTP mediated release from PDEδ in maintaining localization of Rheb, and in turn its signaling activity, is still unknown. The main aim of this thesis was to address the question of regulating spatial organization of Rheb, and to investigate in depth how this localization affects its signaling ability. Additional aim was to uncover the role of PDEδ/Arl2-GTP mediated spatial cycle and confirm its suspected function as a universal mechanism for maintaining localization of all farnesylated proteins. Finally, by using a model for aberrant mTOR signaling (TSC2-null MEFs), we uncovered the coupling of GTPase and spatial cycle of Rheb.

4.1. Arl2-GTP mediated localized release of farnesylated cargo from PDEδ maintains localization of Ras proteins

Prenyl binding factors have been shown to assist in intracellular trafficking of various Ras isoforms. PDEδ was identified as a solubilizing factor of small G proteins from the Ras family, by enhancing their effective diffusion in the cellular cytosol (**Chandra et al. 2012**). Enhanced kinetics of prenylated Ras proteins, mediated by a cytosolic chaperone, counters their tendencies to equilibrate on all membranes. Both Arf-like proteins, Arl2 and Arl3, were shown to interact with PDEδ in a GTP-dependent manner **(Ismail et al. 2011; Linari, Hanzal-Bayer, and Becker 1999)**. Arl2 was shown to be an allosteric displacement factor for low-affinity farnesylated cargo (K-Ras or Rheb) from PDEδ both, *in vitro* and *in vivo* **(Schmick et al. 2014; Ismail et al. 2011; Linari, Hanzal-Bayer, and Becker 1999; Fansa et al. 2016))**. On the other hand, Arl3 has a prominent role in releasing high-affinity farnesylated cargo (inositol polyphosphate-5-phosphatase E; INPP5E) from PDEδ in primary cilia of cells. However, although Arl3 can release low-affinity cargo from PDEδ *in vitro* (K-Ras or Rheb), it does not seem to have this role *in vivo* **(Fansa et al. 2016)**, as the knockdown of Arl2 alone was sufficient to mislocalize K-Ras **(Schmick et al. 2014).** We have shown that only Arl2 knockdown results in mislocalization of Rheb, corroborating its prominent role in release of farnesylated cargo.

It was shown that the Arl2-GTP mediated release from PDEδ must be localized in cells in order to maintain the K-Ras out-of-equilibrium plasma membrane localization. Interestingly, this localized release was not confirmed at the plasma membrane, but the likely site was perinuclear region of the cell. It was corroborated that perinuclear area of the cell is where the active form of Arl2 is present, however, due to technical limitations (overexpressed proteins), it was not shown directly (**Schmick et al. 2014**).

Proximity ligation assay is an antibody-based assay that depicts interaction of two or more proteins in the cell on endogenous level (**Soderberg et al. 2006**). The interaction punctae for Arl2 and PDEδ were prominent in the perinuclear region of the cell, compared to the rest. It indeed showed that the perinuclear

area is the location of Arl2-GTP and PDEδ interaction, which results in displacement of farnesylated cargo. Since Rheb does not reside on organelles exhibiting vesicular transport, it does not accumulate on the plasma membrane. However, the typical perinuclear enrichment it does display could be explained through its displacement from PDEδ via Arl2-GTP activity. Upon treatment with small-molecule PDEδ inhibitor, Deltarasin, both mCherry-Rheb and mCitrine-Rheb HVR have shown the reduced perinuclear accumulation. The fact that mCitrine-Rheb HVR showed perinuclear enrichment pointed additionally that the site of Arl2-GTP mediated release of farnesylated cargo from PDEδ is in this cellular region. Treatment with Deltarasin resulted in decreased enrichment, showing that solubilization through PDEδ is necessary for its maintainance. Altogether, these results demonstrated that spatial cycles mediated by Arl2-GTP and PDEδ represent a universal mechanism, which by countering equilibration tendencies of farnesylated Ras proteins maintains their out-of-equilibrium localization, important for their signaling output.

4.2. Perinuclear Rheb concentration depends on the activity state of Rheb

G domain of small GTPases is the locus of nucleotide binding, GTP-hydrolysis and effector binding. It is a part of the protein that determines its activity (**Wittinghofer and Vetter 2011**). It was reported however, that a C-terminal farnesylated part of the protein responsible for membrane binding, is essential for maintaining its signaling activity **(Clark et al. 1997; Buerger, DeVries, and Stambolic 2006**).

We have uncovered that the interaction between PDEδ and Arl2-GTP is the basis for maintainance of perinuclear localization of Rheb. Both PDEδ knockout and Arl2 knockdown resulted in mislocalization of Rheb, in two different ways: loss of PDEδ resulted in relocalization on all membranes, while loss of Arl2 in increased soluble fraction of Rheb. Since this effect was only visible in TSC2+/+ MEFs, but not in TSC2-null MEFs, this implied that the activity state of Rheb is coupled to generation of this out-of-equilibrium localization.

Unlike all the other small GTPases, where both the interaction and the activation of their respective effectors depend on their GTP-binding, Rheb interacts with mTOR in both GDP and GTP bound state **(Long et al. 2005; Smith et al. 2005**). However, the activation of mTOR occurs only when it is in GTP bound state.

It was reported than amino acid withdrawal inhibits the interaction between Rheb and mTOR (**Sancak et al. 2010; Bar-Peled et al. 2012**). Upon amino acid withdrawal, mTOR relocalizes to the cytosol, while Rag GTPases recruit TSC2 to the lysosome, which inactivates Rheb **(Demetriades, Doumpas, and Teleman 2014**). However, it is known that the TSC2 is inactivating Rheb in the absence of other activating stimuli as well, and that it is active at the lysosome, where it hydrolyzes active Rheb **(Demetriades, Plescher, and Teleman 2016**). Since the perinuclear concentration of mCitrine-Rheb HVR decreased in both TSC2+/+ and TSC2-null sgRNA PDEδ cells, while it remained unchanged in the same cells expressing constitutively active mCitrine-Rheb Q64L, we corroborated that even if the interaction between mTOR and Rheb exists in the GDP bound state; the binding affinity of Rheb GTP-mTOR complex is higher than Rheb GDP-mTOR. Since TSC2-null cells possess constitutively active Rheb, we could only presume that lack of any effect on Rheb localization upon disruption of PDEδ/Arl2 cycle is due to the tight interaction of Rheb-GTP with mTOR, which impairs resolubilization of Rheb and new entrance to the spatial cycle.

4.3. TSC2 GAP activity determines the localization of Rheb

It was reported that the activation of mTORC1 relies on two aspects: activation of Rheb as a result of various upstream stimuli and proper mTOR localization (**Guertin and Sabatini 2007**). Both of these aspects are determined by the activity of the Rheb GAP TSC2. It was widely regarded that the phosphorylation of TSC2 on different residues through Akt completely deactivates it; therefore, Rheb can bind GTP (**Cai et al. 2006**). However*, in vitro* studies have suggested that its GAP activity is largely intact upon Akt phosphorylation, suggesting a different mechanism of its activation **(Menon et al. 2014**). It was reported that depending on the growth factor and amino acid

availability TSC2 translocates to/from the lysosomes where it promotes GTP-hydrolysis on Rheb and blocks mTOR kinase (**Demetriades, Doumpas, and Teleman 2014**). Studies concerning the interaction between Rheb and mTOR have all led to different conclusions. One study reported that the interaction does not depend on the nucleotide-bound state, and that it was stronger with mutants that exist in GDP bound form (**Long et al. 2005**). However, studies made in yeast have shown that the interaction is indeed preferential with GTP bound form (**Urano et al. 2001**). Additionally, since it has been challenging to find Rheb associated with mTORC1 upon in vitro incubation, additional hypothesis arose claiming that the interaction between the two is transient and loose **(Parmar and Tamanoi 2010**). We have shown that nucleotide-binding state of Rheb affects its localization as in cells with constitutively active Rheb its perinuclear concentration was significantly higher compared to cells responsive to growth factors. Since various expression levels of PDEδ had no effect on solubilizing this active Rheb, our presumption is that this Rheb is contained in the perinuclear region, presumably through interaction with mTOR, which is tighter in case of GTP-bound Rheb.

This implies that once the GTPase cycle (GTP/GDP exchange) of Rheb is stopped, and Rheb is locked in the active state, due to the presence of stimuli or mutation, this interaction with mTOR impairs resolubilization and stalls the PDEδ/Arl2 spatial cycle as well.

4.4. mTOR signaling activity relies on perinuclear Rheb concentration

Spatial cycle of all Ras proteins relies on the posttranslational farnesylation and the ability of PDEδ to solubilize these proteins in the cytosol (**Chandra et al. 2012; Schmick et al. 2014; Schmick, Kraemer, and Bastiaens 2015**). Responsiveness to growth factors, a trait necessary for activation of Rheb and proper mTORC1 regulation, proved to be coupled to the spatial cycle. PDEδ and Arl2 localization of Rheb was already disrupted upon interference with its spatial cycle, however, only in growth-factor responsive cells. Signal propagation through mTOR kinase relies on its binding to active, GTP-bound Rheb. The phosphorylation of downstream effector S6 was lower than the

control only in growth factor responsive cells, but not in cells with constitutively active Rheb, where it remained unchanged. TSC2+/+ cells responded to insulin stimulation as well, visible in up regulation of phosphorylation of S6, even the cells with PDEδ knockout. This implies that the spatial cycle is not necessary to maintain responsiveness to growth factors. However, it was reported that mice with an inhibited or downregulated mTORC1 signaling have a lower body weight, liver, and that this has lethal consequences (**Polak et al. 2008; Guridi et al. 2016**). Therefore, to maintain the cellular homeostasis, the spatial cycle is necessary to generate a sufficient pool of Rheb to be activated and interact with mTOR.

Cell growth and cell proliferation are two complex processes regulated through a plethora of activating signals coming from the extracellular environment. mTOR is the main regulator of cell growth; therefore, impairing its proper activation would have an inhibitory effect on this process.

Colony formation assay and RTCA growth curves have shown that the prominent inhibitory effect on cell growth was only visible in TSC2+/+ MEFs with PDEδ knockout. This confirmed the hypothesis that the spatial cycle mediated by PDEδ and Arl2-GTP is necessary to generate sufficient amount of growth factor-responsive Rheb in the perinuclear area to activate mTOR. Interestingly, TSC2-null sgRNA PDEδ MEFs have displayed even a higher rate of growth and colony formation compared to their control. This was in line with the hypothesis that the interaction between mTOR and Rheb-GTP is stable and this Rheb does not dissociate as high as Rheb-GDP, therefore the spatial cycle is stalled. However, in cells with PDEδ knockout, this is even more efficient, as there is no loss to cytosol.

Still, it is known that PI3K/Akt/mTOR and Ras/Erk signaling axis have a lot of intersecting points, enabling crosstalk (**Mendoza, Er, and Blenis 2011**). In order to confirm whether this effect is attributed to the enhanced mTOR activity, the levels of Akt, Erk and other kinases known to intersect with mTOR signaling axis should be monitored in order to confirm that positive growth effect can be attributed to mTOR signaling specifically.

4.5. PDEδ-mediated solibilization is necessary for nucleotide exchange on Rheb

Rheb has been found in unusually high activation state in cells, however guanine nucleotide exchange factors have not yet been identified, and their necessity for guanine nucleotide exchange on Rheb is still not clear **(Im et al. 2002; Inoki et al. 2003)**. It was reported that the intrinsic nucleotide exchange rate of Rheb is markedly higher in solution than upon association with a bilayer membrane **(Mazhab-Jafari et al. 2013)**, which indicates that soluble Rheb will exchange GDP more quickly to GTP, which is in high excess in cells. In addition, it was reported that Rheb has a higher affinity to bind GTP than GDP **(Patel et al. 2003)**, and unlike other GTPases, it possesses an auto inhibited mechanism of GTP-hydrolysis, favoring the GTP-bound state in the absence of GAP activity **(Mazhab-Jafari et al. 2012).** In the absence of upstream stimuli, this GAP activity is present only on the perinuclear lysosomal membranes **(Demetriades, Doumpas, and Teleman 2014; Menon et al. 2014; Demetriades, Plescher, and Teleman 2016)**, allowing for nucleotide exchange on Rheb localized outside this area. Solely farnesylated proteins have a high partitioning rate from membranes to the cytosol (2:1) **(Schmick et al. 2014)**. Therefore, a very high proportion of Rheb is available to bind to PDEδ and be in a soluble state, which favors GTP-binding. This passive process of PDEδ binding to prenylated Ras proteins occurs regardless of their GDP/GTP-bound state. However, for Rheb, solubilization as well results in its removal from the perinuclear-membrane associated TSC2 GAP activity. This promotes exchange of the bound guanine nucleotide to GTP in the cytosol. Therefore, solubilization mediated by PDEδ is a necessary step not only for concentrating Rheb-GTP at the perinuclear membranes via Arl2-GTP activity, but as well in direct promotion of its GTP-binding. This coupling of the generic activity of the PDEδ/Arl2-GTP mechanism to a stimulus-dependent localization of regulatory protein TSC2 enables tunable signal transduction mediated by Rheb and promotion of anabolic processes.

4.6. Spatial cycle of Rheb is coupled to its GTPase cycle

Rheb is farnesylated Ras protein associating with endomembranes. Due to lack of an additional targeting sequence that would associate it with specific membrane compartments, as a solely farnesylated protein it displays a high partitioning rate between endomembranes and the cytosol. In the cytosol, it is sequestered by a GDI-like solubilizing factor PDEδ, which possesses a hydrophobic binding pocket for prenylated proteins. This complex has a high effective diffusion speed and explores intracellular space on a faster rate than Rheb alone. Once it reaches perinucelar area, Arl2-GTP, by binding to PDEδ, causes a conformational change that places hydrophobic pocket in the closed state, initiating displacement of Rheb on the perinuclear membranes. Both Rheb GAP, TSC2 and effector mTOR reside in this region. When cells are deprived of growth factors or hormones, TSC2 promotes GTP hydrolysis on Rheb, disabling perinuclear Rheb from activating mTOR. This results in Rheb dissociation from these membranes and subsequent resolubilization by PDEδ. Since it is spatially segregated from its GAP, Rheb in the cytosol binds GTP, which is in high excess in cells, and reenters the spatial/GTPase cycle. When the cells are stimulated with growth factors, TSC2 is phosphorylated through Akt, and relocalizes from the perinuclear region to the cytosol. Therefore, Rheb-GTP, released from PDEδ through local Arl2-GTP activity can now bind to and activate mTOR, resulting in signal propagation to downstream effectors. As a consequence of this interaction, the spatial cycle, mediated by PDEδ and Arl2-GTP is stalled, as Rheb-GTP is stabilized on the perinuclear membranes through interaction with mTOR and does not dissociate significantly from the perinuclear membranes (**Figure 26**).

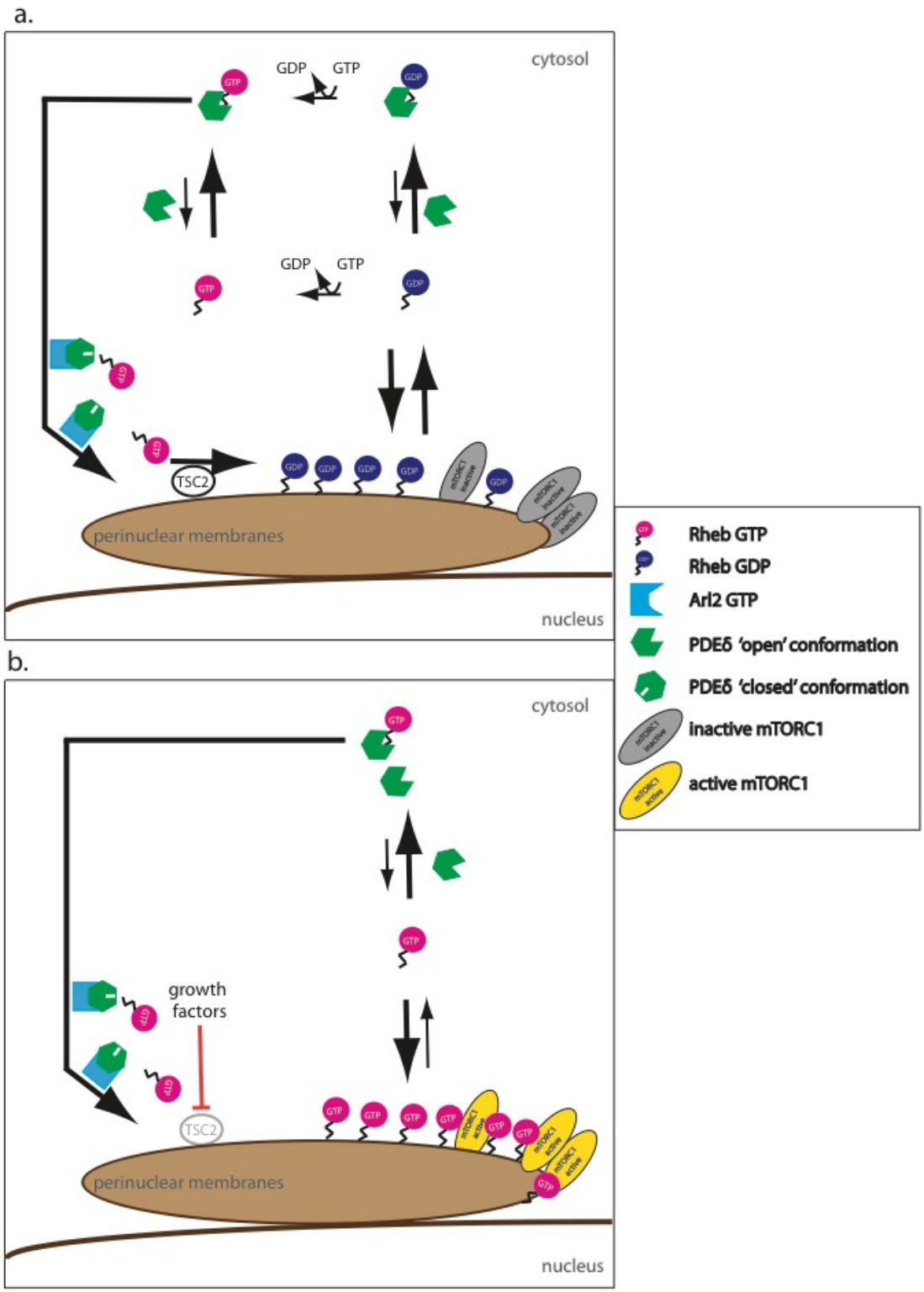

Figure 23. Coupling of GTPase cycle and spatial cycle of Rheb

Model explaining coupling of GTPase and spatial cycle of Rheb. **a.** Soluble GTP-bound Rheb is bound to PDEδ.. Once the complex reaches perinuclear area of the cell, the allosteric displacement factor for farnesylated cargo, Arl2-GTP, binds to PDEδ, resulting in release of farnesylated cargo on perinuclear membranes, including the lysosome. Here, TSC2 hydrolyzes GTP bound to Rheb, and GDP-Rheb, unable to ind and activate mTOR, dissociates from perinuclear membranes to the cytosol, where it can exchange GDP to GTP and get reactivated. **b.** Presence of growth factors inactivates TSC2, therefore, active Rheb on perinucelar membranes, delivered by

PDEδ/Arl2-GTP activity, can bind to and activate mTOR: This results in decreased dissociation from the perinucelar membranes, effectively stopping spatial cycle.

4.6. Conclusion

The work in this thesis focuses on two mechanistically different processes that, by their coupling, enable the protein to exert its functional role in the cell. GTPase cycles determine the activity of G-proteins, but as well the activity of the entire signaling axis in which these proteins are placed. Through their proper regulation, the specificity, tunability and response to environmental signals are enabled.

Spatial cycles are a way of countering entropic tendencies of proteins, arising from their structure, which would result in diluted and inefficient signal propagation.

The intersection of the generic spatial mechanism and specific activity cycle of GTPase represents a unique mechanism for function of small GTPase Rheb and its effector mTORC1. We have shown that the role of solubilizing factor PDEδ is crucial in this particular system, not only as a factor responsible for countering equilibration on all membranes, but as well as an effective “GEF”, promoting efficient nucleotide exchange Rheb. It represents the rate-limiting factor in the entire spatial cycle of Rheb, as its loss results in significant decrease in mTORC1 activity and mislocalization of Rheb.

However, non-functional GTPase cycle impairs the importance of the spatial cycle: if Rheb is permanently GDP-loaded, the spatial cycle is futile, as it cannot exert its function towards mTOR. If Rheb is GTP-loaded, the spatial cycle is halted, due to low dissociation of Rheb from membranes, which results in permanent mTOR activation.

We have shown that regulated GTPase cycle of Rheb, coupled to its spatial cycle enables sensing of the environment through the mTORC1-signaling axis, which results in controlled cellular response.

This coupling allows the cells to sustain a basal level of anabolic processes occurring, and maintains its homeostasis.

LITERATURE

1. Abraham, R. T., and G. J. Wiederrecht. 1996. 'Immunopharmacology of rapamycin', *Annu Rev Immunol*, 14: 483-510.
2. Ahearn, I. M., K. Haigis, D. Bar-Sagi, and M. R. Philips. 2012. 'Regulating the regulator: post-translational modification of RAS', *Nat Rev Mol Cell Biol*, 13: 39-51.
3. Bar-Peled, L., L. D. Schweitzer, R. Zoncu, and D. M. Sabatini. 2012. 'Ragulator is a GEF for the rag GTPases that signal amino acid levels to mTORC1', *Cell*, 150: 1196-208.
4. Bar-Sagi, D. 2001. 'A Ras by any other name', *Mol Cell Biol*, 21: 1441-3.
5. Bastiaens, Philippe I. H., and Anthony Squire. 1999. 'Fluorescence lifetime imaging microscopy: spatial resolution of biochemical processes in the cell', *Trends Cell Biol*, 9: 48-52.
6. Becker, W. 2015. *Advanced Time-Correlated Single-Photon Counting Applications* (Springer).
7. Benvenuto, G., S. Li, S. J. Brown, R. Braverman, W. C. Vass, J. P. Cheadle, D. J. Halley, J. R. Sampson, R. Wienecke, and J. E. DeClue. 2000. 'The tuberous sclerosis-1 (TSC1) gene product hamartin suppresses cell growth and augments the expression of the TSC2 product tuberin by inhibiting its ubiquitination', *Oncogene*, 19: 6306-16.
8. Betz, Charles, and Michael N. Hall. 2013. 'Where is mTOR and what is it doing there?', *The Journal of Cell Biology*, 203: 563-74.
9. Biou, V., and J. Cherfils. 2004. 'Structural principles for the multispecificity of small GTP-binding proteins', *Biochemistry*, 43: 6833-40.
10. Bourne, H. R., L. Wrischnik, and C. Kenyon. 1990. 'Ras proteins. Some signal developments', *Nature*, 348: 678-9.
11. Brown, E. J., M. W. Albers, T. B. Shin, K. Ichikawa, C. T. Keith, W. S. Lane, and S. L. Schreiber. 1994. 'A mammalian protein targeted by G1-arresting rapamycin-receptor complex', *Nature*, 369: 756-8.
12. Buerger, C., B. DeVries, and V. Stambolic. 2006. 'Localization of Rheb to the endomembrane is critical for its signaling function', *Biochem Biophys Res Commun*, 344: 869-80.
13. Cai, S. L., A. R. Tee, J. D. Short, J. M. Bergeron, J. Kim, J. Shen, R. Guo, C. L. Johnson, K. Kiguchi, and C. L. Walker. 2006. 'Activity of TSC2 is inhibited by AKT-mediated phosphorylation and membrane partitioning', *J Cell Biol*, 173: 279-89.
14. Cantley, L. C. 2002. 'The phosphoinositide 3-kinase pathway', *Science*, 296: 1655-7.
15. Chandra, A., H. E. Grecco, V. Pisupati, D. Perera, L. Cassidy, F. Skoulidis, S. A. Ismail, C. Hedberg, M. Hanzal-Bayer, A. R. Venkitaraman, A. Wittinghofer, and P. I. Bastiaens. 2012. 'The GDI-like solubilizing factor PDEdelta sustains the spatial organization and signalling of Ras family proteins', *Nat Cell Biol*, 14: 148-58.
16. Chang, E. H., M. A. Gonda, R. W. Ellis, E. M. Scolnick, and D. R. Lowy. 1982. 'Human genome contains four genes homologous to

transforming genes of Harvey and Kirsten murine sarcoma viruses', *Proc Natl Acad Sci U S A*, 79: 4848-52.
17. Chantranupong, L., R. L. Wolfson, J. M. Orozco, R. A. Saxton, S. M. Scaria, L. Bar-Peled, E. Spooner, M. Isasa, S. P. Gygi, and D. M. Sabatini. 2014. 'The Sestrins interact with GATOR2 to negatively regulate the amino-acid-sensing pathway upstream of mTORC1', *Cell Rep*, 9: 1-8.
18. Chen, J., X. F. Zheng, E. J. Brown, and S. L. Schreiber. 1995. 'Identification of an 11-kDa FKBP12-rapamycin-binding domain within the 289-kDa FKBP12-rapamycin-associated protein and characterization of a critical serine residue', *Proc Natl Acad Sci U S A*, 92: 4947-51.
19. Chiu, M. I., H. Katz, and V. Berlin. 1994. 'RAPT1, a mammalian homolog of yeast Tor, interacts with the FKBP12/rapamycin complex', *Proc Natl Acad Sci U S A*, 91: 12574-8.
20. Clark, G. J., M. S. Kinch, K. Rogers-Graham, S. M. Sebti, A. D. Hamilton, and C. J. Der. 1997. 'The Ras-related protein Rheb is farnesylated and antagonizes Ras signaling and transformation', *J Biol Chem*, 272: 10608-15.
21. Clegg, R. M. 1992. 'Fluorescence resonance energy transfer and nucleic acids', *Methods Enzymol*, 211: 353-88.
22. Correll, R. N., C. Pang, D. M. Niedowicz, B. S. Finlin, and D. A. Andres. 2008. 'The RGK family of GTP-binding proteins: regulators of voltage-dependent calcium channels and cytoskeleton remodeling', *Cell Signal*, 20: 292-300.
23. Cox, A. D., and C. J. Der. 2002. 'Ras family signaling: therapeutic targeting', *Cancer Biol Ther*, 1: 599-606.
24. Demetriades, C., N. Doumpas, and A. A. Teleman. 2014. 'Regulation of TORC1 in response to amino acid starvation via lysosomal recruitment of TSC2', *Cell*, 156: 786-99.
25. Demetriades, C., M. Plescher, and A. A. Teleman. 2016. 'Lysosomal recruitment of TSC2 is a universal response to cellular stress', *Nat Commun*, 7: 10662.
26. DerMardirossian, C., and G. M. Bokoch. 2005. 'GDIs: central regulatory molecules in Rho GTPase activation', *Trends Cell Biol*, 15: 356-63.
27. DeYoung, M. P., P. Horak, A. Sofer, D. Sgroi, and L. W. Ellisen. 2008. 'Hypoxia regulates TSC1/2-mTOR signaling and tumor suppression through REDD1-mediated 14-3-3 shuttling', *Genes Dev*, 22: 239-51.
28. Dibble, C. C., W. Elis, S. Menon, W. Qin, J. Klekota, J. M. Asara, P. M. Finan, D. J. Kwiatkowski, L. O. Murphy, and B. D. Manning. 2012. 'TBC1D7 is a third subunit of the TSC1-TSC2 complex upstream of mTORC1', *Mol Cell*, 47: 535-46.
29. Dirac-Svejstrup, A. B., J. Shorter, M. G. Waters, and G. Warren. 2000. 'Phosphorylation of the vesicle-tethering protein p115 by a casein kinase II-like enzyme is required for Golgi reassembly from isolated mitotic fragments', *J Cell Biol*, 150: 475-88.
30. Domchek, S. M., K. R. Auger, S. Chatterjee, T. R. Burke, Jr., and S. E. Shoelson. 1992. 'Inhibition of SH2 domain/phosphoprotein association by a nonhydrolyzable phosphonopeptide', *Biochemistry*, 31: 9865-70.

31. Dransart, E., A. Morin, J. Cherfils, and B. Olofsson. 2005. 'Uncoupling of inhibitory and shuttling functions of rho GDP dissociation inhibitors', *J Biol Chem*, 280: 4674-83.
32. Etienne-Manneville, S., and A. Hall. 2002. 'Rho GTPases in cell biology', *Nature*, 420: 629-35.
33. Fansa, E. K., S. K. Kosling, E. Zent, A. Wittinghofer, and S. Ismail. 2016. 'PDE6delta-mediated sorting of INPP5E into the cilium is determined by cargo-carrier affinity', *Nat Commun*, 7: 11366.
34. Florio, S. K., R. K. Prusti, and J. A. Beavo. 1996. 'Solubilization of membrane-bound rod phosphodiesterase by the rod phosphodiesterase recombinant delta subunit', *J Biol Chem*, 271: 24036-47.
35. Förster, Th. 1948. 'Zwischenmolekulare Energiewanderung und Fluoreszenz', *Annalen der Physik*, 437: 55-75.
36. French, Todd E., Enrico Gratton, and John S. Maier. 1992. "Frequency-domain imaging of thick tissues using a CCD." In, 254-61.
37. Frias, M. A., C. C. Thoreen, J. D. Jaffe, W. Schroder, T. Sculley, S. A. Carr, and D. M. Sabatini. 2006. 'mSin1 is necessary for Akt/PKB phosphorylation, and its isoforms define three distinct mTORC2s', *Curr Biol*, 16: 1865-70.
38. Gai, Z., W. Chu, W. Deng, W. Li, H. Li, A. He, M. Nellist, and G. Wu. 2016. 'Structure of the TBC1D7-TSC1 complex reveals that TBC1D7 stabilizes dimerization of the TSC1 C-terminal coiled coil region', *J Mol Cell Biol*.
39. Gillespie, P. G., R. K. Prusti, E. D. Apel, and J. A. Beavo. 1989. 'A soluble form of bovine rod photoreceptor phosphodiesterase has a novel 15-kDa subunit', *J Biol Chem*, 264: 12187-93.
40. Goody, R. S., A. Rak, and K. Alexandrov. 2005. 'The structural and mechanistic basis for recycling of Rab proteins between membrane compartments', *Cell Mol Life Sci*, 62: 1657-70.
41. Grecco, H. E., P. Roda-Navarro, and P. J. Verveer. 2009. 'Global analysis of time correlated single photon counting FRET-FLIM data', *Opt Express*, 17: 6493-508.
42. Gromov, P. S., P. Madsen, N. Tomerup, and J. E. Celis. 1995. 'A novel approach for expression cloning of small GTPases: identification, tissue distribution and chromosome mapping of the human homolog of rheb', *FEBS Lett*, 377: 221-6.
43. Guertin, D. A., and D. M. Sabatini. 2007. 'Defining the role of mTOR in cancer', *Cancer Cell*, 12: 9-22.
44. Guridi, M., B. Kupr, K. Romanino, S. Lin, D. Falcetta, L. Tintignac, and M. A. Ruegg. 2016. 'Alterations to mTORC1 signaling in the skeletal muscle differentially affect whole-body metabolism', *Skelet Muscle*, 6: 13.
45. Guzman, C., M. Bagga, A. Kaur, J. Westermarck, and D. Abankwa. 2014. 'ColonyArea: an ImageJ plugin to automatically quantify colony formation in clonogenic assays', *PLoS One*, 9: e92444.
46. Hall, A., C. J. Marshall, N. K. Spurr, and R. A. Weiss. 1983. 'Identification of transforming gene in two human sarcoma cell lines as a new member of the ras gene family located on chromosome 1', *Nature*, 303: 396-400.

47. Hancock, J. F., K. Cadwallader, H. Paterson, and C. J. Marshall. 1991. 'A CAAX or a CAAL motif and a second signal are sufficient for plasma membrane targeting of ras proteins', *Embo j*, 10: 4033-9.
48. Hancock, J. F., A. I. Magee, J. E. Childs, and C. J. Marshall. 1989. 'All ras proteins are polyisoprenylated but only some are palmitoylated', *Cell*, 57: 1167-77.
49. Hancock, J. F., H. Paterson, and C. J. Marshall. 1990. 'A polybasic domain or palmitoylation is required in addition to the CAAX motif to localize p21ras to the plasma membrane', *Cell*, 63: 133-9.
50. Hanker, A. B., N. Mitin, R. S. Wilder, E. P. Henske, F. Tamanoi, A. D. Cox, and C. J. Der. 2010. 'Differential requirement of CAAX-mediated posttranslational processing for Rheb localization and signaling', *Oncogene*, 29: 380-91.
51. Hanzal-Bayer, M., L. Renault, P. Roversi, A. Wittinghofer, and R. C. Hillig. 2002. 'The complex of Arl2-GTP and PDE delta: from structure to function', *Embo j*, 21: 2095-106.
52. Hara, K., Y. Maruki, X. Long, K. Yoshino, N. Oshiro, S. Hidayat, C. Tokunaga, J. Avruch, and K. Yonezawa. 2002. 'Raptor, a binding partner of target of rapamycin (TOR), mediates TOR action', *Cell*, 110: 177-89.
53. Hara, K., K. Yonezawa, Q. P. Weng, M. T. Kozlowski, C. Belham, and J. Avruch. 1998. 'Amino acid sufficiency and mTOR regulate p70 S6 kinase and eIF-4E BP1 through a common effector mechanism', *J Biol Chem*, 273: 14484-94.
54. Hay, N., and N. Sonenberg. 2004. 'Upstream and downstream of mTOR', *Genes Dev*, 18: 1926-45.
55. Heitman, J., N. R. Movva, and M. N. Hall. 1991. 'Targets for cell cycle arrest by the immunosuppressant rapamycin in yeast', *Science*, 253: 905-9.
56. Hsu, Y. C., J. J. Chern, Y. Cai, M. Liu, and K. W. Choi. 2007. 'Drosophila TCTP is essential for growth and proliferation through regulation of dRheb GTPase', *Nature*, 445: 785-8.
57. Huang, J., and B. D. Manning. 2008. 'The TSC1-TSC2 complex: a molecular switchboard controlling cell growth', *Biochem J*, 412: 179-90.
58. Im, E., F. C. von Lintig, J. Chen, S. Zhuang, W. Qui, S. Chowdhury, P. F. Worley, G. R. Boss, and R. B. Pilz. 2002. 'Rheb is in a high activation state and inhibits B-Raf kinase in mammalian cells', *Oncogene*, 21: 6356-65.
59. Inoki, K., Y. Li, T. Xu, and K. L. Guan. 2003. 'Rheb GTPase is a direct target of TSC2 GAP activity and regulates mTOR signaling', *Genes Dev*, 17: 1829-34.
60. Inoki, K., Y. Li, T. Zhu, J. Wu, and K. L. Guan. 2002. 'TSC2 is phosphorylated and inhibited by Akt and suppresses mTOR signalling', *Nat Cell Biol*, 4: 648-57.
61. Ismail, S. A., Y. X. Chen, A. Rusinova, A. Chandra, M. Bierbaum, L. Gremer, G. Triola, H. Waldmann, P. I. Bastiaens, and A. Wittinghofer. 2011. 'Arl2-GTP and Arl3-GTP regulate a GDI-like transport system for farnesylated cargo', *Nat Chem Biol*, 7: 942-9.

62. Jinek, M., K. Chylinski, I. Fonfara, M. Hauer, J. A. Doudna, and E. Charpentier. 2012. 'A programmable dual-RNA-guided DNA endonuclease in adaptive bacterial immunity', *Science*, 337: 816-21.
63. Kandt, R. S., J. L. Haines, M. Smith, H. Northrup, R. J. Gardner, M. P. Short, K. Dumars, E. S. Roach, S. Steingold, S. Wall, and et al. 1992. 'Linkage of an important gene locus for tuberous sclerosis to a chromosome 16 marker for polycystic kidney disease', *Nat Genet*, 2: 37-41.
64. Kim, D. H., D. D. Sarbassov, S. M. Ali, J. E. King, R. R. Latek, H. Erdjument-Bromage, P. Tempst, and D. M. Sabatini. 2002. 'mTOR interacts with raptor to form a nutrient-sensitive complex that signals to the cell growth machinery', *Cell*, 110: 163-75.
65. Kim, D. H., D. D. Sarbassov, S. M. Ali, R. R. Latek, K. V. Guntur, H. Erdjument-Bromage, P. Tempst, and D. M. Sabatini. 2003. 'GbetaL, a positive regulator of the rapamycin-sensitive pathway required for the nutrient-sensitive interaction between raptor and mTOR', *Mol Cell*, 11: 895-904.
66. Konstantinopoulos, P. A., M. V. Karamouzis, and A. G. Papavassiliou. 2007. 'Post-translational modifications and regulation of the RAS superfamily of GTPases as anticancer targets', *Nat Rev Drug Discov*, 6: 541-55.
67. Koos, B., L. Andersson, C. M. Clausson, K. Grannas, A. Klaesson, G. Cane, and O. Soderberg. 2014. 'Analysis of protein interactions in situ by proximity ligation assays', *Curr Top Microbiol Immunol*, 377: 111-26.
68. Lakowicz, J. R. 1988. 'Principles of frequency-domain fluorescence spectroscopy and applications to cell membranes', *Subcell Biochem*, 13: 89-126.
69. Lakowicz, J. R., H. Szmacinski, K. Nowaczyk, K. W. Berndt, and M. Johnson. 1992. 'Fluorescence lifetime imaging', *Anal Biochem*, 202: 316-30.
70. Laplante, M., and D. M. Sabatini. 2012. 'mTOR signaling in growth control and disease', *Cell*, 149: 274-93.
71. Li, G., and X. C. Zhang. 2004. 'GTP hydrolysis mechanism of Ras-like GTPases', *J Mol Biol*, 340: 921-32.
72. Linari, M., M. Hanzal-Bayer, and J. Becker. 1999. 'The delta subunit of rod specific cyclic GMP phosphodiesterase, PDE delta, interacts with the Arf-like protein Arl3 in a GTP specific manner', *FEBS Lett*, 458: 55-9.
73. Long, X., Y. Lin, S. Ortiz-Vega, K. Yonezawa, and J. Avruch. 2005. 'Rheb binds and regulates the mTOR kinase', *Curr Biol*, 15: 702-13.
74. Lowy, D. R., and B. M. Willumsen. 1993. 'Function and regulation of ras', *Annu Rev Biochem*, 62: 851-91.
75. Ma, X. M., and J. Blenis. 2009. 'Molecular mechanisms of mTOR-mediated translational control', *Nat Rev Mol Cell Biol*, 10: 307-18.
76. Maegley, K. A., S. J. Admiraal, and D. Herschlag. 1996. 'Ras-catalyzed hydrolysis of GTP: a new perspective from model studies', *Proc Natl Acad Sci U S A*, 93: 8160-6.
77. Manning, B. D., and L. C. Cantley. 2007. 'AKT/PKB signaling: navigating downstream', *Cell*, 129: 1261-74.

78. Manning, B. D., A. R. Tee, M. N. Logsdon, J. Blenis, and L. C. Cantley. 2002. 'Identification of the tuberous sclerosis complex-2 tumor suppressor gene product tuberin as a target of the phosphoinositide 3-kinase/akt pathway', *Mol Cell*, 10: 151-62.
79. Marshall, C. J., A. Hall, and R. A. Weiss. 1982. 'A transforming gene present in human sarcoma cell lines', *Nature*, 299: 171-3.
80. Marzesco, A. M., T. Galli, D. Louvard, and A. Zahraoui. 1998. 'The rod cGMP phosphodiesterase delta subunit dissociates the small GTPase Rab13 from membranes', *J Biol Chem*, 273: 22340-5.
81. Maurer-Stroh, S., and F. Eisenhaber. 2005. 'Refinement and prediction of protein prenylation motifs', *Genome Biol*, 6: R55.
82. Mazhab-Jafari, M. T., C. B. Marshall, N. Ishiyama, J. Ho, V. Di Palma, V. Stambolic, and M. Ikura. 2012. 'An autoinhibited noncanonical mechanism of GTP hydrolysis by Rheb maintains mTORC1 homeostasis', *Structure*, 20: 1528-39.
83. Mazhab-Jafari, M. T., C. B. Marshall, P. B. Stathopulos, Y. Kobashigawa, V. Stambolic, L. E. Kay, F. Inagaki, and M. Ikura. 2013. 'Membrane-dependent modulation of the mTOR activator Rheb: NMR observations of a GTPase tethered to a lipid-bilayer nanodisc', *J Am Chem Soc*, 135: 3367-70.
84. McMahon, Harvey T., and Emmanuel Boucrot. 2015. 'Membrane curvature at a glance', *J Cell Sci*, 128: 1065-70.
85. Mendoza, M. C., E. E. Er, and J. Blenis. 2011. 'The Ras-ERK and PI3K-mTOR pathways: cross-talk and compensation', *Trends Biochem Sci*, 36: 320-8.
86. Menon, S., C. C. Dibble, G. Talbott, G. Hoxhaj, A. J. Valvezan, H. Takahashi, L. C. Cantley, and B. D. Manning. 2014. 'Spatial control of the TSC complex integrates insulin and nutrient regulation of mTORC1 at the lysosome', *Cell*, 156: 771-85.
87. Michaelson, D., W. Ali, V. K. Chiu, M. Bergo, J. Silletti, L. Wright, S. G. Young, and M. Philips. 2005. 'Postprenylation CAAX processing is required for proper localization of Ras but not Rho GTPases', *Mol Biol Cell*, 16: 1606-16.
88. Misaki, Ryo, Miki Morimatsu, Takefumi Uemura, Satoshi Waguri, Eiji Miyoshi, Naoyuki Taniguchi, Michiyuki Matsuda, and Tomohiko Taguchi. 2010. 'Palmitoylated Ras proteins traffic through recycling endosomes to the plasma membrane during exocytosis', *The Journal of Cell Biology*, 191: 23-29.
89. Mizuki, N., M. Kimura, S. Ohno, S. Miyata, M. Sato, H. Ando, M. Ishihara, K. Goto, S. Watanabe, M. Yamazaki, A. Ono, S. Taguchi, K. Okumura, M. Nogami, T. Taguchi, A. Ando, and H. Inoko. 1996. 'Isolation of cDNA and genomic clones of a human Ras-related GTP-binding protein gene and its chromosomal localization to the long arm of chromosome 7, 7q36', *Genomics*, 34: 114-8.
90. Nan, X., E. A. Collisson, S. Lewis, J. Huang, T. M. Tamguney, J. T. Liphardt, F. McCormick, J. W. Gray, and S. Chu. 2013. 'Single-molecule superresolution imaging allows quantitative analysis of RAF multimer formation and signaling', *Proc Natl Acad Sci U S A*, 110: 18519-24.

91. Nancy, V., I. Callebaut, A. El Marjou, and J. de Gunzburg. 2002. 'The delta subunit of retinal rod cGMP phosphodiesterase regulates the membrane association of Ras and Rap GTPases', *J Biol Chem*, 277: 15076-84.
92. Ng, Tony, Anthony Squire, Gurdip Hansra, Frederic Bornancin, Corinne Prevostel, Andrew Hanby, William Harris, Diana Barnes, Sandra Schmidt, Harry Mellor, Philippe I. H. Bastiaens, and Peter J. Parker. 1999. 'Imaging Protein Kinase Cα Activation in Cells', *Science*, 283: 2085-89.
93. Nie, Z., D. S. Hirsch, and P. A. Randazzo. 2003. 'Arf and its many interactors', *Curr Opin Cell Biol*, 15: 396-404.
94. Northrup, H., M. K. Koenig, D. A. Pearson, and K. S. Au. 1993. 'Tuberous Sclerosis Complex.' in R. A. Pagon, M. P. Adam, H. H. Ardinger, S. E. Wallace, A. Amemiya, L. J. H. Bean, T. D. Bird, N. Ledbetter, H. C. Mefford, R. J. H. Smith and K. Stephens (eds.), *GeneReviews(R)* (University of Washington, Seattle
95. University of Washington, Seattle. GeneReviews is a registered trademark of the University of Washington, Seattle. All rights reserved.: Seattle (WA)).
96. O'Connor, D.V.; Phillips D. 1984. *Time Correlated Single Photon Counting* (Academic Press: London).
97. Oldham, W. M., and H. E. Hamm. 2008. 'Heterotrimeric G protein activation by G-protein-coupled receptors', *Nat Rev Mol Cell Biol*, 9: 60-71.
98. Ong, S. H., Y. R. Hadari, N. Gotoh, G. R. Guy, J. Schlessinger, and I. Lax. 2001. 'Stimulation of phosphatidylinositol 3-kinase by fibroblast growth factor receptors is mediated by coordinated recruitment of multiple docking proteins', *Proc Natl Acad Sci U S A*, 98: 6074-9.
99. Parmar, N., and F. Tamanoi. 2010. 'Rheb G-Proteins and the Activation of mTORC1', *Enzymes*, 27: 39-56.
100. Pasqualato, S., L. Renault, and J. Cherfils. 2002. 'Arf, Arl, Arp and Sar proteins: a family of GTP-binding proteins with a structural device for 'front-back' communication', *EMBO Rep*, 3: 1035-41.
101. Patel, P. H., N. Thapar, L. Guo, M. Martinez, J. Maris, C. L. Gau, J. A. Lengyel, and F. Tamanoi. 2003. 'Drosophila Rheb GTPase is required for cell cycle progression and cell growth', *J Cell Sci*, 116: 3601-10.
102. Pawson, T. 2002. 'Regulation and targets of receptor tyrosine kinases', *Eur J Cancer*, 38 Suppl 5: S3-10.
103. Peng, Min, Na Yin, and Ming O Li. 2014. 'Sestrins Function as Guanine Nucleotide Dissociation Inhibitors for Rag GTPases to Control mTORC1 Signaling', *Cell*, 159: 122-33.
104. Pereira-Leal, J. B., and M. C. Seabra. 2001. 'Evolution of the Rab family of small GTP-binding proteins', *J Mol Biol*, 313: 889-901.
105. Peterson, T. R., M. Laplante, C. C. Thoreen, Y. Sancak, S. A. Kang, W. M. Kuehl, N. S. Gray, and D. M. Sabatini. 2009. 'DEPTOR is an mTOR inhibitor frequently overexpressed in multiple myeloma cells and required for their survival', *Cell*, 137: 873-86.

106. Polak, P., N. Cybulski, J. N. Feige, J. Auwerx, M. A. Ruegg, and M. N. Hall. 2008. 'Adipose-specific knockout of raptor results in lean mice with enhanced mitochondrial respiration', *Cell Metab*, 8: 399-410.
107. Potter, C. J., L. G. Pedraza, and T. Xu. 2002. 'Akt regulates growth by directly phosphorylating Tsc2', *Nat Cell Biol*, 4: 658-65.
108. Preedy, V. R., and P. J. Garlick. 1986. 'The response of muscle protein synthesis to nutrient intake in postabsorptive rats: the role of insulin and amino acids', *Biosci Rep*, 6: 177-83.
109. Qin, J., Z. Wang, M. Hoogeveen-Westerveld, G. Shen, W. Gong, M. Nellist, and W. Xu. 2016. 'Structural Basis of the Interaction between Tuberous Sclerosis Complex 1 (TSC1) and Tre2-Bub2-Cdc16 Domain Family Member 7 (TBC1D7)', *J Biol Chem*, 291: 8591-601.
110. Qin, N., S. J. Pittler, and W. Baehr. 1992. 'In vitro isoprenylation and membrane association of mouse rod photoreceptor cGMP phosphodiesterase alpha and beta subunits expressed in bacteria', *J Biol Chem*, 267: 8458-63.
111. Ran, F. A., P. D. Hsu, J. Wright, V. Agarwala, D. A. Scott, and F. Zhang. 2013. 'Genome engineering using the CRISPR-Cas9 system', *Nat Protoc*, 8: 2281-308.
112. Rehmann, H., M. Brüning, C. Berghaus, M. Schwarten, K. Köhler, H. Stocker, R. Stoll, F. J. Zwartkruis, and A. Wittinghofer. 2008. 'Biochemical characterisation of TCTP questions its function as a guanine nucleotide exchange factor for Rheb', *FEBS Lett*, 582: 3005-10.
113. Repasky, G. A., E. J. Chenette, and C. J. Der. 2004. 'Renewing the conspiracy theory debate: does Raf function alone to mediate Ras oncogenesis?', *Trends Cell Biol*, 14: 639-47.
114. Rocks, O., M. Gerauer, N. Vartak, S. Koch, Z. P. Huang, M. Pechlivanis, J. Kuhlmann, L. Brunsveld, A. Chandra, B. Ellinger, H. Waldmann, and P. I. Bastiaens. 2010. 'The palmitoylation machinery is a spatially organizing system for peripheral membrane proteins', *Cell*, 141: 458-71.
115. Sabatini, D. M., H. Erdjument-Bromage, M. Lui, P. Tempst, and S. H. Snyder. 1994. 'RAFT1: a mammalian protein that binds to FKBP12 in a rapamycin-dependent fashion and is homologous to yeast TORs', *Cell*, 78: 35-43.
116. Sancak, Y., L. Bar-Peled, R. Zoncu, A. L. Markhard, S. Nada, and D. M. Sabatini. 2010. 'Ragulator-Rag complex targets mTORC1 to the lysosomal surface and is necessary for its activation by amino acids', *Cell*, 141: 290-303.
117. Sancak, Y., T. R. Peterson, Y. D. Shaul, R. A. Lindquist, C. C. Thoreen, L. Bar-Peled, and D. M. Sabatini. 2008. 'The Rag GTPases bind raptor and mediate amino acid signaling to mTORC1', *Science*, 320: 1496-501.
118. Sanger, F., and A. R. Coulson. 1975. 'A rapid method for determining sequences in DNA by primed synthesis with DNA polymerase', *J Mol Biol*, 94: 441-8.
119. Sanger, F., S. Nicklen, and A. R. Coulson. 1977. 'DNA sequencing with chain-terminating inhibitors', *Proceedings of the National Academy of Sciences*, 74: 5463-67.

120. Sarbassov, D. D., S. M. Ali, D. H. Kim, D. A. Guertin, R. R. Latek, H. Erdjument-Bromage, P. Tempst, and D. M. Sabatini. 2004. 'Rictor, a novel binding partner of mTOR, defines a rapamycin-insensitive and raptor-independent pathway that regulates the cytoskeleton', *Curr Biol*, 14: 1296-302.
121. Sarbassov, D. D., D. A. Guertin, S. M. Ali, and D. M. Sabatini. 2005. 'Phosphorylation and regulation of Akt/PKB by the rictor-mTOR complex', *Science*, 307: 1098-101.
122. Satoh, T., M. Endo, M. Nakafuku, T. Akiyama, T. Yamamoto, and Y. Kaziro. 1990. 'Accumulation of p21ras.GTP in response to stimulation with epidermal growth factor and oncogene products with tyrosine kinase activity', *Proc Natl Acad Sci U S A*, 87: 7926-9.
123. Schalm, S. S., D. C. Fingar, D. M. Sabatini, and J. Blenis. 2003. 'TOS motif-mediated raptor binding regulates 4E-BP1 multisite phosphorylation and function', *Curr Biol*, 13: 797-806.
124. Scheele, J. S., J. M. Rhee, and G. R. Boss. 1995. 'Determination of absolute amounts of GDP and GTP bound to Ras in mammalian cells: comparison of parental and Ras-overproducing NIH 3T3 fibroblasts', *Proc Natl Acad Sci U S A*, 92: 1097-100.
125. Schlessinger, J. 2002. 'Ligand-induced, receptor-mediated dimerization and activation of EGF receptor', *Cell*, 110: 669-72.
126. Schmick, M., A. Kraemer, and P. I. Bastiaens. 2015. 'Ras moves to stay in place', *Trends Cell Biol*, 25: 190-7.
127. Schmick, M., N. Vartak, B. Papke, M. Kovacevic, D. C. Truxius, L. Rossmannek, and P. I. Bastiaens. 2014. 'KRas localizes to the plasma membrane by spatial cycles of solubilization, trapping and vesicular transport', *Cell*, 157: 459-71.
128. Seabra, M. C., and C. Wasmeier. 2004. 'Controlling the location and activation of Rab GTPases', *Curr Opin Cell Biol*, 16: 451-7.
129. Shaw, R. J., M. Kosmatka, N. Bardeesy, R. L. Hurley, L. A. Witters, R. A. DePinho, and L. C. Cantley. 2004. 'The tumor suppressor LKB1 kinase directly activates AMP-activated kinase and regulates apoptosis in response to energy stress', *Proc Natl Acad Sci U S A*, 101: 3329-35.
130. Shimizu, K, M Goldfarb, M Perucho, and M Wigler. 1983. 'Isolation and preliminary characterization of the transforming gene of a human neuroblastoma cell line', *Proceedings of the National Academy of Sciences*, 80: 383-87.
131. Sigismund, S., S. Confalonieri, A. Ciliberto, S. Polo, G. Scita, and P. P. Di Fiore. 2012. 'Endocytosis and signaling: cell logistics shape the eukaryotic cell plan', *Physiol Rev*, 92: 273-366.
132. Smith, E. M., S. G. Finn, A. R. Tee, G. J. Browne, and C. G. Proud. 2005. 'The tuberous sclerosis protein TSC2 is not required for the regulation of the mammalian target of rapamycin by amino acids and certain cellular stresses', *J Biol Chem*, 280: 18717-27.
133. Soderberg, O., M. Gullberg, M. Jarvius, K. Ridderstrale, K. J. Leuchowius, J. Jarvius, K. Wester, P. Hydbring, F. Bahram, L. G. Larsson, and U. Landegren. 2006. 'Direct observation of individual endogenous protein complexes in situ by proximity ligation', *Nat Methods*, 3: 995-1000.

134. Tabancay, A. P., Jr., C. L. Gau, I. M. Machado, E. J. Uhlmann, D. H. Gutmann, L. Guo, and F. Tamanoi. 2003. 'Identification of dominant negative mutants of Rheb GTPase and their use to implicate the involvement of human Rheb in the activation of p70S6K', *J Biol Chem*, 278: 39921-30.
135. Takahashi, K., M. Nakagawa, S. G. Young, and S. Yamanaka. 2005. 'Differential membrane localization of ERas and Rheb, two Ras-related proteins involved in the phosphatidylinositol 3-kinase/mTOR pathway', *J Biol Chem*, 280: 32768-74.
136. Taylor, J. S., T. S. Reid, K. L. Terry, P. J. Casey, and L. S. Beese. 2003. 'Structure of mammalian protein geranylgeranyltransferase type-I', *Embo j*, 22: 5963-74.
137. Tee, A. R., B. D. Manning, P. P. Roux, L. C. Cantley, and J. Blenis. 2003. 'Tuberous sclerosis complex gene products, Tuberin and Hamartin, control mTOR signaling by acting as a GTPase-activating protein complex toward Rheb', *Curr Biol*, 13: 1259-68.
138. Tsun, Z. Y., L. Bar-Peled, L. Chantranupong, R. Zoncu, T. Wang, C. Kim, E. Spooner, and D. M. Sabatini. 2013. 'The folliculin tumor suppressor is a GAP for the RagC/D GTPases that signal amino acid levels to mTORC1', *Mol Cell*, 52: 495-505.
139. Urano, J., C. Ellis, G. J. Clark, and F. Tamanoi. 2001. 'Characterization of Rheb functions using yeast and mammalian systems', *Methods Enzymol*, 333: 217-31.
140. van Slegtenhorst, M., R. de Hoogt, C. Hermans, M. Nellist, B. Janssen, S. Verhoef, D. Lindhout, A. van den Ouweland, D. Halley, J. Young, M. Burley, S. Jeremiah, K. Woodward, J. Nahmias, M. Fox, R. Ekong, J. Osborne, J. Wolfe, S. Povey, R. G. Snell, J. P. Cheadle, A. C. Jones, M. Tachataki, D. Ravine, J. R. Sampson, M. P. Reeve, P. Richardson, F. Wilmer, C. Munro, T. L. Hawkins, T. Sepp, J. B. Ali, S. Ward, A. J. Green, J. R. Yates, J. Kwiatkowska, E. P. Henske, M. P. Short, J. H. Haines, S. Jozwiak, and D. J. Kwiatkowski. 1997. 'Identification of the tuberous sclerosis gene TSC1 on chromosome 9q34', *Science*, 277: 805-8.
141. Vander Haar, E., S. I. Lee, S. Bandhakavi, T. J. Griffin, and D. H. Kim. 2007. 'Insulin signalling to mTOR mediated by the Akt/PKB substrate PRAS40', *Nat Cell Biol*, 9: 316-23.
142. Vartak, N., and P. Bastiaens. 2010. 'Spatial cycles in G-protein crowd control', *Embo j*, 29: 2689-99.
143. Vartak, Nachiket, Bjoern Papke, Hernan E Grecco, Lisaweta Rossmannek, Herbert Waldmann, Christian Hedberg, and Philippe IH Bastiaens. 2014. 'The Autodepalmitoylating Activity of APT Maintains the Spatial Organization of Palmitoylated Membrane Proteins', *Biophysical Journal*, 106: 93-105.
144. Vetter, I. R., and A. Wittinghofer. 2001. 'The guanine nucleotide-binding switch in three dimensions', *Science*, 294: 1299-304.
145. Vezina, C., A. Kudelski, and S. N. Sehgal. 1975. 'Rapamycin (AY-22,989), a new antifungal antibiotic. I. Taxonomy of the producing streptomycete and isolation of the active principle', *J Antibiot (Tokyo)*, 28: 721-6.

146. Wang, X., L. E. Campbell, C. M. Miller, and C. G. Proud. 1998. 'Amino acid availability regulates p70 S6 kinase and multiple translation factors', *Biochem J*, 334 (Pt 1): 261-7.
147. Welman, A., M. M. Burger, and J. Hagmann. 2000. 'Structure and function of the C-terminal hypervariable region of K-Ras4B in plasma membrane targetting and transformation', *Oncogene*, 19: 4582-91.
148. Willumsen, B. M., A. Christensen, N. L. Hubbert, A. G. Papageorge, and D. R. Lowy. 1984. 'The p21 ras C-terminus is required for transformation and membrane association', *Nature*, 310: 583-6.
149. Winter-Vann, A. M., and P. J. Casey. 2005. 'Post-prenylation-processing enzymes as new targets in oncogenesis', *Nat Rev Cancer*, 5: 405-12.
150. Wittinghofer, A., and I. R. Vetter. 2011. 'Structure-function relationships of the G domain, a canonical switch motif', *Annu Rev Biochem*, 80: 943-71.
151. Wouters, Fred S., and Philippe I. H. Bastiaens. 1999. 'Fluorescence lifetime imaging of receptor tyrosine kinase activity in cells', *Current Biology*, 9: 1127-S1.
152. Wullschleger, S., R. Loewith, and M. N. Hall. 2006. 'TOR signaling in growth and metabolism', *Cell*, 124: 471-84.
153. Yu, Y., S. Li, X. Xu, Y. Li, K. Guan, E. Arnold, and J. Ding. 2005. 'Structural basis for the unique biological function of small GTPase RHEB', *J Biol Chem*, 280: 17093-100.
154. Zerial, M., and H. McBride. 2001. 'Rab proteins as membrane organizers', *Nat Rev Mol Cell Biol*, 2: 107-17.
155. Zhang, H., G. Cicchetti, H. Onda, H. B. Koon, K. Asrican, N. Bajraszewski, F. Vazquez, C. L. Carpenter, and D. J. Kwiatkowski. 2003. 'Loss of Tsc1/Tsc2 activates mTOR and disrupts PI3K-Akt signaling through downregulation of PDGFR', *J Clin Invest*, 112: 1223-33.
156. Zhang, X., N. Tang, T. J. Hadden, and A. K. Rishi. 2011. 'Akt, FoxO and regulation of apoptosis', *Biochim Biophys Acta*, 1813: 1978-86.
157. Zhou, H., and S. Huang. 2011. 'Role of mTOR Signaling in Tumor Cell Motility, Invasion and Metastasis', *Curr Protein Pept Sci*, 12: 30-42.
158. Zimmermann, G., B. Papke, S. Ismail, N. Vartak, A. Chandra, M. Hoffmann, S. A. Hahn, G. Triola, A. Wittinghofer, P. I. Bastiaens, and H. Waldmann. 2013. 'Small molecule inhibition of the KRAS-PDEdelta interaction impairs oncogenic KRAS signalling', *Nature*, 497: 638-42.
159. Zoncu, R., L. Bar-Peled, A. Efeyan, S. Wang, Y. Sancak, and D. M. Sabatini. 2011. 'mTORC1 senses lysosomal amino acids through an inside-out mechanism that requires the vacuolar H(+)-ATPase', *Science*, 334: 678-83.

ACKNOWLEDGEMENTS

"…Keep Ithaka always in your mind.
Arriving there is what you are destined for.
But do not hurry the journey at all.
Better if it lasts for years,
so you are old by the time you reach the island,
wealthy with all you have gained on the way…"- C. P. Cavafy

As it is the case with all the grand and epic journeys in our lives, we tend to reflect on our personal experiences, growth and most importantly, people who participated in them and shaped them significantly for ourselves. I am not an exception, so, at the end of this very important chapter in my life, I would like to express gratitude to all of those who have made a big impact on it. First of all, I need to thank to Philippe for not just seeing the potential in me, but for his constant support- financial, emotional and intellectual, which allowed for that potential to grow every day for the past few years. You have shaped me as a scientist, and I am eternally grateful and honored to have worked with a brilliant man such as yourself. I have to thank to Martin Schuler for his useful comments about the work and agreeing to be the supervisor from the University. As well, I express my gratitude to Michael Ehrmann for agreeing to be my co-supervisor and being very helpful in the process of submission.

This journey wouldn't be nearly as interesting without my fellow passengers to whom I give very big thanks: to my 'three musketeers' - Björn, Nash and Malte, for being my 'science teachers' at the very beginning of my work and setting the base for all the following things I learned or discovered in everyday lab life. To my two big brothers from the office, Wayne and Antonio, for so many serious and amusing discussions about science, politics, pop culture and food. Additionally, a very big thanks to Antonio, for his help and various useful tips in the lab, which were much needed and appreciated. To Aneta and Hernán, for the help in understanding many different concepts, but as well for your approval, kind words and support in my endeavors. To Astrid, for

always knowing to put everything into right perspective and her useful and objective comments and observations. To Jutta, Lisaweta and Manuela, big thanks for the cloning tips and prepping the constructs, and of course, for making lab work always enjoyable. To all of my fellow PhD students and all the crew from Department 2, I give big thanks for sharing all the good and bad with me, and for being amazing colleagues through all of this time. I need to give a special thanks to Angel and Amit, for having the kindest of hearts and being wonderful, understanding and supportive friends. To my sis Ola, for being an amazing person, a shoulder to cry on and a voice of reason in many different situations. To all of my friends from back home, even though so many things in our life have changed, I am thankful that our friendships so many years later have still stayed the same.

On a more personal note, I have to thank to Diego, for endless love, support and encouragement in everything that I do. You were the best partner in this journey, and I am so happy that we have decided to go together on all the others that are waiting ahead. I love you.

Finally, I need to thank to my family, to whom I am dedicating this work. To my parents, Ivan and Doma, and my sisters, Gordana and Josipa, for all the sacrifices you have done so that I can get ahead and for your eternal faith and support in my dreams, even when they seemed so unattainable. Thank you for teaching me what really matters and has a value and for giving me a core strong enough to endure any obstacle on this crazy journey called life.

CURRICULUM VITAE

The biography is not included in the online version for reasons of data protection.

Erklärung:

Hiermit erkläre ich, gem. § 6 Abs. (2) g) der Promotionsordnung der Fakultät für Biologie zur Erlangung der Dr. rer. nat., dass ich das Arbeitsgebiet, dem das Thema „Coupling of spatial and GTPase cycle of Rheb enables growth factor signaling to mTORC1“ zuzuordnen ist, in Forschung und Lehre vertrete und den Antrag von Marija Kovacevic befürworte und die Betreuung auch im Falle eines Weggangs, wenn nicht wichtige Gründe dem entgegenstehen, weiterführen werde.

Essen, den _____ _____

Unterschrift eines Mitglieds der Universität Duisburg-Essen

Erklärung:

Hiermit erkläre ich, gem. § 7Abs. (2) d) + f) der Promotionsordnung der Fakultät für Biologie zur Erlangung des Dr. rer. nat., dass ich die vorliegende Dissertation selbständig verfasst und mich keiner anderen als der angegebenen Hilfsmittel bedient,bei der Abfassung der Dissertation nur die angegeben Hilfsmittel benutzt und alle wörtlich oder inhaltlich übernommenen Stellen als solche gekennzeichnet habe.

Essen, den _____ _____

Unterschrift des/r Doktoranden/in

Erklärung:

Hiermit erkläre ich, gem. § 7Abs. (2) e) + g) der Promotionsordnung der Fakultät für Biologiezur Erlangung des Dr. rer. nat., dass ich keine anderen Promotionen bzw. Promotionsversuche in der Vergangenheit durchgeführt habe und dass diese Arbeit von keiner anderen Fakultät/Fachbereichabgelehnt worden ist.

Essen, den _____ _____

Unterschrift des Doktoranden